Modelling Condensed-Phase Systems

From quantum chemistry to molecular models

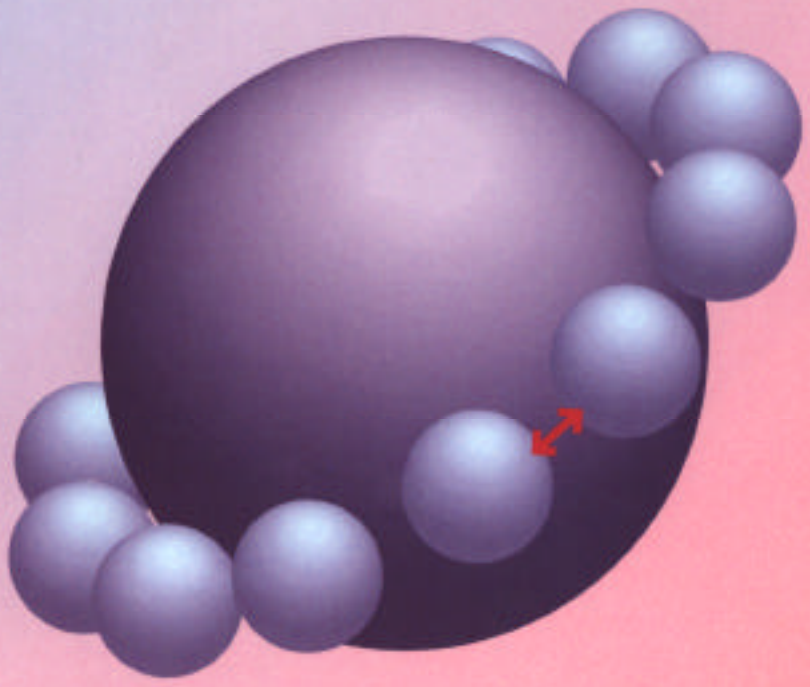

Alex de Vries

MODELLING
CONDENSED-PHASE SYSTEMS
From quantum chemistry to molecular models

Omslag: Michiel Santman

The study described in this thesis was conducted under supervision of and in close collaboration with Dr. P. Th. van Duijnen at the Department of Chemistry of the State University of Groningen, The Netherlands. The research was supported by the Netherlands Foundation for Chemical Research (SON) with financial aid from the Netherlands Organisation for Scientific Research (NWO). Several grants for computing time on various super-computers awarded by the Netherlands National Computer Facilities (NCF) contributed to the results presented in this thesis.

RIJKSUNIVERSITEIT GRONINGEN

MODELLING CONDENSED-PHASE SYSTEMS

From quantum chemistry to molecular models

Proefschrift

ter verkrijging van het doctoraat in de

WISKUNDE en NATUURWETENSCHAPPEN

aan de Rijksuniversiteit Groningen

op gezag van de

Rector Magnificus Dr. F. van der Woude

in het openbaar te verdedigen op

vrijdag 15 december 1995

des namiddags te 1.15 uur precies

door

Alexander Harold de Vries

geboren op 7 mei 1965

te Roden

Promotor

Prof. Dr. W.C. Nieuwpoort

'... They won't make the best of a bad job nowadays. My private schoolmaster used to say, "If a thing's worth doing at all, it's worth doing well." My Church has taught that in different words for several centuries. But these young people have got hold of another end of the stick, and for all we know it may be the right one. They say, "If a thing's not worth doing well, it's not worth doing at all." It makes everything very difficult for them.'

EVELYN WAUGH

Vile Bodies (1930)

Voorwoord/Preface

Op deze plaats wil ik iedereen die mij het leven prettig heeft gemaakt en daardoor mee heeft geholpen aan de voltooiing van dit boekje hartelijk bedanken. Het feit dat je dit boekje in handen hebt gekregen betekent feitelijk dat je tot die groep behoort. Toch wil ik enkelen er even uitlichten.

Joyce, Esther, Edwin, Peter, Mirjam, Piet en Carla vormen een blijvend plezierige thuisbasis.

Mijn begeleider Piet van Duijnen en mijn promotor Wim Nieuwpoort hebben mij *vanaf het begin* op een geweldige manier in het onderzoek gestimuleerd. Beider houding ten aanzien van wetenschap als mensenwerk creëert een warme sfeer waarin kritiek alleen maar opbouwend kan zijn.

Labbewoners uit alle geledingen en door alle jaren heen schiepen een omgeving waarin altijd gelegenheid was de keiharde wereld van de wetenschap even te ontvluchten. Ontmoetingen in wandelgangen, bibliotheek, kantine, sportvelden en vooral luchtbrug waren voor mij essentieel om de jungle te overleven.

Twee hele bijzondere labbewoners waren Marco en Siewert Jan. Ik vind het een hele eer dat zij mij ook bij deze academische passage willen bijstaan.

De volleyeurs en volleyeuses van *Sportclub Groningen* zijn gedurende mijn promotietijd een unieke plaats gaan innemen in mijn leven. De trainings(?)-weekeinden, Amelandtoernooien, absurde feesten en vierde, vijfde en zesde sets onder de douche, in Merleyn en elders zal ik nergens anders vinden. Het greintje waardering dat ik heb voor het Nederlandse lied is uitsluitend jullie verdienste.

The precious moments spent with *all you young quantum chemists* out there, be it at Summerschools, conferences, or at home, have been especially helpful in my finishing this thesis. I dedicate this work to you, in the hope that we will fight for a place to be friends in and that society will *grant* us the pleasure to remain colleagues.

Was gedateerd, december 1995

Inhoudsopgave/Table of contents

1

Concepts and Theory

All beginnings are obscure. Inasmuch as the mathematician operates with the conceptions along strict and formal lines, he, above all, must be reminded from time to time that the origins of things lie in greater depths than those to which his methods enable him to descend. Beyond the knowledge gained from the individual sciences, there remains the task of **comprehending**. In spite of the fact that the views of philosophy sway from one system to another, we cannot dispense with it unless we are to convert knowledge into a meaningless chaos.

HERMANN WEYL

Space Time Matter (1921)

Chemistry of the Multitudes 1.1

Introduction

THE CHEMISTRY discussed in this thesis is the chemistry of solvated molecules: situations in which a relatively small number of molecules of interest, the solute molecules, are surrounded by a large number of other (possibly different) molecules, the solvent. These surroundings undeniably exert some influence on the solute, but the solute may still be recognized as a more or less uncorrupted chemical entity. In experiments that are performed to obtain information on the properties and behaviour of these systems, the total number of molecules present is of the order of 10^{23}—a number exceeding the estimated number of stars in the universe.[1] The size of such samples is what we call macroscopic, or large scale, and the properties obtained reflect the average behaviour of the molecules present, because the detection techniques available cannot discern between specific molecules of the same sort.

In spite of this knowledge, chemists tend to formulate their ideas about the properties of even the largest samples in terms of those of single molecules,[2] and this view has indeed been a very powerful one—since long before individual molecules were actually 'seen' through a microscope.[3] Apparently, molecules, or even fragments of molecules, possess a strong identity, being only weakly disturbed by their particular surroundings. This notion of integrity of matter on the chemical scale is the basis not only of many useful 'rules of thumb', connecting concepts such as electronegativity, electron donor strength, aromaticity, etc. to chemical behaviour as observed in real life, but also of many approximations used in computational approaches to chemistry.

Computational chemistry is the branch of chemistry that pursues the computation of chemical processes from general principles in order to mimic (reproduce), predict, and explain physical experiments, and beyond that to provide concepts that help the creative process of finding new applications in the realm of chemistry. Computational chemistry is therefore a connection between experiment and theory, using mathematical techniques and computer technology. There are many levels on which to practice computational chemistry, depending on the questions asked: from the mixing of chemicals in a reaction vessel to the flow of polymer solutions through a pipe, to the permeation of molecules through membranes, to the spectrum of an impurity in a solid, to the collision of atoms and molecules in beams, in order of increasing spatial detail required to give a pragmatic description. At each level a number of properties are needed in terms of which to describe the problem. Those properties usually have their roots in a level below the one of the actual description, and are the result of a collective or of an average behaviour of smaller entities.[4]

In this thesis the lowest level description of the chemical world will be given in terms of nuclei and electrons, which are thought of as point-like, charged particles that obey the quantum laws. From a study of the behaviour at this level, properties can be computed to serve in the description of molecules in solution at the molecular level, where knowledge of the goings-on of individual nuclei and electrons as such is no longer needed, but only their *collective* effect, typically of one to ten nuclei and one to a hundred electrons, is relevant. Because some of the phenomena computed require explicit description in terms of nuclei and electrons for part of the system, both levels are combined to mimic the experimental conditions. A third level is added and mixed into the description: the collective behaviour of some tens of thousands of molecules in the presence of an applied electric field, the so-called dielectric behaviour. In this way, starting from a microscopic description of matter, the outcome of macroscopic measurements may be computed, at the same time gaining insight into the factors that influence the properties of molecules in solution at a microscopic level.

Survival of the Commonest

Microscopic calculations on macroscopic systems can be meaningful because of the statistical nature of our observations on macroscopic systems. Imagine a box full of elementary particles. There are a lot of possible ways in which the particles may occupy the box. Particle 1 may be in the left bottom corner, while particle 2 is on the right, and number 3 is somewhere in the middle. This arrangement will have certain properties different from another arrangement, for example one in which all three particles are close together in a corner of the box. With millions of millions of millions of particles one can imagine the number of possibilities is unimaginable.

It is precisely this unimaginable number of possibilities that enables us to make the link between the microscopic and the macroscopic.[5] Because of the overwhelming number of possibilities, the properties of the sample will be dominated by the properties of the arrangements that are most common, i.e. most probable. For the molecular description of the condensed phase, the probability p_i of arrangement i is given by the Boltzmann factor, which depends exponentially on the property called energy E_i of the arrangement:

$$p_i = \frac{1}{Z} \exp\left(-E_i / kT\right) \tag{1}$$

where T is the temperature and k the Boltzmann constant. The denominator Z is called the partition function of the system and sums the negative exponent of the energy over all possible arrangements:

$$Z = \sum_j \exp\left(-E_j / kT\right) \tag{2}$$

It is clear that arrangements with high energy do not contribute significantly to the partition function. Thus, the low-energy arrangements (or conformations) are the most important, but becoming less dominant as the temperature rises. All macroscopic properties of the system can be related to the partition function and it is therefore the most central property in the statistical description of matter. For example, the average energy U (as a function of temperature) of the system is given by:

$$U(T) = \sum_i E_i p_i = \frac{1}{Z} \sum_i E_i \exp(-E_i / kT) = kT^2 \frac{\partial \ln Z}{\partial T} \qquad (3)$$

which shows the power of the partition function if it is known as a function of temperature. Sometimes analytical approximations can be found to *Z*, for example for non-interacting particles that are free to move through space independently. For more complicated systems one has to find methods that pick out the most important configurations and to leave it at that. In calculations with classically described particles only, this aspect of chemistry is well developed.[6] In quantum-chemical practice however, the number of conformations considered is usually very small. The techniques developed in the field of molecular simulations on large systems are practicable in quantum chemistry as well, and indeed are gaining importance.[7-9]

In computing energies of physical and chemical processes, the differences between two situations are of interest and require separate computation of the two situations. For example, in this thesis, the energy of solvation is of particular interest. It is the energy associated with the process of bringing one molecule out of the gas phase (where it may be assumed to be completely isolated) into a liquid consisting of a very large number of quite closely packed molecules. To compute the energy of this process, one must compute the energy of the one molecule in the gas phase, the energy of the collection of the molecules in the liquid and finally the energy of all molecules together in the liquid phase. Such a detailed computation is well out of reach of modern technology, and possibly always will be. It is, however, possible to ignore some of the details of the interactions and still obtain a valid description of such macroscopic processes. The remaining sections of this chapter will be devoted to the machinery of this reduction of complexity, starting from the detail of nuclei and electrons as constituent particles, emphasizing the conditions under which these simplifications are justified.

Quantum Chemistry 1.2

Energy is What We're Made Of

Great thinkers of this world throughout the ages have given us the notion that the universe is finally energy, appearing in many forms. A fundamental axiom, never seen to be violated so far, is that the total amount of energy in a closed system remains constant.[10] Thus, in studying nature, we study the ways in which energy *changes form*. The forms to be encountered here are particles (matter) and radiation (light).

To start with particles: the particles relevant for chemists are nuclei and electrons. Both are assumed to be point-like, charged particles with a certain mass. The electrons each carry a single negative charge and the nuclei an integral number of positive charges. A certain composition of nuclei and electrons will be called a system and may be taken to correspond to a sample of matter as one may handle it in the laboratory, or anywhere else. It will be clear that such a sample will never exist on its own, but that there is usually a lot of other matter left over: this left-over matter is called the surroundings. Also, one will never succeed in completely isolating the system from its surroundings, though one may come a long way.

Radiation is a key form of energy in the study of chemical systems: the light absorbed and emitted by samples provides a fingerprint by which it is possible to identify the chemical entities present and to gain insight into the type of interactions in which they are involved. This strongly characterizing potency of light is due to the fact that a system is allowed to possess only very definite amounts of energy if the particles in it are in any way confined. Each amount of energy in the system is associated with a state of the system. In changing from one such state to another, a very definite amount of energy is either absorbed or released in the form of radiation, because the total energy of system and radiation in such a change of states must be constant. As there are many such transitions from state to state, a set of characteristic energy changes will be possible, and together these form the spectrum of the system. It is one of the tasks of quantum chemistry to compute the states and concomitant energies of a system of interest, and thereby the characteristic spectrum, taking as building blocks the nuclei and electrons of the system. This is possible because formulas have been found that give the energy as a function of the mass and velocity of, and the interactions between, the particles.

Schrödinger Equations

The energy-content, or simply energy, of a system is determined by the energy of the particles' movement through space (kinetic energy) and the energy of interaction between the particles of the system. For our purposes the only relevant interaction

between the particles is the Coulomb interaction. In classical mechanics,[11] which describes the behaviour of particles derived from observations on macroscopic amounts of matter, any system with balanced amounts of positive and negative charge would collapse (with the understanding that the energy released in this process is lost to the surroundings by radiation). This does not happen in fact, and the empirical knowledge of this fact has been laid down in a set of rules to which the building blocks of nature must adhere: the quantum laws, and the Pauli principle. These laws are referred to as quantum theory, and the practical implementation of these laws in terms of computable formulae is called quantum mechanics.

Quantum theory as used in this work is built around the concept of a wave function.[12-14] The wave function Ψ is a function of the co-ordinates, or position vectors, $\{\mathbf{r}\}$ of the particles of interest—in chemistry these are nuclei and electrons—, possibly of some intrinsic variable of the particles, such as spin, and of time, t, and contains the information on the motion of the particles through space as a function of time:

$$\Psi = \Psi(\{\mathbf{x}\}; t) \tag{4}$$

in which $\{\mathbf{x}\}$ collects the position vectors and intrinsic variables of the particles. Once the wave function is known all properties of the system can be computed as so-called expectation values, which are integrals of the wave function, normalized to unity, over an operator $\hat{O}$ associated with the property of interest:

$$O(t) = \int_V d\mathbf{x}_1 \int_V d\mathbf{x}_2 ... \int_V d\mathbf{x}_n \, \Psi^*(\mathbf{x}_1, \mathbf{x}_2, ..., \mathbf{x}_n; t) \, \hat{O} \, \Psi(\mathbf{x}_1, \mathbf{x}_2, ..., \mathbf{x}_n; t) \equiv \langle \Psi | \hat{O} | \Psi \rangle \tag{5}$$

where the integration is over all variables of the particles, and the bracket notation is introduced. The motion of the particles is determined by the initial conditions and the interactions between the particles. The energies of motion and of the Coulomb interactions are collected in the Hamiltonian:

$$\hat{H} = -\sum_{i=1}^{N+n} \frac{1}{2 m_i} \hat{\nabla}_i^2 + e^2 \sum_{i=1}^{N+n} \sum_{j<i}^{N+n} \frac{z_i z_j}{|\mathbf{r}_j - \mathbf{r}_i|} \tag{6}$$

for a system with N nuclei and n electrons. m_i and z_i are the mass and charge of particle i, respectively, e is the unit of charge, and $|\mathbf{r}_j - \mathbf{r}_i|$ measures the distance between particles i and j. The first term is the kinetic energy operator, the second is the electrostatic interaction energy operator. The Hamiltonian is expressed in atomic units,[15] in which the familiar factor $1/4\pi\varepsilon_0$ as well as Planck's constant equal 1, so that they do not appear explicitly in the formula. The unit of charge, e, has been left explicit in these formulas for clarity, to concur with the notation in the next chapter in which the effect of nuclei and electrons are analysed separately.

The time-evolution of the system may be found by solving the so-called time-dependent Schrödinger equation. We shall be concerned here only with *stationary states*, for which a simpler equation needs to be solved. In stationary states the

motion of the particles is periodic; the wave function folds back on itself in regular intervals, and the Hamiltonian and properties are independent of time. The equations for the co-ordinates are decoupled from those for time, as the wave function is factored into a time-independent and a time-dependent part $\Psi(\{\mathbf{x}\}; t) = \Psi(\{\mathbf{x}\})\,\Theta(t)$, resulting in two separate equations:

$$\begin{cases} \widehat{\mathrm{H}}\,\Psi(\{\mathbf{x}\}) = E\,\Psi(\{\mathbf{x}\}) \\ \Theta(t) = \mathrm{C}\,\exp(-\,i\,E\,t) \end{cases} \tag{7}$$

in which C is a constant, and the top line of eq. (7) is the time-independent Schrödinger equation. E is the constant of separation and may be identified as the energy of the stationary state. This is the property of the system we are after, because the set of possible energy values determines the spectrum and the statistics of the system. The mathematical construct of decoupling equations will be used a few more times in this thesis as it is the basis of many simplifications in the solution of the Schrödinger equation. Bear in mind that the basis of each decoupling procedure is a fundamental physical observation, valid only in well-defined cases! Here, that is the observation that many systems maintain the same properties over a longer period of time. Note that the periodicity is marked by the energy.

Analysing the motions of individual particles, one may discover that some of the particle periodicities may be much shorter than the overall periodicity. This is often the case for electrons versus nuclei, for reasons of difference of mass (nuclei are at least about two thousand times as heavy as electrons). The energy associated with electronic and nuclear motion may therefore differ several orders, which means that their motions may be only weakly coupled. As a point of departure, the motions of nuclei and electrons may be decoupled, leaving the total function as the direct product of the separate functions:

$$\Psi(\{\mathbf{x}\}) = \Psi_{\mathrm{nuc}}(\{\mathbf{X}\})\quad \Psi_{\mathrm{el}}(\{\mathbf{x}\}\,;\{\mathbf{X}\}) \tag{8}$$

where a change of notation has been made, such that **X** denotes a nuclear co-ordinate and **x** an electronic. This decoupling procedure is called the Born–Oppenheimer (BO) approximation.[16] In applying this approximation one has to be aware that the separation of energy scales may not be as large as expected and that there may indeed be a strong coupling between nuclear and electronic motion, despite their difference in mass. In studying reaction profiles in conjunction with inter-state conversions, one may come across many instances of the breakdown of this approximation.[17]

With the BO approximation in hand, the decoupled equations of motion for nuclei and electrons become:

$$\begin{cases} \widehat{\mathrm{H}}_{\mathrm{el}}(\{\mathbf{X}\})\,\Psi_{\mathrm{el}}(\{\mathbf{x}\}\,;\{\mathbf{X}\}) = E_{\mathrm{el}}(\{\mathbf{X}\})\,\Psi_{\mathrm{el}}(\{\mathbf{x}\}\,;\{\mathbf{X}\}) \\ \left(\widehat{\mathrm{H}}_{\mathrm{nuc}} + E_{\mathrm{el}}(\{\mathbf{X}\})\right)\Psi_{\mathrm{nuc}}(\{\mathbf{X}\}) = E\Psi_{\mathrm{nuc}}(\{\mathbf{X}\}) \end{cases} \tag{9}$$

where the *parametric* dependence of the electronic part of the wave function on the nuclear co-ordinates is made explicit. Solving the nuclear part of the wave function is closely related to the problem of solving the equations of motion for a particle in a potential—in this case, the potential of mean force of the electrons. The standard procedure for this problem is to perform a series of calculations at various fixed nuclear configurations, for which the electronic problem is solved. The series of calculations provides a potential of mean force in which the nuclei move. The equations of motion for the nuclei may then be solved by further quantum-mechanical or classical mechanical techniques,[18] which are by no means trivial, but we shall concentrate here on solving the electronic part of the wave function at a fixed nuclear configuration. This type of calculation is the most common in quantum chemistry and is referred to in general as electronic structure calculation.

The energies normally quoted in electronic structure calculations pertain to the electronic Hamiltonian:[19, 20]

$$\hat{H}_{el}'(\{\mathbf{X}\}) = -\sum_{i=1}^{n} \frac{1}{2} \hat{\nabla}_i^2 - e^2 \sum_{i=1}^{n} \sum_{K=1}^{N} \frac{Z_K}{|\mathbf{R}_K - \mathbf{r}_i|} + e^2 \sum_{i=1}^{n} \sum_{j<i}^{n} \frac{1}{|\mathbf{r}_j - \mathbf{r}_i|} + E_{nuc}(\{\mathbf{X}\}) \qquad (10)$$

where Z_K is the charge of nucleus K in atomic units. Although strictly speaking not appropriate, the electronic Hamiltonian is seen to include the electrostatic interaction between the nuclei [$E_{nuc}(\{\mathbf{X}\})$, which is included in $\hat{H}_{nuc}$ in eq. (9)]. Adding this energy, however, delivers the BO potential energy referred to earlier, which is convenient in handling, because it complies with the classical notion of a potential energy surface.

The Electronic Problem

Before further developing practical methods for solving the electronic structure problem, the consequence of the identical nature of electrons must be considered. Because electrons are indistinguishable, the order in which their variables appear in the wave function should be immaterial to the value of the observables of the system. For the probability density of a two-particle system, given by:

$$\rho(\mathbf{x}_1, \mathbf{x}_2) = \Psi^*(\mathbf{x}_1, \mathbf{x}_2)\,\Psi(\mathbf{x}_1, \mathbf{x}_2) = \Phi^*(\mathbf{x}_2, \mathbf{x}_1)\,\Phi(\mathbf{x}_2, \mathbf{x}_1) \qquad (11)$$

this condition implies either $\Phi(\mathbf{x}_2, \mathbf{x}_1) = \Psi(\mathbf{x}_1, \mathbf{x}_2)$ or $\Phi(\mathbf{x}_2, \mathbf{x}_1) = -\Psi(\mathbf{x}_1, \mathbf{x}_2)$. It has been found that for electrons the wave function should be antisymmetric with respect to particle interchange, i.e. the second relation holds. This requirement on the wave function is called the Pauli principle and adds significantly to the computational effort in solving the Schrödinger equation. The consequence of the Pauli principle is that two identical particles may not occupy the same part of space at the same time. Discussion of the theoretical background of the Pauli principle is not within the scope of this thesis,[21] but the idea behind it is nicely visualized in Erewhonian theology discovered in the previous century:[22]

> Thus they have a law that two pieces of matter may not occupy the same space at the same moment, which law is presided over and administered by the gods of time and space jointly, so that if a flying stone and a man's head attempt to outrage these gods, by 'arrogating a right which they do not possess' (for so it is written in their books), and to occupy the same space simultaneously, a severe punishment, sometimes even death itself, is sure to follow, without any regard to whether the stone knew that the man's head was there, or the head the stone; this at least is their view of the common accidents of life. Moreover, they hold their deities to be quite regardless of motives. With them it is the thing done which is everything, and the motive goes for nothing.

The implementation of the Pauli principle has taken the form of taking the separation of variables to an extreme by starting off from a wave function that is the product function of an independent wave function for each particle:

$$\Psi^{\text{ind. part.}}(\{\mathbf{x}\}) = \psi_1(\mathbf{x}_1) \times \psi_2(\mathbf{x}_2) \times \psi_3(\mathbf{x}_3) \times \ldots \times \psi_n(\mathbf{x}_n) \tag{12}$$

Of course this independent-particle wave function does not obey the antisymmetry requirement for interchanging labels, but the missing terms can easily be generated by performing all possible single, double, triple, etc. interchanges and adding them with the correct sign, at the same time keeping the wave function normalized. This procedure defines the action of the antisymmetrizer:

$$\hat{A}_n = \frac{1}{\sqrt{n!}} \sum_P (-1)^P \hat{P} = \frac{1}{\sqrt{n!}} \left(1 - \sum_{i=1}^{n} \sum_{j>i} \hat{P}_{ij} + \sum_{i=1}^{n} \sum_{j>i} \sum_{k=1}^{n} \sum_{\substack{l>k \\ l>j}} \hat{P}_{ij} \hat{P}_{kl} - \ldots \right) \tag{13}$$

where $\hat{P}_{ij}$ denotes the interchange of labels i and j. For n electrons the antisymmetrizer generates n! terms. Instead of writing all these many terms out, a shorthand notation has been found by recognizing that both number and sign of the n-particle functions are correctly given by the determinant of a matrix having one-particle function and particle label as indices. Such a determinant is called a Slater determinant and is usually denoted by listing the diagonal terms of the matrix:

$$\Psi^{\text{Slater}}(\{\mathbf{x}\}) = \frac{1}{\sqrt{n!}} \begin{vmatrix} \psi_1(\mathbf{x}_1) & \psi_2(\mathbf{x}_1) & \ldots & \psi_n(\mathbf{x}_1) \\ \psi_1(\mathbf{x}_2) & \psi_2(\mathbf{x}_2) & \ldots & \psi_n(\mathbf{x}_2) \\ \ldots & \ldots & \ldots & \ldots \\ \psi_1(\mathbf{x}_n) & \psi_2(\mathbf{x}_n) & \ldots & \psi_n(\mathbf{x}_n) \end{vmatrix} = | \psi_1(\mathbf{x}_1)\, \psi_2(\mathbf{x}_2) \ldots \psi_n(\mathbf{x}_n) | \tag{14}$$

in which Ψ is normalized to unity. It is now clear that the wave function will vanish if two identical electrons have the same wave function, or if there is any linear dependency between the one-particle functions: in either case, the Slater determinant will be zero. With antisymmetrizing the independent-particle wave function *Pauli correlation* has been brought into the electronic wave function, and the wave function obeys the Pauli principle for identical particles. Electrons may be in either of two spin states, called α and β, respectively, between which may be distinguished. Electrons in different spin states are therefore not Pauli correlated, since they are not

identical. This reduces the effort required in the calculations somewhat, but working with the Slater determinant is still a formidable task.

At this point, a closer look at the actual computation of the properties of the system is in order. For the independent-particle wave function [eq. (12)], the expectation values over one- and two-particle operators required in quantum chemistry are simple products of easy one- and two-particle integrals, due to the separation of variables. For the Slater determinant a long sum of those products is required because of all the interchanges. The number of integrals to be computed formally grows at the rate of n^2 for one-particle and n^4 for two-particle integrals, where n is the number of one-particle functions, and becomes a true bottleneck in both CPU and storage demands for quantum-chemical methods. A lot of effort is put into somehow reducing the amount of integrals to be computed, be it through applying numerical cut-offs, exploiting spatial symmetry, simplifying integrals by semi-empirical parameterization, or recognizing Pauli-independent groups of particles. This latter course shall be the one pursued here.

Challenging Mr. Pauli

It is possible to only *partly* antisymmetrize the independent-particle wave function [eq. (12)].[23] We shall call the independent-particle functions which depend on both spatial co-ordinates and spin spin-orbitals. For example, let both spin-orbitals 1 through m be antisymmetrized among each other and spin-orbitals m+1 through n be antisymmetrized among each other, but let the antisymmetrization between spin-orbitals 1 through m on the one hand and m+1 through n on the other hand be excluded:

$$\Psi^{\text{trial}}(\{\mathbf{x}\}) = \hat{A}_m \hat{A}_{n-m}\ \Psi^{\text{ind. part.}}(\{\mathbf{x}\}) = |\,\psi_1(\mathbf{x}_1)...\psi_m(\mathbf{x}_m)\,| \times |\,\psi_{m+1}(\mathbf{x}_{m+1})...\psi_n(\mathbf{x}_n)\,| \qquad (15)$$

This wave function does not obey the Pauli principle throughout, but only in parts. Spin-orbitals 1 through m are Pauli correlated, as are spin-orbitals m+1 through n, but these two groups of spin-orbitals are not Pauli correlated to each other. The consequence of partial antisymmetrization is the disappearance of a lot of terms in the electronic energy expression. The terms that disappear contain overlap, one- or two-particle integrals between one-particle functions belonging to different groups, or combinations thereof. Thus, if the integrals between the one-particle functions belonging to different groups are small, the contribution of the neglected terms to the energy is safely ignored, although the description of the system as a whole does not strictly obey the laws of quantum mechanics.

The smallness of integrals may have two causes. The first is due to integration over spin. If the spin-orbitals have different spin components (α *vs.* β), integration over spin will render the integral zero, and it need not be considered *a priori*. The second cause of smallness of integrals is due to separation in space of the spatial part of the spin-orbitals. Just as the time-dependent wave function can be factored into

components of co-ordinates and time only, the independent-particle functions ψ can be factored into a spatial and a spin component. The spatial components are called *orbitals*. If orbitals are spatially separated, integrals due to implementation of the Pauli principle do not contribute to the properties of the system.

The computational gain of the separation into groups is clear: the number of two-electron integrals to be computed is reduced from n^4 to $\{m^4 + (n-m)^4\}$. Nothing is gained, however, if the groups can be defined or recognized *a posteriori* only, since then a full calculation is required anyway to be able to make the separation at all. Theory shows that with increasing spatial separation of the one-particle functions the magnitude of the integrals associated with inter-group electrostatic interactions decreases exponentially.[23] This observation can be taken as the basis for an *a priori* separation of groups. The neglect of Pauli correlation between molecular fragments is defensible to separations up to the van der Waals distance.[24-27] Application of this technique—and its extension to be discussed later—in condensed phase models is therefore stretching the limit, so one has to be on guard for the breakdown of this approximation.

Electronic Structure Calculations

Having defined the system under study (with or without partitioning the electrons into Pauli-uncorrelated groups), and having chosen the Born–Oppenheimer approximation as our point of departure, the task of computing the one-electron functions and the energy remains. The requirement for the wave function is that it is an eigenfunction of the Hamiltonian, the eigenvalue being the energy [eq. (7)]. Linear algebra provides the tools needed for the solution of such a problem. To this end, a basis set of functions in which to express the wave function is needed, together with the overlap, one- and two-electron integrals over the basis-set functions. One may discern several levels of sophistication of the wave function, depending on its form and the extent of the basis set. Practical molecular quantum chemistry is a matter of expansions within expansions. Usually, one is interested in a limited number of eigenfunctions, notably the one with lowest energy, the ground state. It often happens, or it is supposed to happen, that one or a limited number of terms in the expansions dominate the particular state of interest, reducing the computational demands. As with the *a priori* separation of electrons into groups to circumvent the calculation of a large number of complicated integrals, the truncation of certain expansions must be based on previous experience, and requires careful consideration afterwards.

The most general electronic wave function obeying the Pauli principle is a sum over Slater determinants:

$$\Psi_i(\{\mathbf{x}\}) = \sum_I \Psi_I^{\text{Slater}}(\{\mathbf{x}\})\, C_{Ii} \tag{16}$$

for which the weights C_{Ii} of the Slater determinants are found by solving a so-called secular equation:

$$\left| \left(\mathbb{H} - \mathbb{S} E_i \right) \mathbf{C}_i \right| = 0 \tag{17}$$

in which $\mathbb{H}$ and $\mathbb{S}$ are matrices containing the Hamilton and overlap matrix elements between the Slater determinants in the expansion, and E_i is the energy of the i'th state. A description such as eq. (16) is called a multi-configuration wave function. For any but the smallest systems, the expansion eq. (16) has to be truncated to keep the computation feasible. The quality of the multi-configuration wave function depends on the length of the expansion and whether the one-particle functions are optimized, either for each Slater determinant or for the wave function as a whole.

One-particle functions for the multi-configuration wave functions may be generated from solving an effective one-particle Schrödinger equation. The orbitals $\{\varphi\}$ are expanded in a further basis set of simple spatial functions $\{\chi\}$:

$$\varphi_k(\mathbf{r}) = \sum_{\mu} \chi_\mu(\mathbf{r})\, c_{\mu k} \tag{18}$$

The optimal coefficients c_k for each φ_k are computed analogously to the optimal configuration weights in eq. (17):

$$\left| \left(\mathbb{F} - \mathbb{S} \varepsilon_i \right) \mathbf{c}_i \right| = 0 \tag{19}$$

in which $\mathbb{F}$ is the Fock matrix, and $\mathbb{S}$ the overlap matrix in the basis functions $\{\chi\}$. The ε are the eigenvalues of the problem, which is a pseudo-eigenvalue problem, since the Fock matrix depends on the actual coefficients c. The form of the Fock matrix is determined by restrictions put on the occupation by α- and β-electrons of the orbitals. One very common wave function is the Restricted closed shell Hartree-Fock (RHF) wave function, in which each spatial orbital is occupied by both an α- and a β-electron, a procedure endorsed by experiment which shows that the chemical elements are built up in this way. For such a wave function the Fock matrix is given by:

$$F_{\mu\nu} = \left\langle \chi_\mu(1) \left| \hat{h}_1 \right| \chi_\nu(1) \right\rangle + \sum_{\kappa,\lambda} \left(2 \sum_{i\ \{\mathrm{occ}\}} c^*_{\kappa i}\, c_{\lambda i} \right) \left\langle \chi_\mu(1)\, \chi_\kappa(2) \left| \hat{g}_{12} \left(1 - \frac{1}{2} \hat{P}_{12} \right) \right| \chi_\nu(1)\, \chi_\lambda(2) \right\rangle \tag{20}$$

where the index i denotes all occupied orbitals. The bracketed expression with the sum over the occupied orbitals is the $\kappa\lambda$'th element of the density matrix, which plays a central role in the evaluation of the properties of the system. The operators appearing in the Fock matrix elements correspond to the one- and two-electron operators of the electronic Hamiltonian [eq. (10)]:

$$\hat{h}_i = -\frac{1}{2} \hat{\nabla}^2_i - e^2 \sum_{K=1}^{N} \frac{Z_K}{|\mathbf{R}_K - \mathbf{r}_i|}\ ;\ \hat{g}_{ij} = \frac{e^2}{|\mathbf{r}_j - \mathbf{r}_i|} \tag{21}$$

The appearance of the extra term with the permutation operator in the two-electron part of the Fock matrix is due to the implementation of the Pauli principle and the restriction of α- and β-electrons pairing up into spatial one-electron functions. The procedure to find the optimal orbitals is now clear: from a certain start, calculate the density matrix and the actual Fock matrix; solve the secular problem eq. (19), which gives a new density matrix, etc., until the density matrix doesn't change to within a certain threshold. This procedure is called the self-consistent field (SCF) approximation. Each electron feels the *average* field of all other electrons, which is the main feature of the HF wave function. The multi-configuration approaches serve to repair the deficiencies of the average field description. Nevertheless, the HF wave function often gives very useful information on especially the density of the system.

From the Quantum World to the Classical World 1.3

Particles and Space

THE MOST CENTRAL OBSERVABLE in making the link between the quantum and classical worlds is the (charge) density of a system. The density of a system is the amount of matter present in a small region of space around a given position as a function of the position in space. The density may serve to describe transport phenomena; mechanical, such as liquid flow through a tube, or electrical, as formulated in Maxwell's laws. These theories are classical and conceptually strongly spatial. The quantum world is particle-oriented. The wave function contains information about the behaviour of the particles that build up matter. The wave function itself has no meaning, but for being a mathematical construct. The square of the wave function, however, gives the probability of finding particle 1 at position **x**, particle 2 at position **y**, etc. The *charge distribution* at a position **s** is obtained by collecting these probabilities per small region of space and multiplying by the appropriate charge of the particles, summing over all particles:

$$\rho(\mathbf{s}) = \left\langle \Psi(\{\mathbf{x}\}) \middle| \hat{e}\, \delta(\mathbf{s}) \middle| \Psi(\{\mathbf{x}\}) \right\rangle \hat{=} \int_V d\mathbf{r}_1 \int_V d\mathbf{r}_2 \ldots \int_V d\mathbf{r}_n\, \Psi^*(\{\mathbf{r}\})\, \hat{e}\, \delta(\mathbf{s})\, \Psi(\{\mathbf{r}\}) \qquad (22)$$

where $\hat{e}$ is the charge operator ($-e$ for electrons), and $\delta(\mathbf{s})$ is the Dirac delta function. In the last part of eq. (22) integration over spin, which yields unity, has been performed to connect to the charge-density expression for classical particles which does not contain spin.

Now consider a macroscopic volume described on the quantum-chemical level. The properties of the system follow from the wave function Ψ of the system [eq. (5)], a function of the co-ordinates of all particles, and time, defining a state of the system. In the case of stationary states, time enters only as a phase factor. The wave function can then be found by solving the time-independent Schrödinger equation $\hat{H}\,\Psi = E\,\Psi$, where the Hamiltonian $\hat{H}$ contains the kinetic and interaction operators of all particles.

In pursuing detailed computations on large systems, one must look for a reduction of the computational effort wherever one can. The effort needed for the integration involved in taking an expectation value can be reduced enormously if Ψ vanishes for certain co-ordinates in large parts of space. One then deals with *localized* particles. If a group of particles is localized in the same region in space, say *S*, the integration may be carried out separately over the particles of this group and is confined to the selected volume *S* in space. If no other particle outside the group has a contribution inside the volume, the part of the wave function describing the particles of the group, Ψ_S, may be factored out of the total wave function, leaving Ψ_A for the rest of the particles.

$$\Psi = \Psi_A \; \Psi_S \tag{23}$$

Because of the indistinguishability of electrons writing Ψ as in eq. (23) can never be done in principle, but no error—apart from failing to obey the Pauli requirement throughout—is made if the component functions 'do not overlap', i.e. are spatially separated. The idea of using localized descriptions for explaining chemical behaviour crucially depends on the fulfilment of this requirement. Detailed quantum-chemical studies on the extent of overlap and the effects of neglecting small overlaps between molecular fragments have been carried out.[25, 26] It is perhaps surprising that even at interfragment distances comparable to molecular sizes, the assumption of writing the wave function as a product of fragment functions, ignoring antisymmetry requirements, holds well for both properties and interaction energies. This observation then gives one confidence to exploit the separability of fragments, which leads to a host of possibilities for dealing with larger systems, at a level that is computationally feasible for all-electron quantum-chemical descriptions.

Divide et Impera

In solving the Schrödinger equation, the property of interest is the energy, with its associated Hamilton operator $\widehat{H}$. One may always partition $\widehat{H}$ into a part containing only operations on particles belonging to a group A, $\widehat{H}_A^0$, and a part containing only operations on the particles belonging to a group S, $\widehat{H}_S^0$, and the interaction between particles of groups A and S, $\widehat{V}_{AS}$:

$$\widehat{H} = \widehat{H}_A^0 + \widehat{H}_S^0 + \widehat{V}_{AS}\,; \qquad \widehat{V}_{AS} = \sum_a \sum_A \sum_s \sum_S \frac{z_a z_s}{|\mathbf{r}_a - \mathbf{r}_s|} \tag{24}$$

In calculating the energy E as the expectation value of $\widehat{H}$, one may see the advantage of the separation of the particles of A and S into different regions of space:

$$E = \langle\Psi|\,\widehat{H}\,|\Psi\rangle = \langle\Psi_A|\,\widehat{H}_A^0|\Psi_A\rangle_A + \langle\Psi_S|\,\widehat{H}_S^0|\Psi_S\rangle_S + \Delta E_{\text{int}} \tag{25}$$

Here, the A and S parts of the Hamiltonian may be evaluated separately over their respective parts of space (indicated by the italic capitals *A* and *S*), greatly reducing the dimensionality of the problem. The interaction energy ΔE_{int}, however, requires a double integration, since both fragments contribute to it. This integration may be done in two steps, with a pleasant result at the halfway stage: integration of the A-S interaction part of the Hamiltonian over region *S* gives the operator $\widehat{\Phi}_S$, which yields the potential due to the particles constituting group S in space:

$$\Delta E_{\text{int}} = \langle\Psi_A| \sum_a \sum_A z_a \langle\Psi_S| \sum_s \sum_S \frac{z_s}{|\mathbf{r}_a - \mathbf{r}_s|} |\Psi_S\rangle_S \, |\Psi_A\rangle_A = \langle\Psi_A| \sum_a \sum_A z_a \, \widehat{\Phi}_S(\mathbf{r}_a) \, |\Psi_A\rangle_A \tag{26}$$

Solving the Schrödinger equation (SE) for the whole system can now be partitioned into smaller problems, for which the SE is to be solved in an external potential. The procedure sketched here is a simplified version of the group function approach advocated by McWeeny,[28] which is in fact the basis for any approximate embedding scheme.[29-31] The energy E is minimized in an iterative scheme: starting from some trial functions for subsystems A and S, the potential in A due to S is calculated as in eq. (26); the energy of A in this potential:

$$E_A = \langle \Psi_A | \, \hat{H}_A^0 + \sum_{a \ A} z_a \, \hat{\Phi}_S(\mathbf{r}_a) \, | \Psi_A \rangle_A \tag{27}$$

is minimized, giving a new wave function Ψ_A; next, the potential due to A in S is calculated and in turn Ψ_S is optimized in that potential; a new potential due to S in A is found and applied, etc., until self-consistency is reached.

Making a Gain

The potential just derived deserves closer attention, as it plays a central role in the reduction of the computational effort in condensed matter calculations. An analysis is best made using perturbation theory.[32] In a perturbation formalism the starting function for Ψ_S is the vacuum (ground) state function Ψ_S^0 of the subsystem S. The optimized function is expanded in the orthogonal set of solutions to the vacuum problem $\hat{H}_S^0 \, \Psi_S^m = E_S^m \, \Psi_S^m$ for subsystem S. The original state is altered by the mixing in of excited states as a result of a perturbation, i.e. an external influence. The weights of the mixed-in excited states depend on the strength of the perturbation and the energy difference between ground and excited states.

In this formalism it is easily seen that the potential due to S, $\hat{\Phi}_S$, can be split into two contributions, resulting from the vacuum charge density of S on the one hand, and the density *change* of S induced by subsystem A on the other. The former is called the static potential and the latter the response potential:

$$\begin{aligned} \hat{\Phi}_S(\mathbf{r}_a) &= \langle \Psi_S | \, \hat{\varphi}_S(\mathbf{r}_a) \, | \Psi_S \rangle_S = \langle \Psi_S^0 | \, \hat{\varphi}_S(\mathbf{r}_a) \, | \Psi_S^0 \rangle_S \\ &+ \left\{ 2 \sum_{k \neq 0} c_k \langle \Psi_S^0 | \, \hat{\varphi}_S(\mathbf{r}_a) \, | \Psi_S^k \rangle_S + \sum_{k,m \neq 0} c_k \, \langle \Psi_S^k | \, \hat{\varphi}_S(\mathbf{r}_a) \, | \Psi_S^m \rangle_S \, c_m \right\} \\ &= \hat{\Phi}_S^0(\mathbf{r}_a) + \hat{\Phi}_S^{\text{response}}(\mathbf{r}_a) \end{aligned} \tag{28}$$

in which the coefficients c_k and wave functions are taken to be real.

The static potential may be written in terms of the charge density of fragment S, cf. eq. (22):

$$\hat{\Phi}^0_S(\mathbf{r}_a) = \left\langle \Psi^0_S \right| \sum_{s\ S} \frac{z_s}{|\,\mathbf{r}_a - \mathbf{r}_s\,|} \left| \Psi^0_S \right\rangle_S = \int_V d\mathbf{r}'_s \frac{\rho^0_S(\mathbf{r}'_s)}{|\,\mathbf{r}_a - \mathbf{r}'_s\,|} = V\left(\rho^0_S; \mathbf{r}_a\right) \tag{29}$$

A significant reduction in computational effort may now be made if one could simplify the representation of the charge density. Remember the wave function is expanded in many basis functions, and evaluation of the potential requires the evaluation of many integrals over these basis functions of the type:

$$\hat{J}_{\mu\nu}(\mathbf{r}_a) = -e \int_V d\mathbf{r}'_s\ \chi^*_\mu\left(\mathbf{r}'_s\right) \frac{1}{|\,\mathbf{r}_a - \mathbf{r}'_s\,|} \chi_\nu\left(\mathbf{r}'_s\right) \tag{30}$$

Instead of the representation in terms of basis functions, a charge distribution may be represented in a simplified way, by making a multipole expansion. In a multipolar representation of a charge distribution, the potential operator $1/|\,\mathbf{r}_a - \mathbf{r}'_s\,|$ in eqs. (29) and (30) is first Taylor expanded around a representative point $\mathbf{r}^0_s$ in the charge distribution:

$$\begin{aligned} \frac{1}{|\,\mathbf{r}_a - \mathbf{r}_s\,|} &= \frac{1}{|\,\mathbf{r}_a - \mathbf{r}^0_s\,|} - \frac{(\mathbf{r}_a - \mathbf{r}^0_s)^\dagger}{|\,\mathbf{r}_a - \mathbf{r}^0_s\,|^3}\left(\mathbf{r}'_s - \mathbf{r}^0_s\right) \\ &- \frac{1}{2!}\left(\mathbf{r}'_s - \mathbf{r}^0_s\right)^\dagger \left\{ \frac{\mathbb{I}_3}{|\,\mathbf{r}_a - \mathbf{r}^0_s\,|^3} - \frac{3\,(\mathbf{r}_a - \mathbf{r}^0_s)\,(\mathbf{r}_a - \mathbf{r}^0_s)^\dagger}{|\,\mathbf{r}_a - \mathbf{r}^0_s\,|^5} \right\} \left(\mathbf{r}'_s - \mathbf{r}^0_s\right) + \ldots \end{aligned} \tag{31}$$

in which $\mathbb{I}_3$ denotes the 3-dimensional unit matrix. Inserting eq. (31) in eq. (29), the so-called multipole moment integrals of the charge distribution may be recognized:

$$\hat{\Phi}^0_S(\mathbf{r}_a) = V\left(\rho^0_S; \mathbf{r}_a\right) = \frac{1}{|\,\mathbf{r}_a - \mathbf{r}^0_s\,|} \left\{ \int_V d\mathbf{r}'_s\ \rho^0_S\left(\mathbf{r}'_s\right) \right\} - \frac{(\mathbf{r}_a - \mathbf{r}^0_s)^\dagger}{|\,\mathbf{r}_a - \mathbf{r}^0_s\,|^3} \left\{ \int_V d\mathbf{r}'_s\ \rho^0_S\left(\mathbf{r}'_s\right)\left(\mathbf{r}'_s - \mathbf{r}^0_s\right) \right\} + \ldots \tag{32}$$

The bracketed expressions in eq. (32) are the zeroth moment, i.e. the total charge, and the first, or dipole moment of the charge distribution, respectively. It is clear that they can be evaluated *independently* of the measurement point $\mathbf{r}_a$, for which reason the multipole integrals are a lot easier to calculate than the potential integrals [eq. (30)]. It thus seems highly advantageous to make use of this expansion. However, before doing so, one must look into the convergence of the expansion.

The series in eq. (32) converges for measurement points $\mathbf{r}_a$ outside the charge distribution. A real (quantum-mechanical) charge distribution, however, extends over all space, making the use of any such expansion rather tricky.[24] Also, from the expansion it is seen that the contribution of a higher moment decreases with distance more strongly than that of a lower moment, so that at larger distances the series will converge faster than at shorter distances. A more detailed discussion of the possibilities and choices for devising multipolar charge representations is given in the next section. In the same way as multipoles were defined for the complete charge

distribution, multipoles of the basis charge distributions ($\mu\nu$) [cf. eq(30)] may be defined. We shall use those in section 2.2, where the potentials and fields due to and at a quantum-mechanically described system are expanded in order to calculate the interaction between the quantum system and other parts of the system that are described at the classical level.

To gain insight into the response part of the potential in eq. (28), the Taylor expansion of the potential operator $\hat{\varphi}_S$ around a representative point $\mathbf{r}_s^0$ in S is made once more, so that the weights c_k can be written as:

$$c_k = \frac{\left\langle \Psi_S^k \right| \sum_{s\ S} \frac{z_s}{\left| \mathbf{r}_a' - \mathbf{r}_s \right|} \left| \Psi_S^0 \right\rangle_S}{E_0 - E_k} = - \frac{\left(\mathbf{r}_a' - \mathbf{r}_s^0 \right)}{\left| \mathbf{r}_a' - \mathbf{r}_s^0 \right|^3} \times \frac{\left\langle \Psi_S^k \right| \sum_{s\ S} z_s \left(\mathbf{r}_s' - \mathbf{r}_s^0 \right) \left| \Psi_S^0 \right\rangle_S}{E_0 - E_k} + \ldots \qquad (33)$$

where the orthogonality of the zeroth order functions has been used to get rid of the first term in the expansion. The factor on the left in eq. (33) is the field operator of subsystem A at the representative point in S, whereas in the factor on the right the dipole operator of subsystem S with respect to the representative point again makes its appearance. Inserting eq. (33) in the second term of eq. (28) and making the same expansion for the potential operator, truncating at the dipole term, the second order perturbation expression for the dipole polarizability of subsystem S emerges, thus showing the connection of the second term in eq. (28) to the linear response functions of subsystem S:

$$2 \sum_{k \neq 0} \left\langle \Psi_S^0 \right| \hat{\varphi}_S(\mathbf{r}_a) \left| \Psi_S^k \right\rangle_S c_k = 2 \sum_{k \neq 0} \left\langle \Psi_S^0 \right| \hat{\varphi}_S(\mathbf{r}_a) \left| \Psi_S^k \right\rangle_S \times \frac{\left\langle \Psi_S^k \right| \hat{\varphi}_S\left(\mathbf{r}_a' \right) \left| \Psi_S^0 \right\rangle_S}{E_0 - E_k} =$$

$$- \frac{(\mathbf{r}_a - \mathbf{r}_s^0)}{\left| \mathbf{r}_a - \mathbf{r}_s^0 \right|^3} \times 2 \sum_{k \neq 0} \frac{\left\langle \Psi_S^0 \right| \sum_{s\ S} z_s \left(\mathbf{r}_s' - \mathbf{r}_s^0 \right) \left| \Psi_S^k \right\rangle \left\langle \Psi_S^k \right| \sum_{s\ S} z_s \left(\mathbf{r}_s' - \mathbf{r}_s^0 \right) \left| \Psi_S^0 \right\rangle_S}{E_0 - E_k} \times - \frac{\left(\mathbf{r}_a' - \mathbf{r}_s^0 \right)}{\left| \mathbf{r}_a' - \mathbf{r}_s^0 \right|^3} + \ldots \qquad (34)$$

$$= \hat{E}_a(\mathbf{r}_s^0) \ \alpha_S(\mathbf{r}_s^0) \ \hat{E}_a'(\mathbf{r}_s^0) + \ldots$$

Reading this formula from right to left, its meaning is evident: the field at $\mathbf{r}_s^0$, due to a particle in A, induces a dipole proportional to the polarizability α_S at $\mathbf{r}_s^0$, which in turn gives rise to a (response) potential at a particle in subsystem A. These terms are called *induction* terms, as the change in charge density of subsystem S is induced by the charge density of subsystem A. Higher order responses follow similarly from the continued expansion of the second term, and from the third term in eq. (28), connecting to the quadratic response functions of S.

A second type of property of the subsystem S has now been identified: the multipole polarizabilities. Whereas the multipole moments properties are connected to the charge distribution, the polarizabilities are seen to be linked to the spectrum of

the system. In the dipole polarizability the transition dipoles play a crucial role, as made evident in eq. (34). Again, the transition moments have a classical analogue in the oscillator strengths, measuring the intensity of dipolar transitions.

Interfragment Interactions

The interaction between subsystems A and S [eq. (26)] has now been partly unravelled. The expansion of the wave function for subsystem S into vacuum ground and excited state functions showed that the interaction with the charge distribution of subsystem A could be written as a static plus a response contribution [eq. (28)]. A fuller analysis may be obtained from making the same expansion for subsystem A. To second order in the perturbation (SOP), the interaction then contains the following terms: (1) the electrostatic interaction between the charge densities of A and S as they were in isolation, (2) the interaction of the charge density of A and the *change* in charge density of S, and *vice versa*, and (3) the interaction between instantaneous changes in charge density of both A and S.[33] This last term is called the *dispersion* interaction and has not been encountered before:

$$\Delta E_{\mathrm{SOP}}^{\mathrm{disp}} = \frac{1}{|\mathbf{r}_a^0 - \mathbf{r}_s^0|^6}\left\{\mathbb{1} + \frac{3(\mathbf{r}_a^0 - \mathbf{r}_s^0)(\mathbf{r}_a^0 - \mathbf{r}_s^0)^{\dagger}}{|\mathbf{r}_a^0 - \mathbf{r}_s^0|^2}\right\} \times \sum_{k,m \neq 0} \frac{\left|\langle \Psi_A^0 | \hat{\mu}_A | \Psi_A^k \rangle\right|^2 \left|\langle \Psi_S^0 | \hat{\mu}_S | \Psi_S^m \rangle\right|^2}{E_{A,0} - E_{A,k} + E_{S,0} - E_{S,m}} \tag{35}$$

where $\hat{\mu}_A$ and $\hat{\mu}_S$ are the dipole operators of subsystems A and S, respectively [cf. eq. (32), second term]. The dispersion interaction can be expressed in terms of the polarizabilities of the subsystems by invoking the Unsöld approximation that enables a splitting of the denominator:

$$\frac{1}{E_{A,0} - E_{A,k} + E_{S,0} - E_{S,m}} = \left(\frac{U_A U_S}{U_A + U_S}\right)\left(\frac{-1}{(E_{A,0} - E_{A,k})(E_{S,0} - E_{S,m})}\right)\{1 + \Delta_{km}\};$$

$$\Delta_{km} = \frac{\frac{1}{U_A} - \frac{1}{E_{A,0} - E_{A,k}} + \frac{1}{U_S} - \frac{1}{E_{S,0} - E_{S,m}}}{(E_{A,0} - E_{A,k})^{-1} + (E_{S,0} - E_{S,m})^{-1}} \tag{36}$$

in which U_A and U_S are chosen to minimize the overall error. Inserting eq. (36) into eq. (35), the polarizabilities of A and S are recognized—just as the polarizability of S was recognized in eq. (34)—leading to the approximate dispersion interaction expression:

$$\Delta E_{\mathrm{SOP}}^{\mathrm{disp}} \approx \frac{-1}{|\mathbf{r}_a^0 - \mathbf{r}_s^0|^6} \times \left(\frac{U_A U_S}{U_A + U_S}\right) \times \frac{1}{2}\alpha_A \left\{\mathbb{1} + \frac{3(\mathbf{r}_a^0 - \mathbf{r}_s^0)(\mathbf{r}_a^0 - \mathbf{r}_s^0)^{\dagger}}{|\mathbf{r}_a^0 - \mathbf{r}_s^0|^2}\right\} \frac{1}{2}\alpha_S \tag{37}$$

The dispersion interaction between two systems is always attractive, and always present, in contrast to the electrostatic and induction interactions, which depend on the presence of permanent electrostatic moments in either of the subsystems. In

deriving these interaction formulas, we made the assumption that the total wave function is the direct product of the wave functions for A and S, thus ignoring the Pauli principle. When the subsystems come closer, this assumption is not valid, and one should apply symmetry-adapted perturbation theory (SAPT),[27] which accounts for the effect of antisymmetrization of the subsystem wave functions. Each term encountered in the SOP interaction expression is then found to have a counterpart in the SAPT expressions. The effect of the antisymmetrization is to remove favourable interactions that were included through overlap but violate the Pauli principle. These become dominant when the systems get close and taking them out generates a strong repulsion between the systems because the more unfavourable interactions remain. This effect is quite difficult to treat in the same way as the electrostatic and dispersion interactions, and is usually modelled by an *ad hoc* potential of polynomial or exponential form.

Collective Behaviour

Apart from smartly dividing up the volume of integration, and excluding a large number of electron-electron correlations through ignoring the Pauli requirement, no real progress has been made in the development so far to reduce the dimensionality of the system. The complete system is still treated at the quantum-mechanical level. A real reduction of computational effort should come from reducing the number of degrees of freedom. Let us concentrate on subsystem S for a while, leaving A for what it is. In order to reduce the number of degrees of freedom of the system, the static and response potentials due to S should be mapped on some functional form containing far less parameters than the original number of particles in S. The reduction is achieved by truncating the expansions in the Taylor series of the operators and the order of response theory. In practice, the Taylor series are often truncated at the dipole level and the responses at second order in the perturbation, i.e. linear response only, as shown here. Apart from these truncations, the size of the subsystems of which the properties are determined is also reflected in the sophistication of the mapping on classical models.

The great advantage of the treatment outlined above is that both the permanent moments and the response functions are defined entirely in terms of the subsystem S, and can be obtained from explicit calculation at any level, or from experiment. The permanent moments and the response functions may be regarded as parameters describing the *collective* properties of the particles comprising subsystem S. The progress made by using the collective properties described becomes only really meaningful if the parameters describing the static and response moments prove to be transferable between systems of different nature, but composed of the same building blocks. For example, the parameters for a water molecule should be useful in any system containing a water molecule, whatever type of material is present otherwise. If this was not the case, one would have to go through the whole exercise of deriving the parameters for the new situation.

At this stage, one may anticipate that any set of parameters describing collective properties will have its limits of applicability. The limits are, however, quite well defined, and follow directly from the assumptions made in the derivation of the collective properties. In our case, close scrutiny must be paid to the validity of ignoring the Pauli principle, and the order to which the Taylor expansions are taken into account. The practical implications of the theoretical development made in this section will be discussed in the next, together with the limits of applicability. Only by realizing these limits during a computational investigation a sensible approach will result.

Meandering the Scales 1.4

THE COLLECTIVE PROPERTIES of molecules typically reflect one to twenty nuclei and one to a hundred or so electrons in a volume of tens to hundreds of cubic Bohr. Accurate computation of the electrostatic and response properties of such volumes is well within the current possibilities of *ab initio* quantum chemistry techniques. Thus one has access to the static potential [eq. (29)], as well as the multipole [eq. (32)] and response [eq. (34)] moments. Remains the task of reducing the number of degrees of freedom in the representation of those properties. Because the number of degrees of freedom is reduced, a choice can be made and the best choice may vary according to the system under consideration.

Molecules: Charge Density Representation

The only simplified charge density representation to have a direct counterpart in experiment is the multipole representation, because the multipoles of molecules are experimentally accessible: they are observables.[34-36] (The charge density itself is also accessible, e.g. through X-ray diffraction, but a representation of similar resolution would require another basis set type approach without the drastic computational reduction achieved through truncated multipole representations.) The disadvantage of this first charge-density representation is that it may converge quite slowly, especially close to the molecule and for larger molecules, necessitating complicated prefactors [eqs. (31) and (32)].[35]

In the end, it is the potential of the molecule that is of interest. A second approach is the direct storage of the computed potential [eq. (29)], the reduction in computational effort arising from choosing a grid on which to calculate the potential. A suitable interpolation for the potential between the grid points completes this procedure. This is still very costly: it requires a large number of integrals of the type of eq. (30), and there are problems with the transferability (the grid should move along with the molecule if it changes orientation). It is possible, however, in a fitting procedure, to derive a number of charges located somewhere in the molecule that reproduce the computed potential as well as possible.[37, 38] These so-called potential derived charges (PDCs) are transferable, although the choice of number and position of the grid points determine the quality of the representation.[39]

The PDCs are an example of a distributed monopole representation of the charge distribution. The PDCs are only indirectly derived from the charge density. The last type of charge representations to be discussed here is directly derived from the charge density itself. In quantum-chemical calculations, the wave function is expanded in terms of basis functions [eq. (18)], and the total charge density [eq. (22)] is expressed in terms of delta functions for the nuclear part and overlap distributions of the basis functions for the electronic part:

$$\rho(\mathbf{s}) = e \sum_{N \text{ nuc}} Z_N \, \delta(\mathbf{s} - \mathbf{R}_N) - e \sum_{\mu,\nu} D_{\mu\nu} \, \chi_\mu^*(\mathbf{s}) \, \chi_\nu(\mathbf{s}) \tag{38}$$

The density matrix $D_{\mu\nu}$ expressed in the simple basis $\{\chi\}$, and the configuration basis $\{\Psi^{\text{Slater}}\}$, has the general form:

$$D_{\mu\nu} = \sum_{K,L} C_K^* \, C_L \sum_{i,j \ \{\text{occ}\}} \delta_{\eta_{Ki},\eta_{Lj}} \, c_{\mu i}^* \, c_{\nu j} \tag{39}$$

in which η_{Ki} is the spin part of spin-orbital ψ_i in configuration K, and C_K and $c_{\mu i}$ are the expansion coefficients for the configurations Ψ_K and simple basis functions χ_μ, respectively.

A distributed multipole representation is based on calculating the multipole moments of the charge distributions and assigning a position in space to them. The various approaches differ in the truncation of the multipole expansion and the assignment of the contributions to expansion centres. As the basis functions themselves are usually located on the nuclei, most distributed multipole representations take the nuclei as sole expansion centres. The simplest scheme in this family is the Mulliken analysis,[40] a distributed monopole representation, which simply assigns half of the contribution of any overlap distribution to each centre of its constituent basis functions. The distributed multipole analysis of Stone[41, 42] may keep all multipole moments of overlap distributions, or truncates after the quadrupole, and assigns them to the centre closest to it. Extra centres, such as the midpoints of the nuclei, may be added to gain accuracy. These representations all suffer from the fact that they do not in general preserve the *overall* multipole moments of the molecule (this is a consequence of shifting the contributions to the expansion centres without correcting for the moments induced by the shift), and thus generate an inaccurate potential at larger distances. Usually, these methods already fail to reproduce the overall dipole moment.

The so-called dipole preserving charges (DPCs) by Thole and van Duijnen[43] constitute a distributed monopole representation that is the result of a Mulliken-based population analysis that preserves the overall dipole moment. Starting with the Mulliken charges, charges that rebuild the Mulliken dipoles are added on the charge centres, such that the calculated overall dipole moment is preserved. Because a weighting function ensures the nearest centres to get the largest contributions in the rebuilding procedure, the DPCs have the additional property of maximum preservation of *local* dipole moments.

The problem of defining charges for large molecules (for which *ab initio* calculations are out of the question, and measurements of multipole moments are insufficient for a microscopically accurate representation) is a source of continuing research within the development of atom-based force fields.[44] Rullmann has addressed this problem by joining overlapping fragments, for which calculations are possible,[45] e.g. amino acids joined to a protein.[46] In most atom-based force fields, charge representations are the result of optimizing start values (usually from a Mulliken analysis) by

fitting to computed macroscopic properties,[47, 48] such as the second virial coefficient. These charges are usually not widely transferable between different chemical systems and between force fields because there are many more parameters involved that are also allowed to be optimized and, more importantly, these force fields lack an explicit polarizability representation.

One should not employ the distributed multipole representations within the volume of the charge density from which they were derived, because the representation is not valid inside the charge density. In practice one may, however come across situations in which two charge densities are in close vicinity, and the full Coulomb potential of a point charge is then unrealistically large. An option is then to account for the fact that the source of the potential is a charge *density*, rather than a collection of point charges, by assuming a model shape for the charge density. Several choices are available for this shape function. We have employed a conical and an exponential shape, the width of which depends on the polarizability of the atom. The shape functions that result from this assumption are fairly simple and were shown to be effective in the treatment of interacting polarizabilities by Thole.[49] Note that the smearing out of the charge always has the effect of reducing the potential, for which reason the shape function is also called the screening function.

Molecules: Linear Response Function Representation

Honesty demands to add to the claim that the computation of molecular response moments is well within reach of *ab initio* quantum chemistry that the effort needed for obtaining accurate response moments is much larger than for the static properties.[36] The cause of this is that the density is not quite as sensitive to the length of both basis set and configuration expansions as the spectrum and the transition moments required for the response properties [eq. (34)] are. It is therefore advantageous to investigate response function models based on experimental results. In this work only linear response is considered; for molecules that is the (dipole) polarizability: the extent to which the charge density distorts to form an additional dipole moment as the result of an applied permanent electric field.

Analogous to the static moments, the polarizability of a molecule may be represented by one tensor located at the centre of the molecule, or in a distributed fashion, e.g. by interacting atomic polarizabilities located on the nuclei. Stone[50] and Karlström[51] have developed distributed polarizability representations on the basis of *ab initio* wave functions along the same lines as for the representation of the charge distribution. The polarizability representation used in this work is an empirical distributed atomic polarizability representation developed by Thole.[49] A single polarizability for the elements H, C, N and O, in whatever molecule they participate, together with a screening function described above, suffices to reproduce experimental molecular polarizabilities. The fitting was done on circa twenty molecules, and testing for a number of other molecules always proved to reproduce the experimental polarizability to within 10%.

Bulk Material: Dielectric Continuum Models

The collective properties of bulk material typically reflect the collective behaviour of tens of thousands of molecules in a volume of at least 10^7 cubic Bohr.[52] Accurate computation of the electrostatic and response properties of such volumes is well outside the current possibilities of *ab initio* quantum chemistry techniques, and probably will be for a long time. Thus one has to resort to experimental information on the behaviour of such volumes. Such bulk volumes have no permanent electrostatic moments: the individual molecules take on all sorts of orientations so that on average the potential vanishes. When an electric field is applied across such a bulk volume, the average moments do not vanish, but there will be a preference of individual molecules to align their permanent and response moments with the electric field. The extent to which this preference is present in the bulk is reflected by its dielectric constant.[53] The dielectric constant is measured by reduction of the attractive force between two oppositely charged plates when the bulk material is introduced between them. The dielectric constant measures the linear response, for which the applied field strength should not exceed 10^4 V/cm, or 2 10^{-6} a.u., as departures from linearity are observed at higher field strengths.

On the scale on which the dielectric constant is defined, all molecular detail has been lost: the dielectric constant describes a homogeneous, isotropic medium, or *continuum* of matter. Molecular effects are, however, present in the dielectric constant, but only in an average sense. It is therefore dangerous to attribute effects seen in microscopic models embedded in a dielectric to specific interactions, such as H-bonding. Although all structure has been lost, different contributions to the dielectric constant may be discerned, on the basis of molecular models and frequency dependency of the response of bulk volumes. Instead of applying a permanent electric field across the plates of a condensor, one may apply an oscillating field and monitor the response.

At low frequencies the response will not differ from the response when switching on a permanent field, only its direction will change with the change of direction of the applied field. As the frequency is enlarged, however, sharp drops in the response will be noticeable at certain frequencies. These can be identified as typical frequencies of molecular and atomic motion. For molecules with a permanent electrostatic moment, the change in orientation of the molecule contributes to the dielectric response. As the field changes direction, the molecules tend to align their permanent moments and reorient. In this they are hampered by their neighbours through interaction, and so it takes time to adopt to the new direction of the applied field. If the field has changed direction before the new orientation has been reached, reorientation no longer occurs, thus giving a drop in the response. The component associated with the reorientation of the molecules is called the orientational response.

A minor contribution to the dielectric constant vanishes at higher frequencies and can be associated with the vibrational motions within the molecule. Usually this component is so small that it is ignored altogether. The remaining component is that

of the electronic response. This component is assumed to be able to follow any change in the applied field instantaneously, and is present in materials whether or not the molecules carry permanent moments. In fact, it may be considered to result from the interacting molecular polarizabilities encountered above.

A Sensible Model Under Scrutiny 1.5

A SKETCH of our condensed phase model combining three levels of spatial detail is given in Figure 1. In applications of this model, a partitioning of the system into the appropriate levels is to be made. In this section the *physical* basis for making the partition is given. In Chapter 3 different partitioning schemes will be tested numerically, as we investigate several applications of the model.

Spatial Separation of Molecular Subsystems

The theoretical development so far required fragment separation for more or less formal reasons, and linear response of bulk material for practical reasons, but the separation of two or more systems and the (non-)linearity of their mutual interactions are of course strongly connected. For example, the interactions between the three atoms within a single water molecule are highly non-linear because their charge distributions overlap strongly *and* the electric potentials and fields are too large to expect linear response. As far as the energy is concerned, the only way to deal with this problem is to describe the system in terms of electrons and (effective) nuclei, and solve a set of coupled equations which contain all of the non-linear problems. One of the properties of the resulting molecule is its (dipole) polarizability describing the linear response of this collection of atoms.

In the water dimer at its optimal geometry, the largest overlap between two molecular orbitals is about 0.05.[54] Whether or not this is a 'large' overlap depends on the context in which the overlap criterion is used. One may wonder if the electrostatic interaction between the molecules can be described with a linear response

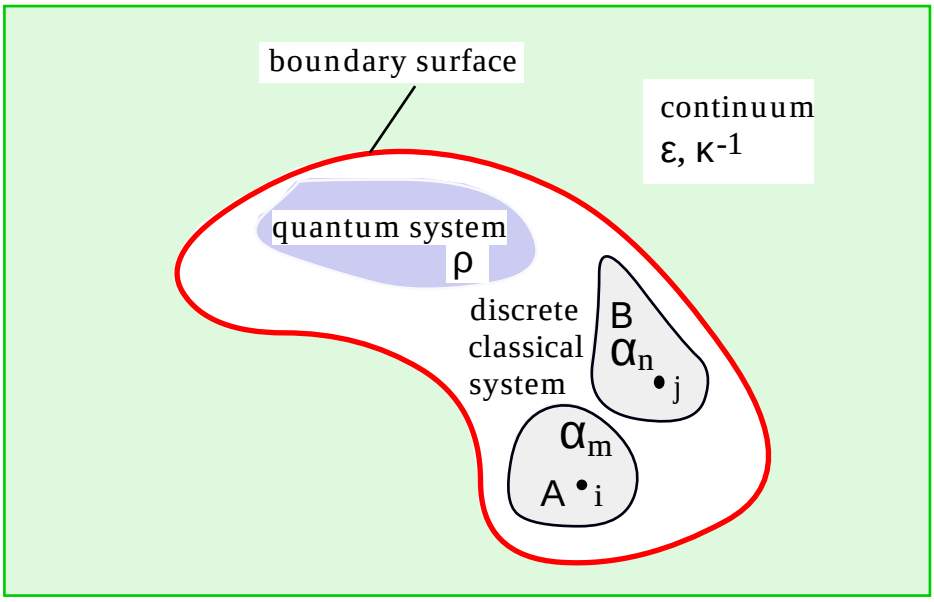

Figure 1. General condensed phase model.

model at this distance, or, more generally, up to what distance this model is acceptable. One possible answer comes from simple electrostatics, and was given by Thole.[49] Consider two isotropic *interacting* polarizabilities α_i and α_j at distance r. The effective polarizability along the axis is:

$$\alpha_{//} = \frac{\alpha_i + \alpha_j + 4\,\alpha_i\alpha_j / r^3}{1 - 4\,\alpha_i\alpha_j / r^6} \tag{40}$$

When r approaches $(4\,\alpha_i\,\alpha_j)^{1/6}$, $\alpha_{//}$ tends to infinity, caused by the co-operative interaction between the two induced dipoles along the axis. The trouble starts when the polarizability volumes—i.e. spheres with radius $\alpha^{1/3}$—start overlapping. Such a situation should be avoided, or one must in some way account for the non-linearities, e.g. by screening the interactions. In our model for reaction potentials we have adopted Thole's method for defining an effective 'many-body' polarizability, in which $d_{ij} = 1.662\,(\alpha_i\,\alpha_j)^{1/6}$ is the minimum distance for two interacting polarizabilities without screening function, where the factor 1.662 and the polarizabilities are model parameters fitted to (experimental or calculated) molecular dipole polarizabilities. If the polarizabilities come closer, the fields of the induced dipoles are damped to account for the overlap of the electronic densities connected to the polarizabilities. In the water dimer we may put the monomer electronic polarizabilities of 10 $Bohr^3$ on the oxygen atoms, which are in the equilibrium geometry about 6 Bohr apart. Thole's criterion shows that already at this distance the mutual induction effects may be treated completely classically,[55] provided the inducing fields correspond to charge distributions which are correct up to at least the dipole term. Apparently both the separation and the linearity requirements are satisfied in this situation.

Spatial Separation from the Bulk

In employing continuum models for solvation it is necessary to define a cavity in the dielectric to contain the solute (and some solvent molecules). The solute's response potential is found by solving Poisson's equation, which is practicable only if no higher order than linear response is allowed. In practice, two methods for solving the Poisson equation are in use: one based on 3-dimensional integration (on some grid),[56] the other based on 2-dimensional integration on the surface enveloping the solute (usually built from small adjacent polygons).[57, 58] The surface defines the boundary between the solute cavity and the solvent bulk. For the second method analytic forms exist but these are applicable only to spherical and elliptical cavities.[59, 60] This makes them less useful for general purposes.

The necessity of defining a cavity around the solute immediately poses the problem of where to put its boundary. Because the reaction potential is very sensitive to the solute–boundary distance, getting 'physically plausible results' strongly depends on the careful definition of the boundary. The surfaces employed in most models resemble a Connolly surface,[61] which is defined by rolling a probe sphere with the size of a solvent molecule over a set of overlapping spheres centred on the

solute's atomic sites (see also Figure 3.6). If the atomic spheres are given the atomic van der Waals radii, Connolly's 'van der Waals surface' is defined by the 'contact points' between probe and atomic spheres. The surface traced by the centre of the probe is usually called the 'solvent accessible' surface.

We want the boundary first to be consistent with the non-overlap requirement, meaning that no significant part of the solute's (electronic) charge is to be found outside the cavity. Obeying this criterion Miertuš *et al.* claim that this leads to 'unrealistically small' reaction potentials.[62] With a nearby boundary, constructed with the standard van der Waals radii, they obtained a 'realistic' reaction potential, but a sizeable amount of electronic density (for water about 1%) was found to extend over the boundary. This means that the overlap of 0.05, mentioned above, is too large for solute–dielectric interaction. To remedy this effect, they made a correction for the 'charge leakage', at the same time scaling up the atomic radii by 20% to reduce the charge distribution outside the cavity to less than 0.5%. The analytic methods employ a cavity with a volume derived from the density of the solute, which leads to a cavity of approximately the same size as defined by the Connolly van der Waals radii, so they may suffer from the same defect. Choices published so far are all of the type 'van der Waals plus something' or 'van der Waals times something' to arrive at 'realistic' solvation energies.

At this point we conclude that the van der Waals surfaces are too close to the solute to be consistent with the non-overlap criterion, and we suggest to increase the 'atomic spheres' by adding at least one solvent radius. In case of a water solute in bulk water, this means that the boundary is located 7.3 Bohr from the centre of mass of the solute. Already here we note that by this procedure the experimental hydration energy cannot be reproduced (which will be demonstrated in Chapter 3).

Next we look into the combined overlap / non-linearity problem. Obviously, no source charge or (induced) dipole may ever be positioned precisely on the boundary, because its reaction potential will then be infinitely large. A measure for the minimal distance can be obtained—at least for a neutral, polarizable solute—by repeating Thole's reasoning for two polarizabilities: the dielectric constant of the bulk is, via the dielectric susceptibility, $\chi_e = (\varepsilon - 1)/4\pi$, connected to the polarizability density which includes, apart from the electronic polarisation, vibrational and rotational contributions. For polar solvents the rotational contribution, i.e. the effect of the permanent dipoles orienting themselves along the applied field, dominates. By simply multiplying the dielectric susceptibility by the volume of one solvent molecule (assuming that the dielectric is homogeneous to a microscopic limit) one gets an effective molecular polarizability. Again taking water as an example, we obtain (from the density and susceptibility at 298K) an effective polarizability of 1240 $Bohr^3$ per molecule. Applying Thole's criterion for the interacting polarizabilities of the central water (10 $Bohr^3$) and an effective neighbouring bulk molecule, the minimum distance should be 8.0 Bohr, which is slightly larger than that derived from the first overlap criterion. This second criterion is not always the strongest. For benzene in benzene, the first criterion (no overlap) would put the boundary at 12.4 Bohr from

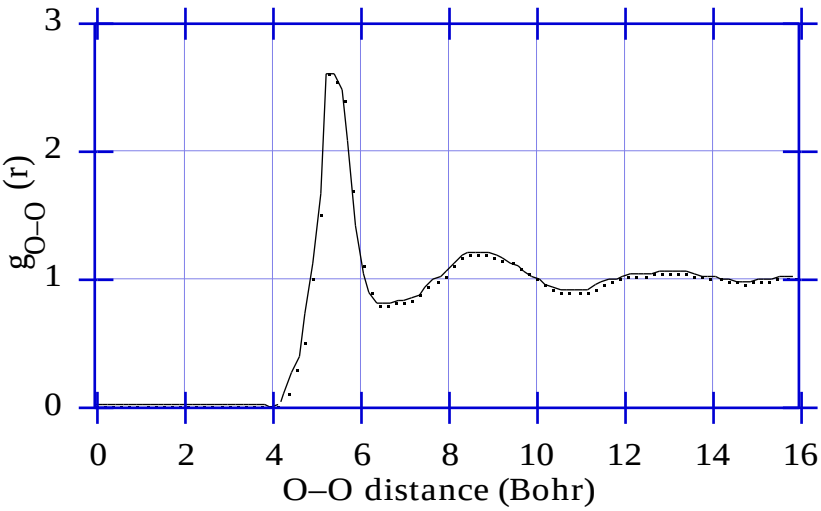

Figure 2. Typical solvent radial distribution function.

the centre of mass, while the interacting polarizabilities criterion would put it at only 7.2 Bohr.

The last possible test regards the linearity of the response *per se*. If the solute's field-strength is too large, non-linear effects will give rise to an enhanced or reduced polarization of the bulk, depending on the type of effect.[53] For polar solvents, the main non-linear effect is saturation: the molecular dipoles become more or less fixed in space with respect to the solute, strongly reducing the orientational contribution to the local polarizability. At the macroscopic level this can be remedied quite satisfactorily by introducing a correction function to the dielectric constant proportional to the square of the field strength, but at the microscopic level the dielectric model breaks down and at least the first solvent layer should be included in a more detailed way in the description. From experiment it is known that non-linear effects show up at field strengths of about $2\ 10^{-6}$ au (10^4 V/cm), which is for example generated by a unit dipole (2.54 D) at 100 Bohr in vacuo! Considering again water in water, with a solute dipole moment equal 1.85 D, the previous criteria look pallid. If the boundary would be put at the required distance (73 Bohr), many layers of solvent water would have to be included to make the model still look like a condensed phase.

In practice, one can probably do with a smaller number of solvent layers, because the collective field of solute and solvent layers will fall off faster than the field of the solute alone. Insight in the minimum number of solvent layers to be included can be gained from the radial distribution functions of the solvent. A typical radial distribution for bulk water after Narten *et al.*[63] is schematically shown in Figure 2. It is clear that at least the first two layers should be considered in detail, since the requirement of homogeneity is not fulfilled.

Conclusion 1.6

THE METHOD outlined in this chapter for relating the nature of microscopically small particles to measurements on macroscopic substances consisting of unimaginably large numbers of those particles appears, in retrospect, too good to be true. It seems almost unbelievable that such a relatively simple scheme could result in accurate and reliable predictions of macroscopic behaviour under strongly varying conditions.

Scepticism is in order—up to a point. Much depends on the process and the properties that are being studied: the conditions must fit the assumptions along which the development of theoretical and computational frames were made. For example, very high-pressure substances cannot be treated in the fashion used in the remainder of this thesis, simply because the Pauli correlation between the molecules will play a crucial role; predictions concerning strictly dynamical processes, such as reaction rates, will not be possible either, unless the properties pursued can be related to nuclear arrangements that fit the Born–Oppenheimer regime. However, by going back to the assumptions the way to proceed in such cases will always be clear. Repairs can be made at the appropriate places, the feasibility being determined by the current (computer) technological state-of-affairs and very often to a large extent by the patience of the computational chemist.

The solvated systems studied in this thesis are on the borderline of the validity of the approach. The molecules do keep their integrity to a large extent, but the density is such that they are always in close vicinity to their neighbours. Special care has to be taken to avoid artefacts caused by the simplified description of the charge distribution and response properties.

It may not always be necessary to go to the lengths described in this book to get accurate and reliable computational results for certain very important and interesting properties. The example of the solvation energy in water will be elaborated on in Chapter 3. It is nevertheless worthwhile to pursue the more detailed description because it provides a better understanding of the nature of the processes that determine the effects of solvation which may be stimulating to further experimental and computational research. It also provides insight into the failure of simple models, reminding us of the saying that only the sun rises free of charge.

2

Implementation

Activity is the only road to knowledge.

BERNARD SHAW

Man and Superman (1906)

Introduction 2.1

THE CONCEPTS and theory of the mixed quantum-mechanical–classical approach discussed in Chapter 1 are to be elaborated in a computational scheme in order to enable numerical testing of the ideas on microscopic condensed-phase modelling. If not for the explicit treatment of molecular polarizability, a chapter on the implementation would hardly be wanted, since the literature yields an ample supply of solvation models: for molecular mechanics type mixing;[64-73] for analytic and numerical dielectric continuum-only reaction fields;[56, 57, 62, 74-92] and for alternative treatments of molecular polarizability.[93-97] Especially the self-consistent coupling of the molecular polarizabilities and the continuum warrant the special attention given to implementation in this chapter. As so often in computational chemistry practice, the scheme doesn't originate with the present author, but has evolved over many years, being added to by various people, as particular interests were being pursued.[29, 98-100] Thus, this chapter presents a transient state-of-the-art.

The quantum chemistry computer code that underlies the work presented in this thesis is the HONDO8.1 suite of programs.[101] Occasionally, specific reference to the way in which this program handles the quantum partition will be made, but the description of the implementation is aimed to be as general as possible; in fact, the present method is currently being implemented in various other (semi-empirical) quantum chemistry codes.

The development of this chapter parallels that of section 1.4. The (electro)static environment potential is treated first, followed by the response, or reaction, potential and field. (The terms reaction potential and reaction field are sometimes somewhat injudiciously used synonymously to indicate the idea of the environment responding to an applied electrostatic influence on it.) The coupling between the responses of the different partitions to each other's influence is treated in some detail. Expressions are given for the different contributions to the total energy. Such an analysis is useful to gain more insight into processes in the condensed phase.

The reaction-field contribution can be coupled to the quantum partition in two ways. One may first determine a charge density of the quantum partition, calculate its reaction field, and couple this back to the quantum partition to determine a new charge density, etc. Alternatively, a reaction-field *operator* may be defined and included in the Hamiltonian. The former is the Average Reaction Field (ARF) approach, because the electrons in the quantum partition experience the reaction field of the charge distribution as a whole, whereas in the latter approach each electron feels the reaction field of itself and the other electrons instantaneously, and is therefore called the Direct Reaction Field (DRF) approach. For single-configuration wave functions, both approaches are possible, but only the ARF approach can be applied to multi-configuration wave functions in a way that is both conceptually and technically unambiguous. The DRF approach has the advantage that an estimate of

the dispersion interaction between quantum and classical partitions can be coupled self-consistently to the quantum system by noting a similarity between two-electron reaction-field integrals and the Unsöld approximation to the SOP expression for dispersion.[55, 102] This feature will be explained and used in section 3.2.

Two features within the present mixed quantum-mechanical–classical approach that have not been described before reflect on two aspects of the phenomena of interest: the time-scale and the thermodynamics. Regarding time-scale, different response components can be distinguished according to the frequency associated with the motions that cause the response (section 1.4).[52, 53] The highest frequencies belong to the electronic motions, modelled by the discrete polarizabilities and the optical dielectric constant ε_∞, which can be derived from the refractive index at high frequency. Next, the shift of equilibrium distances of vibrational motions contributes a fairly high frequency component which is usually not taken into account because it is small. The slower translational and rotational motions of molecules with a permanent dipole moment constitute the origin of the orientation polarization, which is the low-frequency component, and the most important one for polar solvents. It is this component that is unable to directly follow the fast motions or processes in the quantum partition and must therefore be treated with care.[103-105]

For example, if an excitation process is so fast as to prevent the orientation polarization component to 'catch up', the product state experiences the orientational polarization belonging to the ground state. This component is not in equilibrium with the charge distribution of the excited state, and in coupling the reaction field to the excited state it should remain static, while only the electronic component of the response should be allowed to adapt to the excited state charge density.

Conducting experiments at ambient temperatures allows for thermal motion of the system, which can be quite large in weakly bonded systems, like most solutions. Thus the properties of the system are an average over a large number of conformations with approximately the same energy. In calculations with classically described particles only, this aspect of chemistry is well developed.[6] In quantum-chemical practice however, the number of conformations considered is usually very small. The techniques developed in the field of molecular simulations on large systems are practicable in quantum chemistry as well, and indeed are gaining importance.[7-9] With the model presented here a Monte Carlo sampling of the discrete classical degrees of freedom is fairly trivial, albeit time-consuming. The challenge is mainly in the development of interaction functions that fit into the framework outlined in Chapter 1, for which the reader is referred to Chapter 3.

Before closing this section, a word on the partitioning of the system into different regions is in order. In solvation studies a natural choice for the partitions is to treat the solute molecule quantum mechanically, and a number of solvent molecules classically, as groups. A surface around this discrete collection may then serve to separate it from the bulk solvent, treated as a dielectric. The minimum number of explicit solvent layers to be included in the discrete partition may be estimated from (experimental) radial distribution functions. Boundary effects should be minimized

by going beyond the minimum requirement,[106-109] and by carefully considering the distance between the outer molecules and the surface boundary.[110]

In macromolecular problems, such as enzymes, or the cluster approach to the solid state, bonds shall have to be broken between partitions. None of the currently practised solutions to this problem is really satisfactory,[111-116] although saturation with e.g. H-atoms,[117-120] omitting nearest-neighbour interactions have at least provided practicable models. In all instances the employed partitioning should be tested against the properties of interest, especially regarding the degree of localization within the quantum partition.

Expansion of the Potentials and Fields 2.2

WE DEFINE the potential, field, and field-gradient operators, due to a unit point charge at **s**, measured at **x**:[52]

$$V(\mathbf{s};\mathbf{x}) = \frac{1}{|\mathbf{x}-\mathbf{s}|} \tag{1}$$

$$\mathbf{E}(\mathbf{s};\mathbf{x}) = -\nabla_{\mathbf{x}} V(\mathbf{s};\mathbf{x}) = \nabla_{\mathbf{s}} V(\mathbf{s};\mathbf{x}) = \frac{(\mathbf{x}-\mathbf{s})}{|\mathbf{x}-\mathbf{s}|^3} \tag{2}$$

$$\mathbb{T}(\mathbf{s};\mathbf{x}) = \nabla_{\mathbf{x}} \mathbf{E}(\mathbf{s};\mathbf{x}) = -\nabla_{\mathbf{s}} \mathbf{E}(\mathbf{s};\mathbf{x}) = \frac{1}{|\mathbf{x}-\mathbf{s}|^3}\left\{\mathbb{I}_3 - \frac{3(\mathbf{x}-\mathbf{s})(\mathbf{x}-\mathbf{s})^\dagger}{|\mathbf{x}-\mathbf{s}|^2}\right\} \tag{3}$$

where $\mathbb{I}_3$ denotes the 3-dimensional unit matrix. All vectors are defined as column vectors, and set in bold type. Two-dimensional matrices are outlined. A dagger (†) denotes the transpose of a tensor. Atomic units are used throughout.[15]

In the present implementation, the potentials and fields coupling the quantum partition to the classical partitions are not evaluated exactly, but expanded around a number of expansion centres. This greatly simplifies the evaluation of (reaction) field integrals over basis functions and has been shown to retain almost the accuracy of the exact approach for a discrete classical environment.[121] This is due to the slow variation of the reaction field over molecular dimensions, validating an expansion to first order only. If the expansion to first order should not appear to suffice, one could of course consider going to higher order. However, increasing the number of expansion centres might improve the convergence more quickly.

The expansion centres are usually taken to be the nuclei of the quantum partition. However, especially in cases of high symmetry, one or more extra expansion centres (notably the centre of nuclear charge) may be required to avoid symmetry breaking of the wave function. The problem of this type of symmetry breaking originates in assigning the charge distributions to expansion centres. For every charge distribution an expansion centre may be defined by:[121]

$$\mathbf{c}_{ij} = \mathbf{M}'_{ij} / S'_{ij} \tag{4}$$

where $\mathbf{M}'_{ij}$ is the dipole moment integral of the ij'th distribution, taken relative to the centre of nuclear charge, and S'_{ij} is the overlap integral of the same distribution, by treating the orbitals as s-type functions. This definition is rigorous only for s-type basis functions, but we use it for any type. (A similar, but more precise, definition of overlap distribution centres for use in a population analysis has been given by Huzinaga *et al.*[122]) The charge distribution is then assigned to the expansion centre

closest to the computed centre [eq. (4)]. However, one has to be aware of two issues with this scheme:

(i) the computed centre may be equally distant from two or more expansion centres. If the symmetry of the nuclear framework is not imposed on the assignation of the charge distributions, symmetry breaking may occur due to the search algorithm, or due to numerical errors. This may be remedied by defining an extra expansion centre at the computed centre, or assigning all problematic distributions to the centre of nuclear charge.

(ii) S'_{ij} may be very small, whereby $\mathbf{c}_{ij}$ is ill defined. The occurrence of small radial overlap usually involves centres that are quite distant from each other. In general, these overlap distributions have a small dipole moment as well as a small overlap, and therefore often give a negligible contribution to the (reaction) potential. The exact location of their expansion centres will not be very critical, and their contribution may even be discarded altogether. In the case described, we have chosen to define the centre of the overlap distribution as the midpoint of the connecting line between the atoms bearing the basis functions involved, and then to follow the regular procedure.

Other schemes are possible, e.g. just to assign every one-centre overlap distribution to that centre and all two-centre distributions to the centre of nuclear charge. This scheme serves quite well for small molecules, as may be expected if the static and reaction fields vary slowly over molecular dimensions. More elaborate schemes, e.g. with weighting functions according to the distance from an expansion centre can be conceived, but we have not pursued these, as the present schemes are satisfactory.

The potential and field operators due to a unit charge at $\mathbf{s}$ can be expanded around expansion centre $\mathbf{s}_0$. The potential and field measured at $\mathbf{x}$ are, to first order:

$$V(\mathbf{s};\mathbf{x}) \approx V(\mathbf{s}_0;\mathbf{x}) + \nabla_{\mathbf{s}_0} V(\mathbf{s}_0;\mathbf{x})(\mathbf{s}-\mathbf{s}_0) = V(\mathbf{s}_0;\mathbf{x}) - \mathbf{E}(\mathbf{s}_0;\mathbf{x})\cdot\mathbf{s}_0 + \mathbf{E}(\mathbf{s}_0;\mathbf{x})\cdot\mathbf{s} \quad (5)$$

$$\mathbf{E}(\mathbf{s};\mathbf{x}) \approx \mathbf{E}(\mathbf{s}_0;\mathbf{x}) + \nabla_{\mathbf{s}_0}\mathbf{E}(\mathbf{s}_0;\mathbf{x})(\mathbf{s}-\mathbf{s}_0) = \mathbf{E}(\mathbf{s}_0;\mathbf{x}) + \mathbb{T}(\mathbf{s}_0;\mathbf{x})\cdot\mathbf{s}_0 - \mathbb{T}(\mathbf{s}_0;\mathbf{x})\cdot\mathbf{s} \quad (6)$$

The potential and field operators due to a unit charge at $\mathbf{s}$ measured at $\mathbf{x}$, expanded around centre $\mathbf{x}_0$ are, again to first order:

$$V(\mathbf{s};\mathbf{x}) \approx V(\mathbf{s};\mathbf{x}_0) + \nabla_{\mathbf{x}_0} V(\mathbf{s};\mathbf{x}_0)(\mathbf{x}-\mathbf{x}_0) = V(\mathbf{s};\mathbf{x}_0) + \mathbf{E}(\mathbf{s};\mathbf{x}_0)\cdot\mathbf{x}_0 - \mathbf{E}(\mathbf{s};\mathbf{x}_0)\cdot\mathbf{x} \quad (7)$$

$$\mathbf{E}(\mathbf{s};\mathbf{x}) \approx \mathbf{E}(\mathbf{s};\mathbf{x}_0) + \nabla_{\mathbf{x}_0}\mathbf{E}(\mathbf{s};\mathbf{x}_0)(\mathbf{x}-\mathbf{x}_0) = \mathbf{E}(\mathbf{s};\mathbf{x}_0) - \mathbb{T}(\mathbf{s};\mathbf{x}_0)\cdot\mathbf{x}_0 + \mathbb{T}(\mathbf{s};\mathbf{x}_0)\cdot\mathbf{x} \quad (8)$$

The use of these expansions enables very simple evaluation of one- and two-electron integrals, requiring only overlap, first, and second moment integrals of the charge distributions, e.g. for the potential due to the ij'th electronic charge distribution, assigned to $\mathbf{s}_0$, at $\mathbf{x}$:

$$\begin{aligned} V_{ij}(\mathbf{x}) &= -e \left\langle i \middle| V(\mathbf{s}_0; \mathbf{x}) - \mathbf{E}(\mathbf{s}_0; \mathbf{x}) \cdot \mathbf{s}_0 + \mathbf{E}(\mathbf{s}_0; \mathbf{x}) \cdot \mathbf{s} \middle| j \right\rangle \\ &= -e \left\{ \left[V(\mathbf{s}_0; \mathbf{x}) - \mathbf{E}(\mathbf{s}_0; \mathbf{x}) \cdot \mathbf{s}_0 \right] S_{ij} + \mathbf{E}(\mathbf{s}_0; \mathbf{x}) \cdot \mathbf{M}_{ij} \right\} \end{aligned} \tag{9}$$

where $S_{ij} = \langle i | j \rangle$ and $\mathbf{M}_{ij} = \langle i | \mathbf{r} | j \rangle$ are the overlap and dipole moment integrals of the ij'th distribution, and e is the unit positive charge.

In the following sections, explicit formulas will be given for the different contributions to the static and reaction potentials and fields, along with brief discussions of theoretical and practical considerations to the use of these expressions. In the following, we shall denote a general co-ordinate by **x**, discrete classical charge and/or polarizability co-ordinates by $\mathbf{r}_p$ and $\mathbf{r}_q$, representative surface boundary points by $\mathbf{r}_I$ and $\mathbf{r}_J$, nuclear co-ordinates by $\mathbf{R}_N$ and $\mathbf{R}_M$, and expansion centres in the quantum partition by $\mathbf{r}_a$ and $\mathbf{r}_b$.

Static Potentials and Fields 2.3

THE STATIC POTENTIALS and fields due to the discrete classical partition are mediated through a distributed monopole representation of this partition. Usually, the positioning of charges only at the nuclei suffices to provide a fairly accurate potential and field, provided the charges are suitably chosen, but more and other charge centres may be necessary, depending on the accuracy required. (For a discussion on charge representations, refer to section 1.4.) The static potential and field at **x**, due to the discrete classical partition take the form:

$$V_q^{dcl}(\mathbf{x}) = \sum_{p \neq G(\mathbf{x})} f^V(|\mathbf{x} - \mathbf{r}_p|, \alpha_p, \alpha_x)\, q_p\, V(\mathbf{r}_p; \mathbf{x}) \tag{10}$$

$$\mathbf{E}_q^{dcl}(\mathbf{x}) = \sum_{p \neq G(\mathbf{x})} f^E(|\mathbf{x} - \mathbf{r}_p|, \alpha_p, \alpha_x)\, q_p\, \mathbf{E}(\mathbf{r}_p; \mathbf{x}) \tag{11}$$

in which G(**x**) denotes the members of the group in which **x** is positioned, and q_p is the charge at centre p. The exclusion of intra-group interactions between charges is the consequence of the analyses made in sections 1.4 and 1.5, where it was argued that the electrostatic multipoles can be represented by a set of charges, but that the potential is only valid outside the volume of integration, and that intra-group interactions represented by atomic building blocks are highly non-linear and therefore of a form different from Coulomb's law. The analysis also called for a screening function for short-range inter-group interactions.[49] For a conical charge distribution the shape functions f^V, f^E are:

$$f^V(|\mathbf{x} - \mathbf{r}_p|, \alpha_p, \alpha_x) = \begin{cases} v^4 - 2v^3 - 2v\,; & |\mathbf{x} - \mathbf{r}_p| \leq 1.662(\alpha_p\, \alpha_{\mathbf{x}})^{1/6} \\ 1; & |\mathbf{x} - \mathbf{r}_p| > 1.662(\alpha_p\, \alpha_{\mathbf{x}})^{1/6} \end{cases} \tag{12}$$

$$f^E(|\mathbf{x} - \mathbf{r}_p|, \alpha_p, \alpha_x) = \begin{cases} -3v^4 + 4v^3\,; & |\mathbf{x} - \mathbf{r}_p| \leq 1.662(\alpha_p\, \alpha_{\mathbf{x}})^{1/6} \\ 1; & |\mathbf{x} - \mathbf{r}_p| > 1.662(\alpha_p\, \alpha_{\mathbf{x}})^{1/6} \end{cases} \tag{13}$$

where $v = |\mathbf{x} - \mathbf{r}_p| \,/ 1.662(\alpha_p\, \alpha_{\mathbf{x}})^{1/6}$, and α_p and $\alpha_{\mathbf{x}}$ are formal polarizability volumes on the centres p and **x**, associated with the width of the charge distribution. The factor 1.662 is a parameter, obtained from fitting computed molecular polarizabilities from interacting atomic polarizabilities to experimental molecular polarizabilities. The shape function was found to be not very critical to the value of the atomic polarizabilities, so Thole's optimized values for H, C, N and O are used, and Hartree–Fock values[123] for other elements. Another possible choice of the shape function is an exponential one, given by:[49]

$$f^V(|\mathbf{x} - \mathbf{r}_p|, \alpha_p, \alpha_x) = 1 - \left(\frac{1}{2}\, a\, v - 1\right) \exp(-a\, v) \tag{14}$$

$$f^E(|\mathbf{x}-\mathbf{r}_p|, \alpha_p, \alpha_x) = 1 - \left(\frac{1}{2}(a\ v)^2 + a\ v + 1\right)\exp(-a\ v) \tag{15}$$

where $v = |\mathbf{x}-\mathbf{r}_p| \,/\, (\alpha_p\,\alpha_{\mathbf{x}})^{1/6}$, and a is a fitting parameter with the optimized value of 2.089.

The continuum partition has no static potential, as is evident from the assumption that it is homogeneous and isotropic.

As far as the quantum partition is concerned, the nuclear charges generate a static potential and field that are treated completely analogous to those of the discrete classical system (except for the effect on the electrons, which remains to be treated exactly). The expressions are:

$$V_N^{qm}(\mathbf{x}) = \sum_N f^V(|\mathbf{x}-\mathbf{R}_N|, \alpha_N, \alpha_x)\, Z_N\, V(\mathbf{R}_N; \mathbf{x}) \tag{16}$$

$$\mathbf{E}_N^{qm}(\mathbf{x}) = \sum_N f^E(|\mathbf{x}-\mathbf{R}_N|, \alpha_N, \alpha_x)\, Z_N\, \mathbf{E}(\mathbf{R}_N; \mathbf{x}) \tag{17}$$

where Z_N is the charge of the N'th nucleus.

The static and response components of potential and field due to the electronic part of the quantum partition are not treated separately, but are implicitly handled through the electronic density (the nuclei have a static contribution only). Because of the expansion procedure, the evaluation of the potential and field due to the electronic part of the quantum partition is a simple contraction of the density with the potential and field due to unit occupation of the charge distributions at the expansion centres:

$$V_{el}^{qm}(\mathbf{x}) = -e \sum_{ij} d_{ij} \left\{ S_{ij}\left[f^V V(\mathbf{r}_a; \mathbf{x}) - f^E \mathbf{E}(\mathbf{r}_a; \mathbf{x})\cdot \mathbf{r}_a \right] + f^E \mathbf{M}_{ij}\cdot \mathbf{E}(\mathbf{r}_a; \mathbf{x}) \right\} \tag{18}$$

$$\mathbf{E}_{el}^{qm}(\mathbf{x}) = -e \sum_{ij} d_{ij} \left\{ S_{ij}\left[f^E \mathbf{E}(\mathbf{r}_a; \mathbf{x}) + f^T \mathbb{T}(\mathbf{r}_a; \mathbf{x})\cdot \mathbf{r}_a \right] - f^T \mathbb{T}(\mathbf{r}_a; \mathbf{x})\cdot \mathbf{M}_{ij} \right\} \tag{19}$$

where a denotes the expansion centre to which the ij'th charge distribution has been assigned, and d_{ij} is the one-particle density matrix element of the ij'th charge distribution. The screening function f^T for a conical charge distribution is defined as:

$$f^T = f^T(|\mathbf{x}-\mathbf{r}_a|, \alpha_a, \alpha_x) = \begin{cases} -v^4 + 4v^3\,\delta_{\beta\gamma}; & |\mathbf{x}-\mathbf{r}_a| \le 1.662\,(\alpha_a\,\alpha_{\mathbf{x}})^{1/6} \\ 1; & |\mathbf{x}-\mathbf{r}_a| > 1.662\,(\alpha_a\,\alpha_{\mathbf{x}})^{1/6} \end{cases} \tag{20}$$

where the subscripts β and γ denote x,y,z. For an exponential charge distribution f^T is defined as:

$$f^T(|\mathbf{x}-\mathbf{r}_a|, \alpha_a, \alpha_x) = \left(3 + \delta_{\beta\gamma}\right) f^E - \frac{1}{2}(a\ v)^3 \exp(-a\ v) \tag{21}$$

Response Potentials and Fields 2.4

THE RESPONSE POTENTIALS and fields from the discrete classical partition are mediated through dipoles that are induced in the partition. An induced dipole is the result of the action of an electric field due to the rest of the system at the position of a dipole polarizability. The polarizability of the discrete classical partition as a whole is represented by distributed dipole polarizabilities, analogous to the distributed monopole representation for the static potential. Note that the charge density and the polarizability are two independent properties of a system, so that the construction of charge and polarizability representations are independent problems. (For a discussion of the polarizability representation, refer to section 1.4.) The response potential and field at **x**, due to the discrete classical partition take the form:

$$V_{\mu}^{dcl}(\mathbf{x}) = \sum_{p \neq G(\mathbf{x})} f^{E}(|\mathbf{x} - \mathbf{r}_p|, \alpha_p, \alpha_x)\, \mu_p \cdot \mathbf{E}(\mathbf{r}_p; \mathbf{x}) \tag{22}$$

$$\mathbf{E}_{\mu}^{dcl}(\mathbf{x}) = - \sum_{p \neq G(\mathbf{x})} f^{T}(|\mathbf{x} - \mathbf{r}_p|, \alpha_p, \alpha_x)\, \mathbb{T}(\mathbf{r}_p; \mathbf{x}) \cdot \mu_p \tag{23}$$

where μ_p is the induced dipole at p. Note that p may or may not coincide with a discrete classical charge position.

The continuum contribution to the response potential is mediated through dipole and charge densities (the latter only with a finite ionic strength) on the boundary surface separating the discrete and continuum partitions. Because the surface is of arbitrary shape, analytic expressions[59, 60] for the induced densities do not exist, and one must resort to numerical recipes for representing the surface densities.[56-58] We use the so-called constant element representation, where the surface densities are assumed to be constant over a certain area of the surface. The total surface is built from a number of these areas, assumed to be planar, now to be called boundary elements (BEs). The dipole (and charge) densities are then reduced to discrete dipoles (and charges) located at representative points on the BEs.

The accuracy of the continuum contribution depends on the number of BEs. An optimum number of BEs has to be found, trading accuracy and numerical stability for computational effort. It is important for numerical accuracy in the matrix inversion (next section) that the surface is smooth and that the BEs have approximately the same size. This is best achieved with the use of Connolly's solvent accessible surface,[61] which is defined by the trace of the centre of a probe sphere that is rolled over (overlapping) spheres centred on the atoms (see also section 3.3). The formatted output of this program can be used directly. Other methods for manufacturing the surface are available;[56, 57] of these, the triangulation method by Juffer *et al.*[58] has been implemented in the present version of HONDO8.1. Further options provide for

the definition of a triangulated sphere, or a cube (for simple test systems) around the quantum and discrete classical partitions.

The expressions for the potential and field due to the induced surface dipoles ω and charges ζ are:

$$V^{cont}(\mathbf{x}) = \sum_I \left\{ K(\varepsilon, \kappa, \mathbf{n}_I, \mathbf{r}_I; \mathbf{x})\, \omega_I + L(\kappa, \mathbf{r}_I; \mathbf{x})\, \zeta_I \right\} S_I \tag{24}$$

$$\mathbf{E}^{cont}(\mathbf{x}) = \sum_I \left\{ -\ {}_{\mathbf{x}}K(\varepsilon, \kappa, \mathbf{n}_I, \mathbf{r}_I; \mathbf{x})\, \omega_I - {}_{\mathbf{x}}L(\kappa, \mathbf{r}_I; \mathbf{x})\, \zeta_I \right\} S_I \tag{25}$$

with K and L kernels dependent on the continuum parameters ε (the dielectric constant) and κ (inverse Debye screening length):

$$K(\varepsilon, \kappa, \mathbf{n}_I, \mathbf{r}_I; \mathbf{x}) = \left\{ \varepsilon \left[1 + \kappa |\, \mathbf{x} - \mathbf{r}_I \,| \right] \exp(-\kappa |\, \mathbf{x} - \mathbf{r}_I \,|) - 1 \right\} \mathbf{E}(\mathbf{r}_I; \mathbf{x}) \cdot \mathbf{n}_I \tag{26}$$

$$\begin{aligned} {}_{\mathbf{x}}K(\varepsilon, \kappa, \mathbf{n}_I, \mathbf{r}_I; \mathbf{x}) = {} & \left\{ \varepsilon \left[1 + \kappa |\, \mathbf{x} - \mathbf{r}_I \,| \right] \exp(-\kappa |\, \mathbf{x} - \mathbf{r}_I \,|) - 1 \right\} \mathbb{T}(\mathbf{r}_I; \mathbf{x}) \cdot \mathbf{n}_I \\ & - \varepsilon \kappa^2 \exp(-\kappa |\, \mathbf{x} - \mathbf{r}_I \,|)\, \mathbf{E}(\mathbf{r}_I; \mathbf{x}) \cdot \mathbf{n}_I (\mathbf{x} - \mathbf{r}_I) \end{aligned} \tag{27}$$

$$L(\kappa, \mathbf{r}_I; \mathbf{x}) = \left\{ 1 - \exp(-\kappa |\, \mathbf{x} - \mathbf{r}_I \,|) \right\} V(\mathbf{r}_I; \mathbf{x}) \tag{28}$$

$${}_{\mathbf{x}}L(\kappa, \mathbf{r}_I; \mathbf{x}) = \left\{ \left[1 + \kappa |\, \mathbf{x} - \mathbf{r}_I \,| \right] \exp(-\kappa |\, \mathbf{x} - \mathbf{r}_I \,|) - 1 \right\} \mathbf{E}(\mathbf{r}_I; \mathbf{x}) \tag{29}$$

S_I, $\mathbf{r}_I$ and $\mathbf{n}_I$ are the area, the representative point and the outward normal vector of the I'th boundary element, respectively. Note that the surface dipoles are oriented along the outward normal vector of the BEs, and that ω gives their scalar value.

Coupling the Partitions 2.5

THE COUPLING between the different partitions of the system is quite straightforward once the expressions for the induced discrete classical dipoles and surface dipoles and charges are known. The induced discrete classical dipoles are the result of the linear response to the actual field at the location of the polarizabilities:

$$\mu_p = \alpha_p \cdot \left\{ \left[\mathbf{E}_N^{qm}(\mathbf{r}_p) + \mathbf{E}_{el}^{qm}(\mathbf{r}_p) + \mathbf{E}_q^{dcl}(\mathbf{r}_p) \right] + \mathbf{E}_\mu^{dcl}(\mathbf{r}_p) + \mathbf{E}^{cont}(\mathbf{r}_p) \right\} \tag{30}$$

In the same way, the induced surface dipoles ω and charges ζ depend on the potential and field, respectively, at the representative BE points:

$$\omega_I = \frac{1}{2\pi(1+\varepsilon)} \left\{ \left[V_N^{qm}(\mathbf{r}_I) + V_{el}^{qm}(\mathbf{r}_I) + V_q^{dcl}(\mathbf{r}_I) \right] + V_\mu^{dcl}(\mathbf{r}_I) + V^{cont}(\mathbf{r}_I) \right\} \tag{31}$$

(where it is understood that the I'th element itself does not contribute to V^{cont});

$$\zeta_I = \frac{\varepsilon}{2\pi(1+\varepsilon)} \left\{ \begin{array}{l} -\left[\mathbf{E}_N^{qm}(\mathbf{r}_I) + \mathbf{E}_{el}^{qm}(\mathbf{r}_I) + \mathbf{E}_q^{dcl}(\mathbf{r}_I) \right] \cdot \mathbf{n}_I - \mathbf{E}_\mu^{dcl}(\mathbf{r}_I) \cdot \mathbf{n}_I \\ + \sum_{J \neq I} \left[M(\kappa, \mathbf{n}_I, \mathbf{n}_J, \mathbf{r}_J; \mathbf{r}_I)\, \omega_J + N(\varepsilon, \kappa, \mathbf{n}_I, \mathbf{r}_J; \mathbf{r}_I)\, \zeta_J \right] S_J \end{array} \right\} \tag{32}$$

where the kernels M and N are defined by:

$$M(\kappa, \mathbf{n}_I, \mathbf{n}_J, \mathbf{r}_J; \mathbf{r}_I) = \left[\begin{array}{l} \left\{ [1 + \kappa |\mathbf{r}_I - \mathbf{r}_J|] \exp(-\kappa |\mathbf{r}_I - \mathbf{r}_J|) - 1 \right\} (\mathbb{T}(\mathbf{r}_J; \mathbf{r}_I) \cdot \mathbf{n}_J) \\ \quad - \kappa^2 \exp(-\kappa |\mathbf{r}_I - \mathbf{r}_J|) (\mathbf{E}(\mathbf{r}_J; \mathbf{r}_I) \cdot \mathbf{n}_J)(\mathbf{r}_I - \mathbf{r}_J) \end{array} \right] \cdot \mathbf{n}_I \tag{33}$$

$$N(\varepsilon, \kappa, \mathbf{n}_I, \mathbf{r}_J; \mathbf{r}_I) = \left\{ \frac{1}{\varepsilon} [1 + \kappa |\mathbf{r}_I - \mathbf{r}_J|] \exp(-\kappa |\mathbf{r}_I - \mathbf{r}_J|) - 1 \right\} \mathbf{E}(\mathbf{r}_J; \mathbf{r}_I) \cdot \mathbf{n}_I \tag{34}$$

At this point, note that a self-consistent solution of the induced classical dipoles and surface dipoles and charges may be calculated, given any input potential and field [in eq. (31): $V^0 = V_N^{qm} + V_{el}^{qm} + V_q^{dcl}$], by solving a set of coupled linear equations, that may be cast into matrix form:[120, 124]

$$\begin{pmatrix} \alpha_p^{-1} + \mathbb{T}'_{qp} & {}_p\mathbb{K}_{Ip}\,\mathbf{S}_I & {}_p\mathbb{L}_{Ip}\,\mathbf{S}_I \\ \frac{-1}{2\pi(1+\varepsilon)}\mathbb{E}_{pI} & \mathbb{1} - \frac{\mathbb{K}'_{JI}\,\mathbf{S}_J}{2\pi(1+\varepsilon)} & -\frac{\mathbb{L}'_{JI}\,\mathbf{S}_J}{2\pi(1+\varepsilon)} \\ \frac{-\varepsilon}{2\pi(1+\varepsilon)}\mathbb{T}_{pI}\cdot\mathbf{N}_I & -\frac{\varepsilon\,\mathbb{M}'_{JI}\,\mathbf{S}_J}{2\pi(1+\varepsilon)} & \mathbb{1} - \frac{\varepsilon\,\mathbb{N}'_{JI}\,\mathbf{S}_J}{2\pi(1+\varepsilon)} \end{pmatrix} \begin{pmatrix} \mathbf{M} \\ \Omega \\ Z \end{pmatrix} = \begin{pmatrix} \mathbf{E}_p^0 \\ \frac{1}{2\pi(1+\varepsilon)}\mathbf{V}_I^0 \\ \frac{-\varepsilon}{2\pi(1+\varepsilon)}\mathbf{E}_I^0\cdot\mathbf{N}_I \end{pmatrix} \tag{35}$$

or $\mathbb{R}\mathbf{i}=\mathbf{s}^0$. Subscripts have been added for clarity. The primes denote exclusion of the elements with identical subscripts, and the source potentials and fields have been labelled by a superscript 0. $\mathbf{N}_I$ is the super-vector containing all BE outward normal vectors. By inverting the coupling matrix $\mathbb{R}$, usually called relay matrix, the induced moments may be found: $\mathbf{i}=\mathbb{R}^{-1}\,\mathbf{s}^0$. In practice, the solution of the linear coupling equations is achieved in two steps through the LU-decomposition scheme.[125] This procedure has a great advantage over an iterative procedure,[62] in which the induced moments due to the input field are calculated first, followed by the response field due to the induced moments elsewhere in the system, which results in an updated field and updated moments, etc. In the LU-decomposition scheme the relay matrix needs to be built and decomposed only once for a given geometry, ε, and κ, after which it can be used to get the self-consistent induced moments in the classical partitions for *any* source field. Of course, for very large problems (the order of the relay matrix is maximally $3\times N_{pol} + 2\times N_{BE}$, where N_{pol} is the number of polarizabilities and N_{BE} the number of boundary elements) it may be cumbersome (or even impossible) to store and LU-decompose the large relay matrix. For this reason, we intend to also implement the iterative procedure, which requires a minimum amount of memory.

The formulation of the coupling given here for the continuum contribution is the linearized version of the Poisson–Boltzmann equations. If κ=0, one may choose between surface dipoles and surface charges for the representation of the continuum contribution to the reaction field. The representations are equivalent, only numerical accuracy is much better for the surface dipole representation, because the inhomogeneity over the BEs of the inducing potential is smaller.[58] Therefore we have chosen to use the surface dipoles when κ=0. In that case the relay matrix is reduced to the top-left blocks. In the absence of a continuum, only the $(\mathbb{a}^{-1} + \mathbb{T}')$-block of the relay matrix is retained. Alternatively, in the absence of a discrete classical part the relay matrix consists only of the $(\mathbb{1} - \mathbb{K}\mathbf{S})$-block (if κ=0).

In the present model three types of source fields may be distinguished: those from the nuclei, those from the electrons, and those from the external charges, as is made explicit in eqs. (30)-(32). Because of the linearity, the source fields may be treated either separately or summed. By treating them separately, different energy contributions may be identified. As an example, consider the nuclear interaction energy, which is given by:

$$\Delta U_{nuc} = \sum_M Z_M \left\{ \frac{1}{2} V_N^{qm}(\mathbf{R}_M) + \mathbf{v}^R(\mathbf{R}_M)^\dagger \, \mathbb{R}^{-1} \, \mathbf{v}_N^{S,qm} \right\} \tag{36}$$

$\mathbf{v}^S$ and $\mathbf{v}^R$ are super-vectors containing the source fields and reaction potentials, respectively. In this case $\mathbf{v}_N^{S,qm}$ contains the source fields due to all nuclei at the polarizabilities and BEs, and $\mathbf{v}^R(\mathbf{R}_M)$ the reaction potential at nucleus M, due to unit induced moments at the polarizabilities and / or BEs:

$$\mathbf{v}_{\mathrm{N}}^{\mathrm{S},qm} = \begin{pmatrix} \mathbf{E}_{\mathrm{N}}^{qm}(\mathbf{r}_{\mathrm{p}}) \\ \vdots \\ \frac{1}{2\pi(1+\varepsilon)} \mathrm{V}_{\mathrm{N}}^{qm}(\mathbf{r}_{\mathrm{I}}) \\ \vdots \\ \frac{-\varepsilon}{2\pi(1+\varepsilon)} \mathbf{E}_{\mathrm{N}}^{qm}(\mathbf{r}_{\mathrm{I}}) \cdot \mathbf{n}_{\mathrm{I}} \\ \vdots \end{pmatrix}; \qquad \mathbf{v}^{\mathrm{R}}(\mathbf{R}_{\mathrm{M}}) = \begin{pmatrix} \mathbf{E}(\mathbf{r}_{\mathrm{p}}; \mathbf{R}_{\mathrm{M}}) \\ \vdots \\ \mathrm{K}(\mathbf{r}_{\mathrm{I}}; \mathbf{R}_{\mathrm{M}}) \\ \vdots \\ \mathrm{L}(\mathbf{r}_{\mathrm{I}}; \mathbf{R}_{\mathrm{M}}) \\ \vdots \end{pmatrix} \tag{37}$$

Thus $\mathbf{v}^{\mathrm{R}}(\mathbf{x})^{\dagger}\, \mathbb{R}^{-1}\, \mathbf{v}^{\mathrm{S}}$ in eq. (36) is the sum of the response potentials $\mathbf{v}^{\mathrm{R}}(\mathbf{x})$ at the given point in space $\mathbf{x}$ from the self-consistent solution of the induced moments $\mathbf{i}=\mathbb{R}^{-1}\, \mathbf{v}^{\mathrm{S}}$, due to the given source field $\mathbf{v}^{\mathrm{S}}$. Note the implicit double summation over all polarizabilities and BEs in this notation. The factor $1/2$ in the first term of eq. (36) accounts for the double counting. The second term is the interaction of the nuclei through the polarizable environment. Its effect is to weaken the repulsion between the nuclei, and is therefore often called the screening of the nuclear repulsion. In eq. (36), the cost to make the induced dipoles (the polarization energy) has not yet been accounted for. When the system is at equilibrium, this cost equals exactly half the stabilization energy, i.e. the energy gained by the interaction with the polarizable environment.[52] Expressions for all energy contributions are given in the Appendix (section 2.10).

Finally, let us turn to the electronic density, which is determined by the Fock equations, accounting for the nuclear, electronic, and external static and response potentials. For a closed-shell RHF wave function, the Fock matrix is, in the atomic basis [cf. eq. (1.20)]:

$$\mathrm{F}_{\mathrm{ij}} = \left\langle \mathrm{i} \middle| \mathrm{h}^{0} + \mathrm{h}^{\mathrm{Stat}} + \mathrm{h}^{\mathrm{R}} \middle| \mathrm{j} \right\rangle + \sum_{\mathrm{kl}} \mathrm{d}_{\mathrm{kl}} \left\langle \mathrm{ij} \middle| \mathrm{g}^{0} + \mathrm{g}^{\mathrm{R}} \middle| \mathrm{kl} \right\rangle \tag{38}$$

where $\mathrm{d}_{\mathrm{kl}} = \sum_{\mathrm{i}}^{\mathrm{occ}} 2\, c_{\mathrm{ki}}^{*}\, c_{\mathrm{li}}$ is the kl'th density matrix element. The regular expressions for h^0 and g^0 are evaluated exactly (using the standard code):

$$\mathrm{h}^{0} = -\frac{1}{2} \nabla^{2} - e\, \mathrm{V}_{\mathrm{N}}^{qm}(\mathbf{r}) \tag{39}$$

$$\mathrm{g}^{0} = \left(1 - \frac{1}{2} \mathrm{P}_{12}\right) \frac{e^{2}}{\mathrm{r}_{12}} \tag{40}$$

whereas the external and reaction field integrals are all expanded. Below we give the expanded operators, and explain each term. The electronic charge has been left explicit in these formulas for reasons of clarity.

The expanded static external potential operator is given by:

$$\mathrm{h}^{\mathrm{Stat}} = -e \left[\mathrm{V}_{\mathrm{q}}^{dcl}(\mathbf{r}_a) + \mathbf{E}_{\mathrm{q}}^{dcl}(\mathbf{r}_a) \cdot \mathbf{r}_a - \mathbf{E}_{\mathrm{q}}^{dcl}(\mathbf{r}_a) \cdot \mathbf{r} \right] \tag{41}$$

and describes the effect of the external charges on the electronic density. It is understood that $\mathbf{r}_a$ is the expansion centre to which the ij'th charge distribution is assigned. The one-electron response terms may be distinguished according to their origin:

$$h^R = h^R_{dcl} + h^R_N + h^R_{el} \tag{42}$$

The first term describes the effect of the induced moments due to the discrete classical charges' source field:

$$h^R_{dcl} = -e\left[\, \mathbf{v}^R(\mathbf{r}_a) + \mathbb{e}^R(\mathbf{r}_a)\cdot\mathbf{r}_a - \mathbb{e}^R(\mathbf{r}_a)\cdot\mathbf{r}\,\right]^\dagger \mathbb{R}^{-1}\,\mathbf{v}^{S,dcl}_q \tag{43}$$

where $\mathbb{e}^R(\mathbf{r}_a) = -\,_{\mathbf{r}_a}\mathbf{v}^R(\mathbf{r}_a)$ is the super-matrix containing the vector derivatives of the response potentials [eq. (37)] at expansion centre $\mathbf{r}_a$. This term may be seen as a static contribution as well, as it originates from the interaction between the classical partitions only, before any interaction with the quantum-mechanical partition. The second term originates from the response potential due to the nuclear source field:

$$h^R_N = -e\left[\, \mathbf{v}^R(\mathbf{r}_a) + \mathbb{e}^R(\mathbf{r}_a)\cdot\mathbf{r}_a - \mathbb{e}^R(\mathbf{r}_a)\cdot\mathbf{r}\,\right]^\dagger \mathbb{R}^{-1}\,\mathbf{v}^{S,qm}_N \tag{44}$$

The third term contains the response due to the electronic density at the classical charges and the nuclei, as well as at the electrons themselves:

$$h^R_{el} = h^{R,dcl}_{el} + h^{R,N}_{el} + \gamma h^{R,self}_{el} \tag{45}$$

where γ is a scaling parameter to be discussed shortly.

$$h^{R,dcl}_{el} = -e\left[\, \sum_p q_p\,\mathbf{v}^R(\mathbf{r}_p)\,\right]^\dagger \mathbb{R}^{-1}\left[\, \mathbf{v}^S_a - \mathbb{e}^S_a\cdot\mathbf{r}_a + \mathbb{e}^S_a\cdot\mathbf{r}\,\right] \tag{46}$$

$$h^{R,N}_{el} = -e\left[\, \sum_N Z_N\,\mathbf{v}^R(\mathbf{R}_N)\,\right]^\dagger \mathbb{R}^{-1}\left[\, \mathbf{v}^S_a - \mathbb{e}^S_a\cdot\mathbf{r}_a + \mathbb{e}^S_a\cdot\mathbf{r}\,\right] \tag{47}$$

$$h^{R,self}_{el} = \frac{e^2}{2}\left[\, \mathbf{v}^R(\mathbf{r}_a) + \mathbb{e}^R(\mathbf{r}_a)\cdot\mathbf{r}_a - \mathbb{e}^R(\mathbf{r}_a)\cdot\mathbf{r}'\,\right]^\dagger \mathbb{R}^{-1}\left[\, \mathbf{v}^S_a - \mathbb{e}^S_a\cdot\mathbf{r}_a + \mathbb{e}^S_a\cdot\mathbf{r}\,\right] \tag{48}$$

where $\mathbb{e}^S$ is defined as $-\,_{\mathbf{r}_a}\mathbf{v}^S$. Note that $\mathbf{v}^S_a$ is the super-vector for the source fields due to a *unit* charge at expansion centre $\mathbf{r}_a$, and $\mathbb{e}^S_a$ similarly for a dipole. In eq. (48) the factor $1/2$ accounts for the polarization energy cost included in this term. There can be no non-equilibrium contribution for this term (as it is coupled to the electronic response only). Eqs. (46) and (47) are the reverse terms of eqs. (43) and (44), respectively.

Finally, the two-electron reaction field operator g^R for a closed-shell RHF wave function is given by:

$$g^R = e^2\left(\, 1 - \frac{\gamma}{2}\,P_{12}\,\right)\times\left[\, \mathbf{v}^R(\mathbf{r}_a) + \mathbb{e}^R(\mathbf{r}_a)\cdot\mathbf{r}_a - \mathbb{e}^R(\mathbf{r}_a)\cdot\mathbf{r}(1)\,\right]^\dagger \mathbb{R}^{-1}\left[\, \mathbf{v}^S_b - \mathbb{e}^S_b\cdot\mathbf{r}_b + \mathbb{e}^S_b\cdot\mathbf{r}(2)\,\right] \tag{49}$$

Note that now, in contrast to eq. (48), there are *two* expansion centres: in the first term $\mathbf{r}_a$ for the ij'th charge distribution and $\mathbf{r}_b$ for the kl'th; in the second $\mathbf{r}_a$ for the ik'th charge distribution and $\mathbf{r}_b$ for the jl'th, respectively. The scaling parameter γ is the same as in eq. (45). It serves to switch between the average ($\gamma=0$) and direct ($0<\gamma\leq1$) reaction-field approaches. As was discussed in the introduction, in the ARF approach the reaction field is induced by the average field of the quantum partition (meaning the electronic part of it), whereas in the DRF approach the reaction-field operators are included in the Hamiltonian, so the electrons 'feel' their reaction fields instantaneously. The latter has the advantages that the total energy can be expressed as the expectation value of the Hamiltonian,[29] and that an *estimate* of the dispersion interaction between quantum and classical partition may be given.[29, 55, 102] In the DRF approach, γ serves as a scaling parameter which can be derived from comparing the second order perturbation expression for the dispersion energy to the self and exchange RF contributions [eqs. (48) and (49, second term)—see also section 3.2]. It is connected to the excitation energies of the quantum and classical partitions ($\gamma=0.5$ if the spectra of the quantum and classical partitions are identical).

The static and response potentials may be added to the Hamiltonian at will, generating a variety of approaches: the static potential may be treated self-consistently allowing the electronic density to adapt, later adding the RF contributions as a perturbation; or the RF may be treated self-consistently as well, by including it in the Hamiltonian, whether average or direct. The expressions for RF operators are the same for the UHF wave function. However, the Fock matrix is different, because of the separate treatment of α- and β-spin orbitals. For ROHF and GVB wave functions coupling coefficients should be inserted into the two-electron terms according to the state of interest; otherwise, the given RF operators apply. If the RF contributions are put into the two-electron integrals prior to the SCF procedure (see below), the program handles the coupling automatically.

For post-HF calculations (CI, MCSCF), only the ARF option can be applied easily, because it needs the density only,[30, 74, 83] and it has been implemented in the present code. The screening of the self-interactions cannot be calculated straightforwardly, nor can the RF interactions be put into the Hamiltonian, as for the HF wave functions.

Formal Reaction Field Interactions and Integrals 2.6

BECAUSE THE SOURCE AND REACTION FIELDS due to and at the quantum partition are expanded, it suffices to solve the coupling equations [eq. (35)] only a limited number of times, namely for unit charges and dipoles located at the expansion centres, and once for the collection of external charges. The potentials and fields of the induced moments are coupled back to charges and dipoles at the expansion centres, to give unit RF interactions between expansion centres. These formal interactions may then be contracted with the zeroth, first, and (if $\gamma \neq 0$) second moment integrals to get the RF Fock matrix elements, and consequently with the density to obtain the actual RF contributions to the energy. The formal RF interactions between expansion centres are collected in the super-matrix $\mathbb{\Omega}$:

$$\mathbb{\Omega}_{ba} = \begin{pmatrix} -\mathbb{e}^{R}(\mathbf{r}_b) \\ \mathbf{v}^{R}(\mathbf{r}_b) + \mathbb{e}^{R}(\mathbf{r}_b)\cdot\mathbf{r}_b \end{pmatrix}^{\dagger} \mathbb{R}^{-1} \begin{pmatrix} \mathbb{e}^{S}_{a} \\ \mathbf{v}^{S}_{a} - \mathbb{e}^{S}_{a}\cdot\mathbf{r}_a \end{pmatrix} \tag{50}$$

where $\mathbb{\Omega}_{ba}$ is a 4×4 matrix containing the RF contributions of a unit dipole and charge source at $\mathbf{r}_a$, at a unit dipole and charge at $\mathbf{r}_b$. The dimension of $\mathbb{\Omega}$ is thus $4N_{exp}\times 4N_{exp}$, with N_{exp} the number of expansion centres. $\mathbb{\Omega}$ may be augmented by two rows and columns, containing the formal RF interaction of a unit dipole and charge at the expansion centres with all external charges and nuclei, respectively. Consider e.g. the RF contribution to the nuclear attraction energy (also called the screening of the nuclear attraction):

$$\Delta U^{snua} = -e \sum_{ij} d_{ij} \left\{ \sum_{N} \left[\begin{pmatrix} \mathbf{M}_{ij} \\ S_{ij} \end{pmatrix}^{\dagger} \mathbb{\Omega}_{an} Z_N \begin{pmatrix} \mathbf{M}_N \\ 1 \end{pmatrix} + Z_N \begin{pmatrix} \mathbf{M}_N \\ 1 \end{pmatrix}^{\dagger} \mathbb{\Omega}_{na} \begin{pmatrix} \mathbf{M}_{ij} \\ S_{ij} \end{pmatrix} \right] \right\} \tag{51}$$

with *n* denoting the expansion centre at which the N'th nucleus is located, and $\mathbf{M}_N$ is the dipole vector of the N'th nucleus w.r.t. the origin. The summation over the nuclei may be carried out first, using a limited part of $\mathbb{\Omega}$ only (because of the zeros), producing a column and row vector, which may be added to $\mathbb{\Omega}$.

$$\Omega_{aN} = \sum_{N} \left[\mathbb{\Omega}_{an} Z_N \begin{pmatrix} \mathbf{M}_N \\ 1 \end{pmatrix} \right]; \qquad \Omega^{\dagger}_{Na} = \sum_{N} \left[Z_N \begin{pmatrix} \mathbf{M}_N \\ 1 \end{pmatrix}^{\dagger} \mathbb{\Omega}_{na} \right] \tag{52}$$

and eq. (51) simplifies to:

$$\Delta U^{snua} = -e \sum_{ij} d_{ij} \left\{ \begin{pmatrix} \mathbf{M}_{ij} \\ S_{ij} \end{pmatrix}^{\dagger} \Omega_{aN} + \Omega^{\dagger}_{Na} \begin{pmatrix} \mathbf{M}_{ij} \\ S_{ij} \end{pmatrix} \right\} \tag{53}$$

Because the bracketed expression can be evaluated before entering the SCF procedure, it may be included in the one-electron Fock matrix elements. In practice, Ω_{aN}

and $\Omega_{Na}^{\dagger}$ are calculated by first summing the source fields and reaction potentials [eq. (37)], respectively, before solving the coupling equations:

$$\Omega_{aN} = \begin{pmatrix} -\mathbb{e}^{\mathrm{R}}(\mathbf{r}_a) \\ \mathbf{v}^{\mathrm{R}}(\mathbf{r}_a) + \mathbb{e}^{\mathrm{R}}(\mathbf{r}_a)\cdot\mathbf{r}_a \end{pmatrix}^{\dagger} \mathbb{R}^{-1}\mathbf{v}_{\mathrm{N}}^{\mathrm{S},\,qm} \tag{54}$$

$$\Omega_{Na}^{\dagger} = \left[\mathbf{v}_{\mathrm{N}}^{\mathrm{R},\,qm}\right]^{\dagger}\mathbb{R}^{-1}\begin{pmatrix} \mathbb{e}_a^{\mathrm{S}} \\ \mathbf{v}_a^{\mathrm{S}} - \mathbb{e}_a^{\mathrm{S}}\cdot\mathbf{r}_a \end{pmatrix} = \left[\sum_{\mathrm{M}} Z_{\mathrm{M}}\,\mathbf{v}^{\mathrm{R}}(\mathbf{R}_{\mathrm{M}})\right]^{\dagger}\mathbb{R}^{-1}\begin{pmatrix} \mathbb{e}_a^{\mathrm{S}} \\ \mathbf{v}_a^{\mathrm{S}} - \mathbb{e}_a^{\mathrm{S}}\cdot\mathbf{r}_a \end{pmatrix} \tag{55}$$

The same is done for the discrete classical charges, constructing $\mathbf{v}_{\mathrm{q}}^{\mathrm{R},dcl}$, Ω_{aQ} and $\Omega_{Qa}^{\dagger}$. This procedure is advantageous because of the great reduction in the number of times the coupling equations need to be solved and is achievable because of the linearity of the coupling problem. Furthermore, the number of input-field super-vectors $\mathbf{v}^{\mathrm{S}}$ and reaction-field super-vectors $\mathbf{v}^{\mathrm{R}}$ (to be stored for later use) is greatly reduced. Expressions similar to eq. (53) can be obtained for the other one-electron reaction-field contributions, and they are given in the Appendix. The screening of the electronic self-interaction is also a one-electron term, but is a little bit different from the ones discussed so far:

$$\Delta U_{\mathrm{el}}^{self} = \frac{\gamma e^2}{2}\sum_{\mathrm{ij}} \mathrm{d}_{\mathrm{ij}}\left\{\sum_{\alpha,\beta=1}^{4}\left(\mathbb{M}_{\mathrm{ij}}^{\dagger}\right)_{\alpha\beta}\left(\mathbb{Q}_{aa}\right)_{\alpha\beta}\right\};\ \mathbb{M}_{\mathrm{ij}} = \begin{pmatrix} \mathbb{Q}_{\mathrm{ij}} & \mathbf{M}_{\mathrm{ij}} \\ \mathbf{M}_{\mathrm{ij}}^{\dagger} & \mathrm{S}_{\mathrm{ij}} \end{pmatrix} \tag{56}$$

where $\mathbb{Q}_{\mathrm{ij}}$ is a 3×3 matrix, containing the second moment integrals of the ij'th charge distribution: $\left(\mathbb{Q}_{\mathrm{ij}}\right)_{\alpha\beta} = \langle\, \mathrm{i}\,|\,\mathbf{r}\,\mathbf{r}^{\dagger}|\,\mathrm{j}\,\rangle_{\alpha\beta}$, where $\alpha,\beta \in \{x,y,z\}$. Again, the bracketed expression may be evaluated prior to the SCF procedure.

The two-electron RF terms in eq. (38) may be calculated on the fly in each iteration, or be included in the two-electron integrals prior to the SCF in a similar fashion as the one-electron RF terms can be included in the Fock matrix. Consider the J- and K-like RF integrals:

$$\begin{aligned} \mathrm{J}_{\mathrm{ijkl}}^{\mathrm{R}} &= e^2\left\{\begin{pmatrix} \mathbf{M}_{\mathrm{ij}} \\ \mathrm{S}_{\mathrm{ij}} \end{pmatrix}^{\dagger}\mathbb{Q}_{ab}\begin{pmatrix} \mathbf{M}_{\mathrm{kl}} \\ \mathrm{S}_{\mathrm{kl}} \end{pmatrix} + \begin{pmatrix} \mathbf{M}_{\mathrm{kl}} \\ \mathrm{S}_{\mathrm{kl}} \end{pmatrix}^{\dagger}\mathbb{Q}_{ba}\begin{pmatrix} \mathbf{M}_{\mathrm{ij}} \\ \mathrm{S}_{\mathrm{ij}} \end{pmatrix}\right\}; \\ \mathrm{K}_{\mathrm{ijkl}}^{\mathrm{R}} &= \gamma e^2\left\{\begin{pmatrix} \mathbf{M}_{\mathrm{ik}} \\ \mathrm{S}_{\mathrm{ik}} \end{pmatrix}^{\dagger}\mathbb{Q}_{cd}\begin{pmatrix} \mathbf{M}_{\mathrm{jl}} \\ \mathrm{S}_{\mathrm{jl}} \end{pmatrix} + \begin{pmatrix} \mathbf{M}_{\mathrm{jl}} \\ \mathrm{S}_{\mathrm{jl}} \end{pmatrix}^{\dagger}\mathbb{Q}_{dc}\begin{pmatrix} \mathbf{M}_{\mathrm{ik}} \\ \mathrm{S}_{\mathrm{ik}} \end{pmatrix}\right\} \end{aligned} \tag{57}$$

where c and d denote the expansion centres to which the ik'th and jl'th overlap distributions are assigned, respectively. If $\gamma=1$, $\mathrm{K}^{\mathrm{R}}_{\mathrm{ijkl}}=\mathrm{J}^{\mathrm{R}}_{\mathrm{ikjl}}$, as for the vacuum J- and K-integrals,[101] and the two-electron RF contributions may be added to the vacuum integrals because all two-electron integrals to be computed are of the form:

$$\langle\, \mathrm{ij}\,|\,\mathrm{kl}\,\rangle' = \langle\, \mathrm{ij}\,|\,\mathrm{kl}\,\rangle + e^2\left\{\begin{pmatrix} \mathbf{M}_{\mathrm{ij}} \\ \mathrm{S}_{\mathrm{ij}} \end{pmatrix}^{\dagger}\mathbb{Q}_{ab}\begin{pmatrix} \mathbf{M}_{\mathrm{kl}} \\ \mathrm{S}_{\mathrm{kl}} \end{pmatrix} + \begin{pmatrix} \mathbf{M}_{\mathrm{kl}} \\ \mathrm{S}_{\mathrm{kl}} \end{pmatrix}^{\dagger}\mathbb{Q}_{ba}\begin{pmatrix} \mathbf{M}_{\mathrm{ij}} \\ \mathrm{S}_{\mathrm{ij}} \end{pmatrix}\right\} \tag{58}$$

enabling the scaling according to the coincidences among the two-electron integral indices applied in HONDO. If $\gamma \neq 1$, however, this formalism may not be employed, since the relation $K^R_{ijkl}=J^R_{ikjl}$ no longer holds. However, the super-matrix formalism can be employed with any value of γ, as can be seen from the form of its elements:

$$
\begin{aligned}
P'_{ijkl} &= \langle ij \mid kl \rangle + e^2 \left\{ \begin{pmatrix} \mathbf{M}_{ij} \\ S_{ij} \end{pmatrix}^{\dagger} \mathbb{\Omega}_{ab} \begin{pmatrix} \mathbf{M}_{kl} \\ S_{kl} \end{pmatrix} + \begin{pmatrix} \mathbf{M}_{kl} \\ S_{kl} \end{pmatrix}^{\dagger} \mathbb{\Omega}_{ba} \begin{pmatrix} \mathbf{M}_{ij} \\ S_{ij} \end{pmatrix} \right\} \\
&- \frac{1}{4} \left[\begin{array}{l} \langle ik \mid jl \rangle + \gamma e^2 \left\{ \begin{pmatrix} \mathbf{M}_{ik} \\ S_{ik} \end{pmatrix}^{\dagger} \mathbb{\Omega}_{cd} \begin{pmatrix} \mathbf{M}_{jl} \\ S_{jl} \end{pmatrix} + \begin{pmatrix} \mathbf{M}_{jl} \\ S_{jl} \end{pmatrix}^{\dagger} \mathbb{\Omega}_{dc} \begin{pmatrix} \mathbf{M}_{ik} \\ S_{ik} \end{pmatrix} \right\} + \\ \langle il \mid kj \rangle + \gamma e^2 \left\{ \begin{pmatrix} \mathbf{M}_{il} \\ S_{il} \end{pmatrix}^{\dagger} \mathbb{\Omega}_{ef} \begin{pmatrix} \mathbf{M}_{kj} \\ S_{kj} \end{pmatrix} + \begin{pmatrix} \mathbf{M}_{kj} \\ S_{kj} \end{pmatrix}^{\dagger} \mathbb{\Omega}_{fe} \begin{pmatrix} \mathbf{M}_{il} \\ S_{il} \end{pmatrix} \right\} \end{array} \right]
\end{aligned}
\tag{59}
$$

Similarly, for open shell problems, the K'_{ijkl} combination to be stored separately equals the second part of the expression given for P'_{ijkl}, so that RHF, UHF, ROHF and GVB wave functions can be treated with all RF options. If the RF is treated as a perturbation, and the ARF option is used, $\mathbb{\Omega}$ is not constructed, since then the source field of the total electron density is used, and the coupling equations need only be solved three times (instead of $4\times N_{exp}+2$): once for the external charges, once for the nuclei and once for the collected electrons.

Non-equilibrium Reaction Fields 2.7

THE NON-EQUILIBRIUM REACTION FIELDS are either mediated through the induced moments in equilibrium with another microstate (whether electronic or conformational) of the system, or coupled directly. In the former case, the induced moments are being stored, along with the polarization energy cost to induce these moments. The polarization energy equals half the stabilization energy if the system is at equilibrium with the polarization.[53] This option requires the geometry of the classical partitions to be the same for all quantum partition microstates. Alternatively, the equilibrium reaction potential at the expansion centres is stored, requiring the expansion centres to be appropriate for all quantum partition microstates to be considered.

The induced moments generate an external potential, which may be included in the one-electron terms of the Hamiltonian (in expanded form):

$$h^{R}_{neq} = - e \left[\mathbf{v}^{R}(\mathbf{r}_a) + \mathbb{e}^{R}(\mathbf{r}_a) \cdot \mathbf{r}_a - \mathbb{e}^{R}(\mathbf{r}_a) \cdot \mathbf{r} \right]^{\dagger} \begin{pmatrix} \mathrm{M} \\ \Omega \\ \mathrm{Z} \end{pmatrix}_{\mathrm{neq}} \tag{60}$$

For the calculation of excited electronic states it may be important to distinguish between electronic and orientational (static) response contributions of the continuum.[103-105] These responses are associated with different time-scales. The responses due to the electronic and orientational motions in the dielectric are not additive; to separate them one has to perform two calculations: one with the total dielectric constant ε_0, and one with the optical dielectric component ε_∞ only. The static response is defined as the difference between these two responses:

$$h^{R,\,stat}_{neq} = h^{R,\,\varepsilon_0}_{neq} - h^{R,\,\varepsilon_\infty}_{neq} \tag{61}$$

It will be clear that two sets of induced moments need to be stored in this case.

Monte Carlo Sampling 2.8

THE DEFINITION of groups in the discrete classical partition enables an easy and efficient way of generating an ensemble average over certain degrees of freedom in that partition, thus making a step in the direction of an integrated approach to thermodynamic properties within the framework of the combined quantum-mechanical–classical approach. Eventually, the scheme—which is the logical continuation of the work initiated by Rullmann and van Duijnen[98, 99]—may lead to a Molecular Dynamics type of program, combining quantum chemistry with all classically described reaction field options discussed in this paper. The combination of quantum and molecular mechanically treated subsystems has been the subject of a number of studies already.[64-69, 72, 73] The major task will be the development of a consistent force field, with a smooth transition between quantum-mechanically and classically described interactions, which is especially tasking for the short-range interactions. We have used a modified parameterization of the repulsive 12-term from CHARMM[126] between quantum and classical atoms, to avoid the quantum partition moving into the classical partition in geometry optimizations (see also section 3.2). The problem with this model potential is that the electrons do not 'feel' it, so the Pauli principle may be violated.

The sampling over the rotational and translational degrees of freedom of the discrete classical groups follows the standard Monte Carlo (MC) scheme: in each step, a group is selected, rotated around its centre of polarizability over a randomly chosen angle (within bounds), followed by a random translation along the Cartesian co-ordinates; the energy of the configuration is evaluated and compared to that of the previous step; if the energy is lower, the configuration is accepted; if not, it is accepted with such a probability as to ensure Boltzmann statistics over the ensemble.[6]

In practice, in each Monte Carlo step, V_q^{dcl} [eq. (10)] and $\mathbf{v}_q^{S,dcl}$ [cf. eq. (37)] are updated according to the move of the selected group. As far as the relay matrix is concerned, the diagonal 3×3 block, containing $\mathbb{\alpha}^{-1}$ of the rotated group requires updating, since the groups are rotated around the position of the group polarizability. Only that particular polarizability tensor changes with the rotation. If translation of the groups is allowed the coupling matrix elements along the rows and columns belonging to the updated group, and V_μ^{dcl} [eq. (22)] need updating as well. With the updated static and response fields, the energy of the system is recomputed, using an updated $\mathbb{\Omega}$ matrix if required, and the acceptance test is applied. If the new configuration is accepted, the updated fields and relay matrix replace those of the previous configuration.

Conclusion 2.9

BASED ON THE THEORETICAL DEVELOPMENT of partitioning the elementary particles in a dense medium into groups, a practicable computational scheme has been developed to numerically test the consequences of the theory, make useful conceptual analyses, and predict properties of new systems. The sheer number of particles considered in studying condensed phases implies the occurrence of an enormous amount of interactions between them. A computational study of such systems therefore requires the most advanced computational resources: the latest computer systems allow exploration of hitherto unattainable accuracy and detail, but are never quite up to the mark.

Nevertheless, sensible computational chemistry is not restricted to the 'super'-computers of our day: the (conceptually) simple models of Chapter 1 warrant meaningful computations even on personal computers. However, one should not only be interested in obtaining 'the right number'. The more detailed models and computations have provided, and must continue to provide, a justification and validation of the simpler representations and serve to find the answer to the question most prominent in every computational researcher's mind: did we 'get the right number for the right reason'?

Appendix 2.10

Formulas for the Static and Reaction Field Energy Contributions

For any (i.e. RHF, UHF, ROHF and GVB) wave function, the total energy expression may be analysed as:

$$\Delta U_{tot} = \Delta U_{clas} + \Delta U_{qm} + \Delta U_{int} + \Delta U_{pol} + \Delta U_{neq} + \Delta U_{disp} \tag{A.1}$$

The classical energy is:

$$\Delta U_{clas} = \Delta U_{elst}^{dcl} + \Delta U_{int}^{scee} + \Delta U_{disp}^{S\text{-}K} + \Delta U_{rep}^{CHARMM} \tag{A.2}$$

The first two terms are the classical electrostatic energy:

$$\Delta U_{elst}^{dcl} = \frac{1}{2} \sum_{p} q_p \, V_q^{dcl} \left(\mathbf{r}_p \right) \tag{A.3}$$

and the screening of the classical electrostatic energy, i.e. the interaction of the discrete classical charges with the polarizable environment:

$$\Delta U_{int}^{scee} = \left[\mathbf{v}_q^{R,\,dcl} \right]^{\dagger} \mathbb{R}^{-1} \, \mathbf{v}_q^{S,\,dcl} \tag{A.4}$$

where $\mathbf{v}_q^{R,\,dcl}$ is defined analogous to $\mathbf{v}_N^{R,\,qm}$ [eq. (55)]. The third term in eq. (A.2) is the dispersion interaction, as estimated by the Slater–Kirkwood formula,[127] employing either isotropic or anisotropic group polarizabilities, or distributed atomic polarizabilities. The last term is a reparameterized version of the pairwise additive, atom-based, 12-type model repulsion taken from the CHARMM force field.[126] Paramters may be found in Appendix 1 to Chapter 3 (section 3.7).

The second term in eq. (A.1):

$$\Delta U_{qm} = \Delta U_{nuc} + \Delta U_{el} + \Delta U_{nua} \tag{A.5}$$

is the energy of the quantum partition in vacuo, with the SCF density. The terms are well known:

$$\Delta U_{nuc} = \frac{1}{2} \sum_{M} Z_M \, V_N^{qm} \left(\mathbf{R}_M \right) \tag{A.6}$$

is the nuclear repulsion energy; for a closed-shell RHF function,

$$\Delta U_{el} = \Delta U_{el}^{kin} + \frac{e^2}{2} \sum_{ij,kl} d_{ij} \, d_{kl} \left\{ \langle ij \,|\, kl \rangle - \frac{1}{2} \langle ik \,|\, jl \rangle \right\} \tag{A.7}$$

is the vacuum electronic energy; and the nuclear attraction energy is:

$$\Delta U_{nua} = - e \sum_{ij} d_{ij} \left\langle i \left| V_N^{qm} (\mathbf{r}) \right| j \right\rangle \tag{A.8}$$

The interaction energy [the third term in eq. (A.1)] can be split into a static, an ambiguous and a response term:

$$\Delta U_{int} = \Delta U_{elst}^{int} + \Delta U_{amb}^{int} + \Delta U_{resp}^{int} \tag{A.9}$$

The electrostatic terms are clearly:

$$\Delta U_{elst}^{int} = \Delta U_{elst}^{N\text{-}dcl} + \Delta U_{elst}^{el\text{-}dcl} \tag{A.10}$$

where the electrostatic interaction between nuclei and external charges is:

$$\Delta U_{elst}^{N\text{-}dcl} = \sum_{p} q_p V_N^{qm} (\mathbf{r}_p) = \sum_{M} Z_M V_q^{dcl} (\mathbf{R}_M) \tag{A.11}$$

and the electrostatic interaction between electrons and external charges is:

$$\Delta U_{elst}^{el\text{-}dcl} = - e \sum_{ij} d_{ij} \left\{ S_{ij} \left[V_q^{dcl} (\mathbf{r}_a) + \mathbf{E}_q^{dcl} (\mathbf{r}_a) \cdot \mathbf{r}_a \right] - \mathbf{M}_{ij} \cdot \mathbf{E}_q^{dcl} (\mathbf{r}_a) \right\} \tag{A.12}$$

The ambiguous term arises from the (reaction) field induced by the discrete classical charges, if the classical partition is itself split up into interacting fragments. If the reference state is one in which this interaction is already accounted for before interaction with the quantum partition is allowed, this induced field can be regarded a static field with respect to the quantum system, and could by rights be added to the electrostatic term in the analysis. However, if the reference state is one where all partitions are non-interacting, this field is a true response component and could be added to the response term in the analysis. It is given by:

$$\Delta U_{amb}^{int} = \Delta U_{amb}^{class\text{-}N} + \Delta U_{amb}^{class\text{-}el} \tag{A.13}$$

where

$$\Delta U_{amb}^{class\text{-}N} = \left[\mathbf{v}_N^{R,\,qm} \right]^{\dagger} \mathbb{R}^{-1} \mathbf{v}_q^{S,\,dcl} \tag{A.14}$$

[$\mathbf{v}_N^{R,\,qm}$ has been defined in eq. (55)] and

$$\Delta U_{amb}^{class\text{-}el} = - e \sum_{ij} d_{ij} \begin{pmatrix} \mathbf{M}_{ij} \\ S_{ij} \end{pmatrix}^{\dagger} \Omega_{aQ} \quad ; \qquad \Omega_{aQ} = \begin{pmatrix} - \mathbb{e}^R (\mathbf{r}_a) \\ \mathbf{v}^R (\mathbf{r}_a) + \mathbb{e}^R (\mathbf{r}_a) \cdot \mathbf{r}_a \end{pmatrix}^{\dagger} \mathbb{R}^{-1} \mathbf{v}_q^{S,\,dcl} \tag{A.15}$$

The response term is given by:

$$\Delta U^{int}_{resp} = \Delta U^{N\text{-}class}_{RF} + \Delta U^{el\text{-}class}_{RF} + \Delta U^{snr} + \Delta U^{self}_{el} + \Delta U^{ste} + \Delta U^{snua} \tag{A.16}$$

with

$$\Delta U^{N\text{-}class}_{RF} = \left[\mathbf{v}^{R,\,dcl}_{q} \right]^{\dagger} \mathbb{R}^{-1}\, \mathbf{v}^{S,\,qm}_{N} \tag{A.17}$$

$$\Delta U^{el\text{-}class}_{RF} = -\,e \sum_{ij} d_{ij}\; \Omega^{\dagger}_{Qa} \begin{pmatrix} \mathbf{M}_{ij} \\ S_{ij} \end{pmatrix}; \qquad \Omega^{\dagger}_{Qa} = \left[\mathbf{v}^{R,\,dcl}_{q} \right]^{\dagger} \mathbb{R}^{-1} \begin{pmatrix} e^{S}_{a} \\ \mathbf{v}^{S}_{a} - e^{S}_{a} \cdot \mathbf{r}_{a} \end{pmatrix} \tag{A.18}$$

the interaction of the discrete classical partition with the RF induced by the nuclei and electrons, respectively. Furthermore,

$$\Delta U^{snr} = \left[\mathbf{v}^{R,\,qm}_{N} \right]^{\dagger} \mathbb{R}^{-1}\, \mathbf{v}^{S,\,qm}_{N} \tag{A.19}$$

is the screening of the nuclear repulsion,

$$\Delta U^{self}_{el} = \frac{\gamma e^{2}}{2} \sum_{ij} d_{ij} \left\{ \sum_{\alpha,\beta=1}^{4} \left(\mathbb{M}^{\dagger}_{ij} \right)_{\alpha\beta} \left(\mathbb{Q}_{aa} \right)_{\alpha\beta} \right\}; \; \mathbb{M}_{ij} = \begin{pmatrix} \mathbb{Q}_{ij} & \mathbf{M}_{ij} \\ \mathbf{M}^{\dagger}_{ij} & S_{ij} \end{pmatrix} \tag{A.20}$$

the screening of the electronic self energy,

$$\Delta U^{ste} = \Delta U^{ste}_{coul} - \Delta U^{ste}_{exch} \tag{A.21}$$

$$\Delta U^{ste}_{coul} = e^{2} \sum_{ij \le kl} d_{ij}\, d_{kl} \left[\begin{pmatrix} \mathbf{M}_{ij} \\ S_{ij} \end{pmatrix}^{\dagger} \mathbb{Q}_{ab} \begin{pmatrix} \mathbf{M}_{kl} \\ S_{kl} \end{pmatrix} + \begin{pmatrix} \mathbf{M}_{kl} \\ S_{kl} \end{pmatrix}^{\dagger} \mathbb{Q}_{ba} \begin{pmatrix} \mathbf{M}_{ij} \\ S_{ij} \end{pmatrix} \right] \tag{A.22}$$

$$\Delta U^{ste}_{exch} = \frac{\gamma e^{2}}{4} \sum_{ij \le kl} d_{ij}\, d_{kl} \left[\begin{pmatrix} \mathbf{M}_{ik} \\ S_{ik} \end{pmatrix}^{\dagger} \mathbb{Q}_{cd} \begin{pmatrix} \mathbf{M}_{jl} \\ S_{jl} \end{pmatrix} + \begin{pmatrix} \mathbf{M}_{jl} \\ S_{jl} \end{pmatrix}^{\dagger} \mathbb{Q}_{dc} \begin{pmatrix} \mathbf{M}_{ik} \\ S_{ik} \end{pmatrix} \right] \tag{A.23}$$

the screening of the two-electron Coulomb and exchange interactions, where the factor $1/4$ in eq. (A.23) is composed of a factor $1/2$ for double counting, and a factor $1/2$ for the inherent polarization energy cost, which is also present in the screening of the self energy [eq. (A.20)], recall the discussion of eq. (48). Finally:

$$\Delta U^{snua} = -\,e \sum_{ij} d_{ij} \left\{ \begin{pmatrix} \mathbf{M}_{ij} \\ S_{ij} \end{pmatrix}^{\dagger} \Omega_{aN} + \Omega^{\dagger}_{Na} \begin{pmatrix} \mathbf{M}_{ij} \\ S_{ij} \end{pmatrix} \right\} \tag{A.24}$$

is the screening of the nuclear attraction energy.

In addition to these interaction terms, the same model repulsion term that acts between the discrete classical groups may be added. This repulsion is not felt by the electrons, and thus the Pauli principle may be violated. Effective potentials that are in some way felt by the electrons are much more elaborate—a good description will require the computation of at least overlap integrals with some (temporary) basis set on the classical partition.[114, 116, 128] It will be worthwhile to pursue this line of research in the development of a more consistent combined quantum–classical force field.

The polarization energy is the cost to make the induced moments. It is calculated from the equilibrium response interactions for the source fields. For equilibrium response, it can be shown that the polarization energy equals exactly half the stabilization energy.

$$\Delta U_{\mathrm{pol}} = \Delta U_{\mathrm{pol}}^{clas} + \Delta U_{\mathrm{pol}}^{qm} \tag{A.25}$$

$$\Delta U_{\mathrm{pol}}^{clas} = -\frac{1}{2}\,\Delta U_{\mathrm{int}}^{scee} \tag{A.26}$$

$$\Delta U_{\mathrm{pol}}^{qm} = -\frac{1}{2}\,\Delta U_{\mathrm{stab}}^{\mathrm{eq}} = -\frac{1}{2}\left\{\Delta U^{snr} + \Delta U_{\mathrm{coul}}^{ste}\right\} \tag{A.27}$$

It has been mentioned that the nuclear, electronic, and discrete classical source fields may be added before contracting with the relay matrix (section 2.5). In that case, the analysis [eqs. (A.26) and (A.27)] for the polarization energy cannot be made. However, the polarization energy is still half the *total* stabilization energy from the reaction field, and is calculated as such.

The interaction with the non-equilibrium RF is (elaborated for the case in which the *static* component of the dielectric response is not in equilibrium, and the induced moments carry the non-equilibrium response):

$$\Delta U_{\mathrm{neq}} = \Delta U_{dcl}^{\mathrm{neq}} + \Delta U_{N}^{\mathrm{neq}} + \Delta U_{el}^{\mathrm{neq}} \tag{A.28}$$

$$\Delta U_{dcl}^{\mathrm{neq}} = \left[\mathbf{v}_{\mathrm{q},0}^{\mathrm{R},dcl}\right]^{\dagger}\begin{pmatrix}\mathrm{M}\\ \Omega\\ \mathrm{Z}\end{pmatrix}_{\mathrm{neq}}^{\varepsilon_0} - \left[\mathbf{v}_{\mathrm{q},\infty}^{\mathrm{R},dcl}\right]^{\dagger}\begin{pmatrix}\mathrm{M}\\ \Omega\\ \mathrm{Z}\end{pmatrix}_{\mathrm{neq}}^{\varepsilon_\infty} \tag{A.29}$$

$$\Delta U_{N}^{\mathrm{neq}} = \left[\mathbf{v}_{\mathrm{N},0}^{\mathrm{R},qm}\right]^{\dagger}\begin{pmatrix}\mathrm{M}\\ \Omega\\ \mathrm{Z}\end{pmatrix}_{\mathrm{neq}}^{\varepsilon_0} - \left[\mathbf{v}_{\mathrm{N},\infty}^{\mathrm{R},qm}\right]^{\dagger}\begin{pmatrix}\mathrm{M}\\ \Omega\\ \mathrm{Z}\end{pmatrix}_{\mathrm{neq}}^{\varepsilon_\infty} \tag{A.30}$$

$$\Delta U_{el}^{neq} = -e \sum_{ij} d_{ij} \begin{pmatrix} \mathbf{M}_{ij} \\ S_{ij} \end{pmatrix}^{\dagger} \left\{ \begin{pmatrix} -\mathbb{e}_0^R(\mathbf{r}_a) \\ \mathbf{v}_0^R(\mathbf{r}_a) + \mathbb{e}_0^R(\mathbf{r}_a)\cdot\mathbf{r}_a \end{pmatrix}^{\dagger} \begin{pmatrix} M \\ \Omega \\ Z \end{pmatrix}_{neq}^{\varepsilon_0} - \begin{pmatrix} -\mathbb{e}_\infty^R(\mathbf{r}_a) \\ \mathbf{v}_\infty^R(\mathbf{r}_a) + \mathbb{e}_\infty^R(\mathbf{r}_a)\cdot\mathbf{r}_a \end{pmatrix}^{\dagger} \begin{pmatrix} M \\ \Omega \\ Z \end{pmatrix}_{neq}^{\varepsilon_\infty} \right\} \tag{A.31}$$

where the total dielectric is denoted by 0 and the optic (fast) component by ∞.

The dispersion energy between quantum partition and surroundings may be estimated in our RF formalism, owing to the separate evaluation of the screening of the self [eq. (A.20)] and exchange [eq. (A.23)] interactions.[29, 55] Here, γ serves to correct for the error made in the prefactor of the DRF-expression in comparison to that of the Unsöld approximation to the second order perturbation expression [eq. (1.35)] for the dispersion interaction. This prefactor should be $U_A\ U_S/(U_A + U_S)$, whereas it actually is U_A, where U_A and U_S denote the mean excitation energies of the quantum and classical partitions, respectively. Thus:

$$\gamma = \frac{U_S}{U_A + U_S} \tag{A.32}$$

implying that if the spectra of the classical and quantum partitions are identical, γ=1/2. The estimate of the dispersion energy is given by:

$$\Delta U_{disp} = \Delta U_{el}^{self} - \Delta U_{exch}^{ste} \tag{A.33}$$

If a dielectric continuum is present, the dispersion is calculated with the optic component of the dielectric response only, because it is that component that reflects the electronic response of the bulk. The configuration of the discrete classical partition may strongly influence the magnitude of the dispersion estimate, as has been shown by Thole and van Duijnen for the water dimer.[55] A more reliable estimate may then be obtained by recalculating the dispersion estimate with quantum and classical partitions interchanged, and averaging over the two constellations.

3

Practice

Mother Nature is a bitch.

TENTH COROLLARY TO MURPHY'S LAW

Murphy's Law (1981)

Introduction 3.1

THE PROOF of the pudding is in the eating. The practical models derived on the basis of theoretical arguments must now be put to the test. We address a number of questions concerning our model. First of all the internal consistency of the classical description as being derived from quantum-chemical calculations is investigated. The interaction energy of the water dimer is calculated fully quantum chemically, in a mixed quantum-chemical–classical description, and fully classically. The interaction energies should come out quite comparable between these three approaches, not only in total, but in their components as well, and indeed they do. The confidence in the approach gained by the water-dimer experience is subsequently confirmed in the calculation of the interaction energy between entirely different molec-ules, viz. benzene and substituted benzenes.

Solvated systems consist of an unimaginably large number of molecules. The molecular models that perform well for dimers need not be suitable when many are thrown in together. Conversely, the detail provided by the molecular model may not be required in condensed-phase calculations. The explicit versus continuum approach is studied for the solvation of a number of solutes in water. In some instances the dielectric continuum model may be used to calculate solvation (free) energies reliably, but we find it is severely limited. A more serious problem with the continuum model is its lack of generality with respect to application to solvents other than water.

The explicit solvent model is generally applicable to all solvents, but it is much more costly in terms of computational effort. Nevertheless, the solvatochromism—i.e. the change of electronic spectra on change of solvent—of acetone in water, acetonitrile, and tetrachloromethane, could only be reproduced both qualitatively and quantitatively with the explicit model, demonstrating once more that the lack of molecular detail in the continuum model must not be taken lightly.

Finally an analysis of dielectric behaviour is given. In spite of the fact that the dielectric model was conceived for macroscopic systems, it has found application in microscopic calculations, e.g. in screening factors for electrostatic interactions in atomic force fields. By breaking the dielectric down to microscopic dimensions it is explicitly shown that true dielectric behaviour is not scaleable to the microscopic dimensions at which computational chemistry operates.

Interaction Functions 3.2

Introduction

THE DIRECT REACTION FIELD (DRF) APPROACH to the description of the condensed phase as presented in Chapter 1 provides a consistent route from a quantum-chemical to an all-classical force-field calculation of intermolecular interactions. This transition is based on the perturbation-theoretical analysis of the interaction energy in terms of molecular electrostatic and response properties. The attraction of modelling molecular properties in this setting is twofold. First, the description may be *systematically* improved according to the required accuracy by increasing the number of expansion centres for charge and polarizability representations. The approach shares this aspect with *ab initio* quantum chemistry which allows larger basis-set and configuration state function expansions with eventual convergence to exact results. Second, the theoretical analysis provides a check on the validity of the classical model, which makes it easy to pinpoint those parts of the force field that need reparation if things go wrong, *without rendering other parts of the parameterization obsolete*.

The molecular properties of interest for the calculation of intermolecular interactions (section 1.3) are the electrostatic multipole (charge, dipole, quadrupole, etc.) and response moments (dipole polarizability and higher-order response moments). These may be modelled in various ways and to certain degrees of sophistication. The choices—it is important to stress these are choices!—made in this work for distributed representations of both static and response moments, and for stopping at the exact representation of the overall dipole moment and at linear response have been amply described in section 1.4. Here we test the model both against internal consistency as we go from a fully quantum-chemical through a mixed to a fully classical description of molecular dimers and against experimental data. The latter is important for estimating the reliability of interaction energies of molecular complexes predicted by the classical force field.

The interaction energy between two molecules is analysed in the following terms, be it for quantum-chemical, mixed, or classical descriptions:

$$\Delta U_{\mathrm{int}} = \Delta U^{int}_{\mathrm{elst}} + \Delta U^{int}_{\mathrm{rep}} + \Delta U^{int}_{\mathrm{resp}} + \Delta U^{int}_{\mathrm{disp}} \qquad (1)$$

or electrostatic, repulsion, response, and dispersion. This analysis is straightforward for the classical and mixed descriptions, but contains elements of arbitrariness at small intermolecular distances for the quantum-chemical approach because of the inseparability of the total wave function into fragment functions (cf. the discussion in section 1.3). At larger intermolecular distances there is no problem; the fragments are recognizable and non-overlapping.

As soon as the fragment wave functions start overlapping the integrity of the fragments is violated and analysis becomes cumbersome.[23, 27, 129] Straightforward analysis starts with calculation of the total energy—in the Hartree–Fock approximation, accounting for basis-set extension errors by the counterpoise method[130, 131]—of the molecular complex by superimposing the fragment densities, U^{HF}_{A+S}. The energy difference of U^{HF}_{A+S} with the sum of the isolated fragment energies is the electrostatic interaction energy if the fragments are non-overlapping. If the fragment wave functions do overlap, the superimposed state is unphysical, however, because it then violates the Pauli principle. The first physically meaningful interaction energy can be defined only after this principle has been implemented by orthogonalizing the fragment wave functions, 'contributing' ΔU^{HF}_{orth}. Thus, in a fully quantum-chemical treatment, the electrostatic and repulsion terms are best collected, and denoted ΔU_0:

$$\Delta U_0 = U^{HF}_{A+S} - \left(U^{HF}_{A} + U^{HF}_{S}\right) + \Delta U^{HF}_{orth} \quad \Delta U_{elst} + \Delta U_{rep} \tag{2}$$

At large intermolecular distances the orthogonalization has no effect, so that it is meaningful to use the superimposed state to define the electrostatic interaction energy.

From the orthogonalized state the fragment wave functions may be allowed to relax to accommodate their mutual influence. The energy difference between the fully relaxed state and the orthogonalized state is the response contribution to the interaction energy. At smaller intermolecular distances the relaxation of the wave function may aggravate the problem of dealing in terms of recognizable fragments as chemical bonding starts to become important. One may still attempt to analyse the contributions in terms of fragments by localizing the orbitals as much as possible, ascribing each orbital to a fragment according to its character. The resulting energy analysis is somewhat arbitrary because there are many different localization schemes. Good localization is even more important for the calculation of the dispersion interaction. This interaction is not included at the Hartree–Fock level, which lacks the instantaneous electron–electron interactions that define the dispersion. Calculation at a correlated level includes the dispersion interaction which may, however, only be analysed as such if properly localized occupied as well as virtual fragment orbitals are available. Again, this requirement is easily fulfilled at large intermolecular distances, but no longer as the fragments start overlapping. For weakly interacting systems (including the water dimer) the dependence on the localization was found to have little effect on the analysis, though.[132]

The most fruitful and physically viable approach is then to maintain the long-range analysis as much as possible, bearing in mind the invalidity of the transition from quantum-chemical to mixed and classical descriptions as the intermolecular separation becomes small. It is allowable, however, to stretch the classical model a bit by accounting for overlap effects. At intermediate intermolecular separations quantum-chemical results may yield good models for damping functions which account for the spatial extent of the fragment electronic density within a classical description. The advantage of the classical representation of the charge density lies in the drastic reduction of detail by using just a small number of charge-points

instead of the large number of basis functions covering large parts of space used in quantum-chemical methods. The neglect of the spatial extent of the charge distribution by the charge-point representation may be repaired without too much computational effort by assuming the charge to be distributed in simple volumes, instead of being concentrated in one point in space. Thole has investigated several of these volumes with their shape-functions and found them to be useful even at typical *intramolecular* interatomic distances.[49]

Having constructed a molecular force field based on the long-range interaction energy analysis, and maintaining it with plausible damping functions at intermediate distances, the task of avoiding flagrant violation of the Pauli principle by some *ad hoc* repulsive interaction function remains. Ideally, one would like a functional form that puts a high penalty on the penetration of the electrons treated explicitly into the regions of space that are already claimed by the electrons that underlie classically modelled molecules. Such functional forms do exist, but are computationally highly demanding because they are almost at the level of the original quantum-chemical description itself.[111, 112, 114-116] (To add to the complexity of this task, the effective potentials should not neglect the give-and-take character of the antisymmetrization in the valence region.) Indeed it is hardly to be expected that such a far-reaching requirement as the antisymmetry due to the Pauli principle can be modelled by a simple functional form. For the molecular systems of interest in this thesis such an elaborate procedure would miss its mark, because the basic assumption for using the molecular model is the non-, or low-overlap of the molecular fragments. If, however, bonds are to be cut in the separation of quantum and classical fragments the development of effective fragment potentials is essential.

The *ad hoc* repulsive potential chosen here is taken from the existing CHARMM force field,[126] be it with slightly different values of the parameters in order to converge on the other parts of the DRF force field. The CHARMM-repulsion has the form:

$$\Delta U_{rep}^{CHARMM} = \sum_{i<j} \frac{3}{4} \frac{\alpha_i \alpha_j (r_i + r_j)^6}{\left(\sqrt{\alpha_i / n_i} + \sqrt{\alpha_j / n_j} \right)} r_{ij}^{-12} \qquad (3)$$

in which α_i, n_i, and r_i are the isotropic polarizability, number of valence electrons, and radius of atomic centre i, respectively, and r_{ij} is the distance between centres i and j. We use the integral number of valence electrons of an atom, and the same atomic polarizabilities that go into the electrostatic (for the damping function), response, and dispersion terms, leaving only the atomic radii as independent parameters to be optimized. By noting that the radius of an atom may be related to its polarizability—classically, the polarizability of a conducting sphere of radius r is r^3—the number of parameters can be reduced further. Note also that we use one set of parameters for each atom, independent of its chemical functionality.

Theoretically, the repulsion term should have exponential distance dependence,[23] and the 12-type repulsion model is known to be too steeply repulsive at

shorter contacts. We note again that the repulsion serves to avoid situations that can only be described properly by a fully quantum-chemical treatment.

The calculation of the electrostatic and response interaction energies in the mixed and fully classical descriptions have been amply discussed in Chapter 2, with formulas given in the Appendix. An elaboration on the dispersion interaction is in order at this point as it has been hinted at being connected to the second order perturbation (SOP) expression but not explicitly shown to be so. We wish to make amends for that at this point. The estimate of the dispersion interaction between a quantum-chemically described molecule A and a classically described molecule S emerges from the comparison of the (SOP) expression in the Unsöld approximation to the two-electron reaction-field contributions to the total energy.[29, 55, 102] Recall the SOP expression for the dispersion interaction [eq. (1.35)] and the Unsöld approximation for the energy-denominator [eq. (1.36)]. Insertion of the Unsöld approximation in the SOP expression and rewriting the interaction operator in its original form leads to:

$$\Delta U_{\mathrm{SOP}}^{\mathrm{disp}} \approx \frac{1}{2} \times \left\{ \frac{U_S}{U_A + U_S} \right\} \times \sum_{k \neq 0} \left\langle \Psi_A^0 \middle| \left(\widehat{E}_\mu(\mathbf{s};\mathbf{a})\, \widehat{\mu}_A \right) \middle| \Psi_A^k \right\rangle^\dagger \mathbb{\alpha}_S \left\langle \Psi_A^k \middle| \widehat{E}_\mu(\mathbf{a};\mathbf{s})\, \widehat{\mu}_A \middle| \Psi_A^0 \right\rangle \tag{4}$$

in which $\widehat{\mu}_A$ is the dipole operator of subsystem A and $\widehat{E}_\mu(\mathbf{s};\mathbf{a})$ is the operator that gives the field at $\mathbf{r}_a^0$ of a dipole located at $\mathbf{r}_s^0$:

$$\widehat{E}_\mu(\mathbf{s};\mathbf{a}) = \widehat{E}_\mu\left(\mathbf{r}_s^0;\mathbf{r}_a^0\right) = \frac{1}{\left|\mathbf{r}_a^0 - \mathbf{r}_s^0\right|^3} \left\{ \mathbb{1} - \frac{3\left(\mathbf{r}_a^0 - \mathbf{r}_s^0\right)\left(\mathbf{r}_a^0 - \mathbf{r}_s^0\right)^\dagger}{\left|\mathbf{r}_a^0 - \mathbf{r}_s^0\right|^2} \right\} \tag{5}$$

In eq. (4) the polarizability of S is inserted, but the sum-over-states expression for A is retained. Addition and subtraction of the k=0 term to eq. (4) yields a fluctuation formula for the dispersion:

$$\Delta U_{\mathrm{SOP}}^{\mathrm{disp}} \approx \left\{ \frac{U_S}{U_A + U_S} \right\} \times \left\{ \begin{array}{c} \frac{1}{2} \left\langle \Psi_A^0 \middle| \left(\widehat{E}_\mu(\mathbf{s};\mathbf{a})\, \widehat{\mu}_A \right)^\dagger \mathbb{\alpha}_S\, \widehat{E}_\mu(\mathbf{a};\mathbf{s})\, \widehat{\mu}_A \middle| \Psi_A^0 \right\rangle \\ - \frac{1}{2} \left\langle \Psi_A^0 \middle| \left(\widehat{E}_\mu(\mathbf{s};\mathbf{a})\, \widehat{\mu}_A \right) \middle| \Psi_A^0 \right\rangle^\dagger \mathbb{\alpha}_S \left\langle \Psi_A^0 \middle| \widehat{E}_\mu(\mathbf{a};\mathbf{s})\, \widehat{\mu}_A \middle| \Psi_A^0 \right\rangle \end{array} \right\} \tag{6}$$

Both terms within the rightmost brackets in eq. (6) are computed within the DRF approach [eqs. (2.A.20) and (2.A.23)], but note that the DRF operator is not restricted to the dipole term only. This leaves the prefactor as a scaling between the SOP estimate and the computed DRF value. In most applications the ionization energies of the molecules A and S have been used to calculate the prefactor. If A and S are identical the prefactor, called γ, equals 0.5.

To complete the journey from fully quantum-chemical through the mixed to the fully classical description, the dispersion between classically described molecules is given by the Slater–Kirkwood version of the SOP expression,[127] expressing the prefactor in terms of the polarizability (again!) and number of valence electrons, rather than excitation energies, as in the mixed [eq. (6)] and classical London dispersion formulas:

$$\Delta U_{\text{disp}}^{S-K} = \sum_{i<j} \frac{1}{4} \frac{\mathrm{Tr}\left(\alpha_i \hat{E}_{\mu ij}^{2} \alpha_j\right)}{\left(\sqrt{\alpha_i / n_i} + \sqrt{\alpha_j / n_j}\right)} \tag{7}$$

The summation may be over atomic or group polarizabilities, which may be treated as isotropic or anisotropic, according to the polarizability representation of choice.

The Water Dimer

The water dimer fulfils the role for force fields that the hydrogen molecule fulfils for the representation of the chemical bond and the helium dimer for the accurate calculation of intermolecular interactions. The literature abounds with water–water potentials to varying degrees of accuracy, derived from quantum-chemical computations and from experimental data and from mixtures.[99, 133-143] Aspects of the water model presented here have been discussed before.[55, 99] Here, the exposition aims at demonstrating the derivation of the classical force field from quantum-chemical calculations. The extensive quantum-chemical studies of the water-dimer Potential Energy Surface (PES) of Jeziorski and van Hemert (I),[144] Vos *et al.* (II),[132] and Szalewicz *et al.* (III)[145] serve as our reference, together with the accurate calculation of the well-depth at the minimum-energy conformation of van Duijneveldt-van de Rijdt and van Duijneveldt (IV).[146] A comprehensive review of the water–water interaction by *ab initio* methods was published by Scheiner.[147] The molecular electrostatic properties of water in our model are derived from the LCAO–RHF wave function with a basis set of double-ζ quality in the valence shell plus a polarization function (DZP).[148] The comparison is therefore with literature results of similar quality. Finally we proceed to comparison to experimental results[149] in order to test the model for its potential to predict binding energies of molecular complexes.

Comparison to *ab initio* results

The computed water dipole and quadrupole moments and dipole polarizability are collected in Table 1, together with the values of these properties given by the classical model. The classical model consists of three point charges and three atomic polarizabilities, located at the nuclei. The point charges are the Dipole Preserving Charges (DPCs) discussed in section 1.4.[43] The atomic polarizabilities were chosen to reproduce the computed polarizability within Thole's model.[49] (The standard polarizabilities in Thole's model reproduce *experimental* molecular polarizabilities, a standard computations at the DZP-level cannot attain.) Two shape-functions were studied, corresponding to a linearly (LIN) and an exponentially (EXP) decaying volume for the charge, respectively. It is not yet our aim to reproduce experimental values, so the values in Table 1 serve to illustrate the correspondence between quantum-chemical and classical model properties.

Table 1. Water properties[a] from *ab initio* calculations and classical models.

Model	μ_x	Θ_{xx}	Θ_{yy}	Θ_{zz}	α_{xx}	α_{yy}	α_{zz}
DZP (CHF)[b]	.878	-.08	1.82	-1.74	5.42	7.18	3.03
DZP (SOP)[c]					5.50	6.65	3.53
LIN[d,e]	.878	-.06	1.26	-1.19	4.95	6.97	3.66
EXP[d,f]	.878	-.06	1.26	-1.19	5.12	6.31	4.28
exp.[g]	.728	-.10	1.96	-1.86	9.5	9.7	9.2

[a] All values in atomic units. The tensor components not given all equal zero in the geometry studied. [b] Polarizability from Coupled Hartree–Fock calculation. [c] Polarizability from second-order perturbation calculation with non-empirical Unsöld correction for finite basis-set size (ref. 150). [d] Atomic charges: O: -.796; H: +.398. [e] Atomic polarizabilities: O: 2.417; H: 1.442, damping parameter a=1.662 with conical charge-volume (ref. 49). [f] Atomic polarizabilities: O: 2.666; H: 1.448, damping parameter a=2.089 with exponentially decaying charge-volume (ref. 49). [g] Experimental water properties. Dipole from ref. 151; quadrupole from ref. 152; semi-empirical polarizability from ref. 153.

The interaction components of the water dimer were studied in the orientation of the experimental water-dimer minimum-energy conformation,[149] shown in Figure 1. The quantum-mechanical (QM) water was treated both as H-bond donor and as H-bond acceptor in order to investigate the orientation dependence of the mixed description. The comparisons of the zeroth-order, relaxation, and dispersion components of the interaction energy of the water dimer as a function of O–O distance are shown pictorially in Figure 2.

Only the results for the exponential damping function are shown here. At O–O distances above 6 Bohr, the results for the linear damping function are virtually identical to those obtained with the exponential damping function. As the monomers close in, the linear damping function does not behave as smoothly as the exponential one. Instead, it results in a deeper and narrower potential well. Bearing in mind that at room temperature RT corresponds to 2.5 kJ/mol, Figure 2 shows that the interaction-energy components in the mixed and classical descriptions start deviating seriously from the *ab initio* results only at intermolecular distances shorter than 5.5 Bohr, where the relaxation and dispersion energies differ notably from the fully QM results, pointing to an over-damping of the classical model.

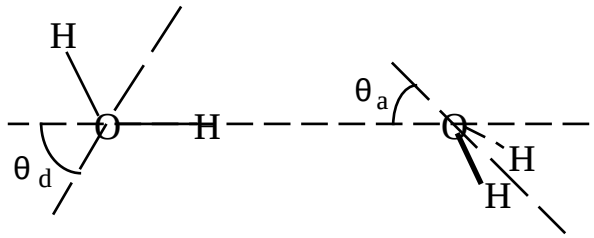

Figure 1. Experimental water-dimer orientation. θ_d*=51°;* θ_a*=57°.*

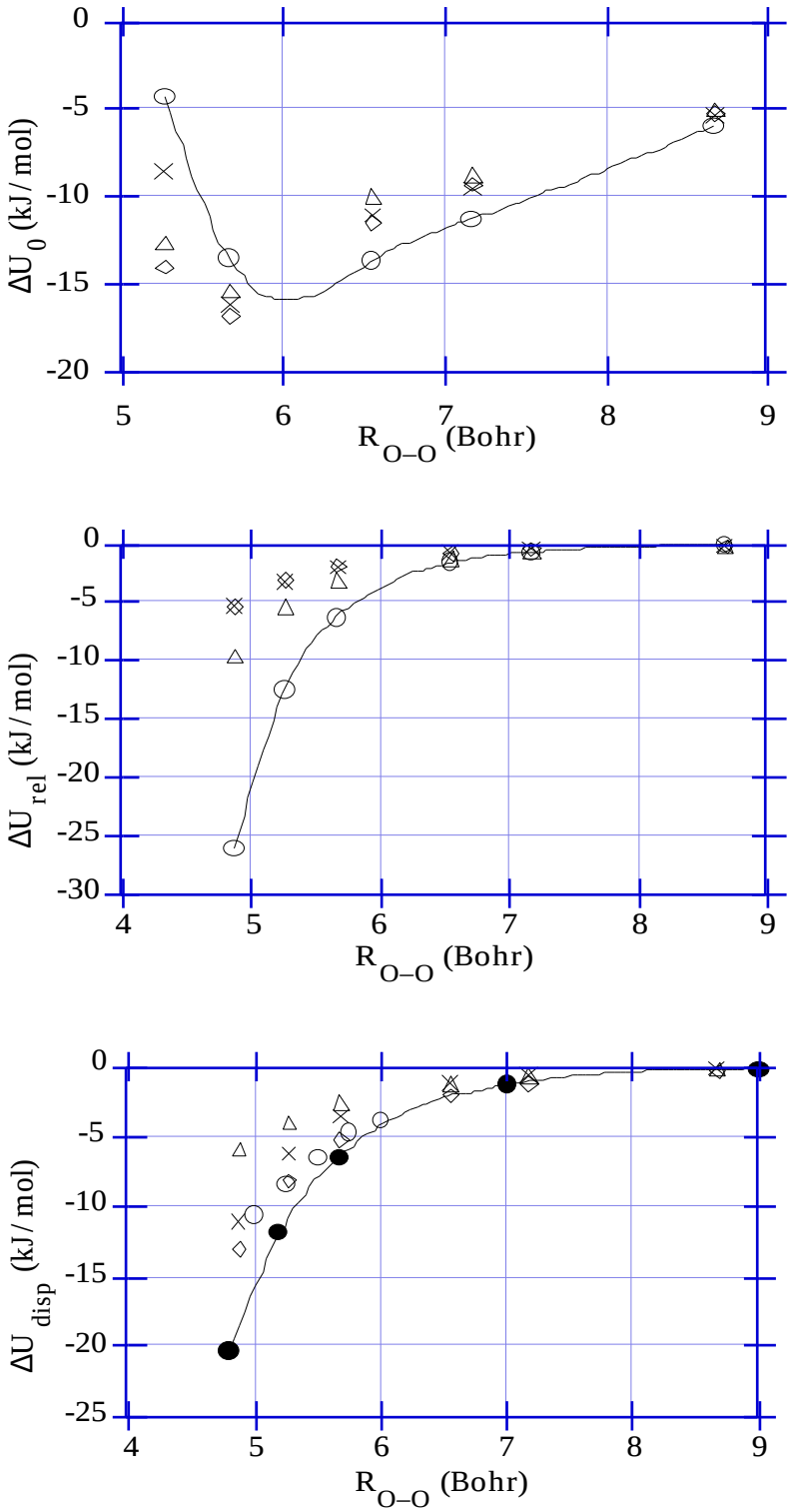

Figure 2. Comparison of the interaction-energy components of the water dimer in various descriptions, as a function of O–O distance (see Figure 1). Top: figure 2a: zeroth-order interaction, eq. (2); middle: figure 2b: relaxation energy interaction; bottom: figure 2c: dispersion interaction. Legend: ○: fully QM description (for the dispersion component this is QM I); ●: fully QM description II (curves fit with a cubic spline); △: mixed description with QM water as H-bond donor; ◇: mixed description with QM water as H-bond acceptor; × : fully classical description.

This over-damping can be repaired, but in the mixed model this might lead to the polarization catastrophe discussed in section 1.5 for the linear damping model. Furthermore, one should not expect the classical model to be satisfactory well inside the overlap region, where typically quantum-chemical effects due to the operation of the Pauli principle govern the distribution of the electrons.

Another feature worth some attention is the orientation dependence of the interaction components in the mixed description. This was already noted by Thole and van Duijnen,[55] and reflects an imbalance in the distributed charge and polarizability representations used. The problem is mainly due to the short H–O distance due to hydrogen bonding. Hence, the relaxation energy of the QM H-bond donor is larger than that of the QM H-bond acceptor because the donor molecule 'sees' a large charge on O quite nearby, whereas the acceptor 'sees' a small charge on H, to which the vacuum densities respond accordingly. On the other hand, the dispersion interaction is larger for the QM H-bond acceptor because there are some eight electrons 'seeing' a H-polarizability, compared to about one electron 'seeing' an O-polarizability, which is not even twice that of H. The imbalance vanishes as the distance between the molecules increase, as it should when local effects disappear.

The imbalance can be repaired for the dispersion interaction by using a group-polarizability representation. The group polarizability will be located quite near the O-atom, hardly changing things for the QM H-bond donor, but causing a drop in the dispersion interaction for the QM H-bond acceptor because of the increased distance of the polarizability to the acceptor O.

Finally, suffice it to conclude that the fully quantum-chemical, mixed, and fully classical models are compatible at long and intermediate intermolecular distances. The fact that even the H-bonded water dimer is accommodated quite well within this model demonstrates its scope. Thus we expect to be able to predict van der Waals minima of *ab initio* quality with the classical model for molecular complexes of molecules other than water. This may not be good enough, however, for practical purposes which are geared to the prediction of experimental interaction energies. The improvements required for attaining experimental standards are the subject of the next section.

Comparison to experimental results

The DZP-derived classical model polarizability of water is rather small compared to experiment (see Table 1), resulting in an underestimation of the induction and dispersion interaction energies compared to accurate calculations. If the model is to be used to yield interaction energies comparable to experimental values, the polarizability is the prime candidate for improvement. Of course correlated large basis-set calculations[36] could be invoked to calculate molecular polarizabilities that can then be reproduced by Thole's model. The standard atomic polarizabilities of Thole's model do, however, yield molecular ground-state polarizabilities of experimental quality for molecules outside the learning set, disposing of the immediate need to perform costly *ab initio* calculations. (For excited states there is a call for such

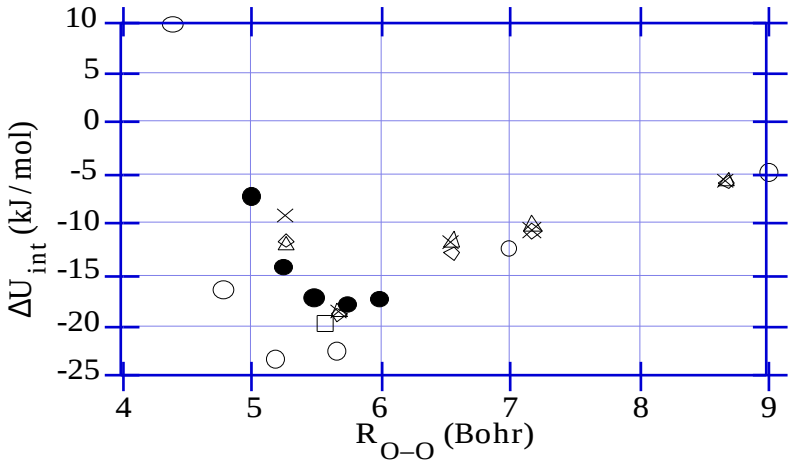

Figure 3. Comparison of the total interaction energy of the water dimer in various descriptions, as a function of O–O distance (see Figure 1). ○*: fully QM description I;* ●*: fully QM description II;* □*: estimated* ab initio *limit (QM IV);* △*: mixed description with QM water as H-bond donor;* ◇*: mixed description with QM water as H-bond acceptor;* ×*: fully classical description.*

calculations[154] because of the limited availability of experimentally determined polarizabilities.[154, 155]) For instance, water was not in Thole's learning-set but its experimental polarizability is reproduced quite well by the model (parameters are given in Appendix 1). With the group polarizability thus obtained, the total interaction energy curve of the water dimer was recalculated in the mixed and classical descriptions, and is shown in Figure 3.

The agreement between the standard DRF force-field and high-quality *ab initio* calculations for both mixed and fully classical descriptions is excellent at the minimum. In this discussion it must be borne in mind that the minimum energy by van Duijneveldt-van de Rijdt and van Duijneveldt (IV) should be regarded as the best available value, comparing very well to experiment after thermodynamic corrections. The deeper wells obtained earlier (I and III) are mostly due to the dispersion contribution which was shown to be sensitive to the exponent of the polarization function.[146] The short-range interaction is too repulsive, in accord with the exaggerated steepness of the 12-type repulsion term. Reparation of the dipole polarizability of the water monomers provides the major correction to the DZP-level results. Further sophistication of the description of the monomer properties is not deemed necessary for the purposes pursued in this thesis. For calculation of e.g. rotation–vibration spectra the DRF scheme is too crude. The small splittings encountered there require accurate description of higher-order molecular properties.[156] We conclude that the transition from (accurate) *ab initio* QM descriptions through mixed to the fully classical DRF force field is very satisfactory for the calculation of intermolecular interaction energies as long as we keep in mind that the approach is bound to break down at intermolecular distances that enter the region of covalency.

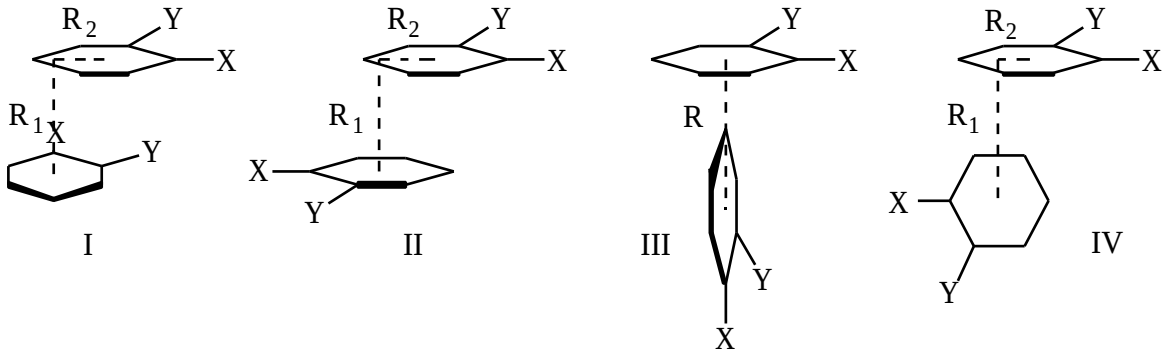

Figure 4. Substituted-benzene dimer conformations. I: parallel–displaced; II: anti-parallel–displaced; III: head-on perpendicular; IV: side-on perpendicular.

Complexes of Benzene and its Derivatives

The benzene dimer has been regarded as a prototype for the study of π–π-interactions in (macro)molecular complexes and in proteins.[157, 158] The observed preference for parallel–displaced (I, II) and perpendicular (III, IV) (see Figure 4) over parallel–stacked orientations in these compounds has been ascribed to the electrostatic interaction between the π-systems. The repulsion of the electron charge-clouds above and below the molecular plane of π-systems dominates in the parallel orientation, whereas in the perpendicular and displaced orientations the overall electrostatic interaction is favourable. The main contribution to the *binding energy* of the benzene dimer is however not from the electrostatic, but from the dispersion interaction. The dispersion is claimed to be hardly orientation dependent[157, 159] and thus not to prefer a particular intermolecular structure.

The leading electrostatic moment of benzene is the quadrupole. In proteins phenyl rings are always attached to the back-bone, introducing a possibly large dipole moment which may dominate the electrostatic interaction with the surroundings. If the phenyl rings are further substituted with e.g. hydroxyl groups the dipole moment becomes even more prominent. The study of benzene derivatives, such as toluene, xylene, and fluorobenzene, is expected to shed light on the consequences of the substitution of phenyl rings on interaction energy and conformation. Molecular beam experiments on clustering have been performed on some benzene derivatives, both of the pure substance and of mixtures.[160] For the interpretation of these experiments a number of parameters are required that are not all that easy to determine independently, one of them being the binding energy. The experimental determination of the binding energy is quite difficult[161-163] and accurate calculation is therefore warranted as a check on the experiments.[159, 164]

Accurate computation of dispersion interactions requires excellent description of the molecular electronic spectrum, which can only be done by using both large one-electron and large configuration basis-set expansions in current *ab initio* methods. Only very few such studies have been published. The problem with the arenes is that they are planar but an important portion of their electron density resides outside the

plane. Standard one-electron basis-set expansions tie their basis functions to the nuclei, and provide insufficient opportunity for the electrons to distribute themselves in the regions above and below the molecular plane. This deficiency may be repaired only at great costs as the computational effort formally grows with the sixth power of the number of basis functions. Reliable (semi-) empirical models for the computation of the dispersion interaction in molecular complexes are therefore very valuable to supplement state-of-the-art quantum chemistry.

The DRF force field provides a fairly good estimate of the dispersion interaction because experimental molecular polarizabilities are represented very well by Thole's model. Although the interaction energy gained by going beyond the Hartree–Fock level in *ab initio* treatments includes more than just the dispersion connected to the dipole polarizabilities, the major contribution is captured by the DRF model for the water dimer. Here we investigate a number of molecular arene complexes, starting with the benzene dimer. The standard all-classical DRF force field is shown to agree on the binding energy and preferred orientation with the best *ab initio* study published for this dimer.

The benzene dimer

The benzene dimer potential has been studied extensively.[159, 165-168] Accurate *ab initio* calculations are sparse, the best published by Hobza *et al.*,[159] who find a parallel–displaced conformation (I) to be slightly more stable than a head-on perpendicular one (III). From experimental determination of the principal moments of inertia, the preferred orientation of the benzene molecules was found to be slightly tilted away from being perpendicular.[169, 170] The experiment reflects the thermodynamic average of all possible conformations, and it is to be expected that perpendicular conformations are more numerous than parallel–displaced ones, outweighing them in the thermodynamic average.

The minimum-energy conformations found by Hobza *et al.* were studied with our all-classical DRF force field. DP charges (DPCs) located at the nuclei only were derived from a HF-level calculation in a basis of STO4-31G quality. These do not fully reproduce the experimental quadrupole moment (but are better than those obtained from a DZP-quality HF wave function), as can be seen from Table 2 in which computed and experimental molecular properties are collected.

Two other sets of charges that do reproduce the quadrupole moment were investigated as well. The first set is obtained by simply scaling the DP charges (SDPC), the second set by adding extra charge-points 1.0 Å above and below the C-atoms and constructing the quadrupole moment by shifting the appropriate amount of charge from the C-atoms to the extra charge-points (EDPC). For the molecular polarizability three representations were studied as well. The first is Thole's standard model (P): atomic polarizabilities on the nuclei only. These yield a molecular polarizability that is more than 10% below the experimental value (see Table 2). Interestingly, the shortcoming of the polarizability in Thole's model is almost entirely due to the falling short of the out-of-plane component, which indicates that benzene is a special

Table 2. Computed and experimental molecular properties of benzene.[a]

Model	$-\theta_{zz}$[b]	α_{xx}[c]	α_{zz}	$\langle\alpha\rangle$[d]
DZP[e]	7.10	71.8	27.1	56.9
DPC[f] from DZP	2.82			
DPC[f] from STO4-31G	4.66			
P[g]		74.2	36.3	61.6
SP[h]		84.6	40.2	69.8
EP[i]		76.4	53.4	69.8
Hobza *et al.*, DZ+2P[j]	7.38	73.0	33.5	59.8
Hobza *et al.*, best[k]	7.08	79.2	44.5	67.7
Experimental[l]	7.4 ± .5			69.6

[a] All properties in atomic units. [b] Buckingham quadrupole, ref. 35. Note that $\theta_{xx}=\theta_{yy}=-\theta_{zz}/2$ because of the molecular symmetry. [c] $\alpha_{yy}=\alpha_{xx}$. [d] Isotropic molecular polarizability. [e] Expectation values from DZP-level HF for quadrupole and Coupled HF for polarizabilities. [f] DPCs at the nuclei from HF wave function. [g] Standard Thole model polarizabilities at the nuclei, exponential damping function. [h] Scaled polarizabilities at the nuclei. [i] Added polarizabilities 1 Å above and below the molecular plane. [j] Taken from Hobza *et al.*; basis set used for calculation of binding energy. [k] Hobza's best values; basis set includes 2 polarization functions on C and H, extra valence functions on C and H, and f-functions on C. [l] Refs. 171 and 172.

molecule and gives the same problems to Thole's model as it does to *ab initio* calculation of the polarizability. The failure of Thole's model can be repaired by scaling the polarizabilities (SP), or by adding polarizabilities above and below the plane (EP). For the latter we chose the same points as for the EDPCs. Parameters are given in Appendices 2 and 3. The computed binding energies with their interaction components are collected in Table 3.

The results presented in Table 3 deserve close inspection because they give insight into some of the particulars of the DRF force field. Consider the electrostatic interaction. First note the error in the analysis of Hobza *et al.*, who report an attractive quadrupole–quadrupole interaction in the parallel–displaced dimer. Using the quadrupole tensors and interaction expression given by Buckingham,[35] displacing a parallel benzene can indeed give electrostatic attraction, but the displacement should be quite a bit more than the 1.6 Å of the present minimum-energy conformation, in which the electrostatic interaction is definitely repulsive. The electrostatic interaction is reproduced qualitatively by the standard DPCs, but because they recover only 60% of the overall quadrupole moment they yield electrostatic interaction energies that are smaller than they should be. The scaled DPCs do not quite reproduce the quadrupole–quadrupole interaction either, but this is not to be expected due to local effects and the operation of the damping function. This is better seen from the EDPCs, which are supposed to model the electronic clouds above and below the molecular plane by extra charge-points. With these charges the electrostatic attraction and repulsion diminish with respect to the scaled DPCs. The spreading of the charge from the C-atoms causes the major contributions to be dipole–dipole,

Table 3. Computed total and component binding energies of the benzene dimer.[a]

Model / Orientation	Perpendicular (III)			Parallel–displaced (I)		
	ΔU_{elst}[b]	ΔU_{disp}[c]	ΔU_{tot}[d]	ΔU_{elst}[b]	ΔU_{disp}[c]	ΔU_{tot}[d]
DPC–P	-2.0	-11.7	-7.8	+3.3	-17.3	-9.0
SDPC–P	-4.9	-11.7	-10.9	+8.0	-17.3	-5.1
EDPC–P	-3.7	-11.7	-9.9	+7.6	-17.3	-6.6
SDPC–SP	-4.9	-13.6	-12.8	+8.0	-20.5	-8.4
EDPC–EP	-3.7	-24.6	-15.8	+7.6	-48.2	-13.3
Hobza *et al.*[e]	-5.7	-3.4	-8.8	-6.2	-16.1	-9.5
QQ–London[f]	-5.7	-4.8		+11.3	-22.9	

[a] All energies in kJ / mol. The head-on perpendicular (R=5.0 Å) and parallel–displaced (R_1=3.5 Å; R_2=1.6 Å) geometries are structures a and e taken from Hobza *et al.* [b] Electrostatic interaction energy. [c] Dispersion contribution to interaction energy by eq. (7) with distributed polarizabilities. [d] Total binding energy. [e] Hobza's analysis (ref. 159), made in terms of computed overall quadrupole moments and polarizabilities. [f] Overall quadrupole–quadrupole interaction and London dispersion interaction from experimental polarizability and ionization energy.

rather than charge–charge interactions, leaving the electrostatic interactions less pronounced. In addition to the local effects, the damping function further reduces the interactions as it compensates for overlap effects.

The distributed polarizability representation strongly affects the dispersion energy for the perpendicular geometry, giving larger interactions than obtained from the London formula with isotropic molecular polarizabilities.[33] For the parallel–displaced geometry the DRF dispersion interactions are smaller, except for the EP-representation which seems to overestimate the interaction, perhaps because the extra polarizabilities are too far from the molecular plane. The anisotropy of the distributed representation is essential for a balanced description of the correlation interaction, though. The *ratio* between the DRF dispersion energies for parallel–displaced and perpendicular geometries (1.5-2) is much closer to that from the ΔE^{MP2}-values given by Hobza *et al.* (2.3, not shown) than that from the London dispersion energies (4.8). With anisotropic molecular polarizabilities the ratio is about 2.6, emphasizing the inadequacy of the isotropic polarizability representation. The anisotropy of the benzene polarizability tensor is quite large, and the observation that the dispersion interaction is less orientation dependent than the electrostatic interaction[157, 159] is not valid for the benzene dimer.

The question of the relative stabilities of perpendicular and parallel–displaced geometries is unresolved by the DRF force field. Only the standard (DPC–P) DRF force field agrees with the best *ab initio* results available in giving preference to the parallel–displaced geometry. Any improvement of the description of molecular properties results in the perpendicular geometry being the more stable, however. We conjecture this corroborates better with experiments, noting that Hobza's best results are obtained with a basis set that underestimates the out-of-plane molecular

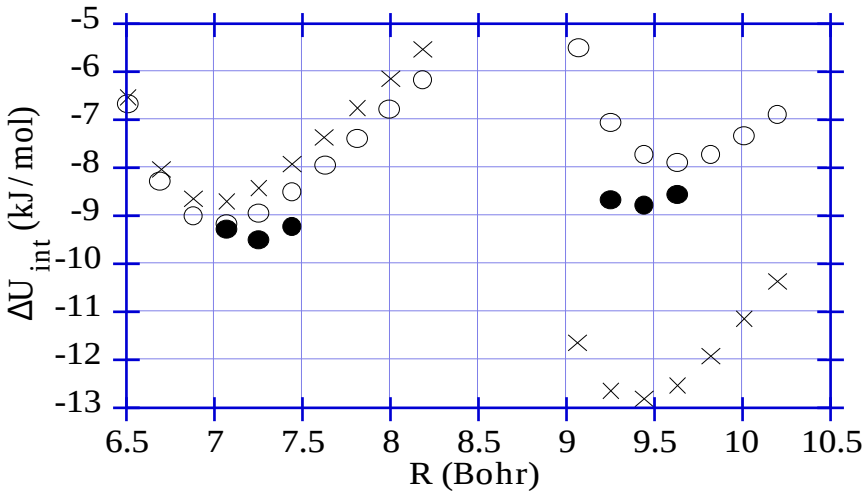

Figure 5. Benzene dimer interaction energy as a function of intermolecular distance. Left: parallel–displaced orientation; right: perpendicular orientation. ○: DPC–P parameters; ×: SDPC–SP parameters; ●: Hobza et al.

polarizability, thereby putting the perpendicular geometry at a disadvantage with respect to the parallel–displaced one. As for the binding energy of the benzene dimer, a value of 10-12 kJ/mol seems to be the limit, which is somewhat larger than the experimental value of 7±1 kJ/mol. Correction for zero-point energy lifts the experimental value to 9±1 kJ/mol, however.[162] As a final check on the DRF force field binding energy and structure a potential energy surface (PES) scan was performed with the DPC–P and SDPC–SP parameter sets. The results are shown in Figure 5.

The conclusions that may be drawn from the minimum-energy search and PES-scan presented in Figure 5 are that the standard parameterization corresponds to the present *ab initio* results, whereas the extended parameterization points to possible improvements, corroborating with experimental results on structure, suggesting too small a value of the experimental binding energy.

Dimers of benzene derivatives

The dimers of toluene, *o*-xylene, and fluorobenzene, along with some mixed dimers were investigated by the standard DRF force field. Controlled PES scans along the intermolecular vector (R_1) were performed starting at perpendicular and parallel(–displaced) orientations. Starting from the minimum-energy structures found in the PES scan, a modest Monte Carlo search was performed to find even lower-energy conformations. Geometry and charge parameters of the monomers may be found in Appendix 2. The results of these calculations have been collected in Table 4.

Table 4. Minimum energies[a] and corresponding structures[b] of molecular complexes between benzene derivatives.

Complex[c]	ΔU_{min}[d]	ΔU_{elst}	ΔU_{disp}	Structure	ΔU_{MC}[e]	Lit.[f]
B–B	-9.0	+3.3	-17.3	Parallel–displaced (I); R_1=6.4; R_2=2.9 Bohr	-9.8	-7±1; *-9.6*
B–T	-11.9	-0.2	-18.6	Parallel–displaced (I); R_1=6.1; R_2=5.2 Bohr	-14.0	-13±2
T–T	-14.3	+2.8	-26.8	Anti-parallel–displaced (II); R_1=6.7; R_2=0.4 Bohr	-15.0	-15±2
T–X	-16.8	+2.1	-32.1	Anti-parallel–displaced (II); R_1=6.6; R_2=-0.3 Bohr	-17.5	-17±3
X–X	-19.9	+0.6	-35.2	Anti-parallel–displaced (II); R_1=6.7; R_2=0.3 Bohr	-20.3	-21±3
F–F	-15.2	-1.8	-24.8	Anti-parallel–displaced (II); R_1=6.4; R_2=1.0 Bohr	-15.3	

[a] All energies in kJ/mol. The parameter sets used were the standard DPCs and Thole's polarizabilities with the exponential damping function. [b] For general features of the structures see Figure 4.
[c] Abbreviations used: B: benzene (X=Y=H); T: toluene (X=CH_3, Y=H); X: *o*-xylene (X=Y=CH_3); F: fluorobenzene (X=F, Y=H). [d] Binding energy at minimum-energy conformation in controlled PES scan. [e] Binding energy at minimum-energy conformation in a Monte Carlo sampling run at 100 K, starting from controlled PES-scan minimum. [f] Literature experimental (ref. 163) and computed binding energies. Italicized numbers are computational results. B–B from Hobza *et al.*

The preferred orientation of the aromatic rings is parallel in all minimum-energy structures. This preference for parallel structures may be explained by the dominance of the dispersion contribution to the binding energy. A parallel orientation of the aromatic rings allows a much closer contact than a perpendicular arrangement, resulting in a larger dispersion interaction. The unfavourable electrostatic quadrupole–quadrupole interaction is a price worth paying. In the substituted benzenes some of the electrostatic repulsion between the quadrupoles may be made good by favourable dipole–dipole interactions. This explains the preference for anti-parallel arrangements.

The model calculations seem to contradict experimental findings in proteins that phenyl rings are often in some perpendicular arrangement.[158] For all complexes except the *o*-xylene dimer we found perpendicular arrangements, mostly side-on to benefit from dipole–dipole attraction, that were within 5 kJ/mol of the (anti-)parallel minimum-energy structure. Improved description of the out-of-plane component of the polarizability is expected to bring these structures down in energy, like it did for the benzene dimer, and thus there seems to be no strong intrinsic dislike for perpendicular arrangements between substituted arenes.

The simple standard DRF force field yields binding energies for the molecular complexes of benzene derivatives that agree very well with experimental values. Only the benzene dimer itself is calculated to be more stable than what is found experimentally. In view of the underestimation of the polarizability in the DRF force field for benzene (Table 2) we suggest that the experimental binding energy of benzene is too small. We cannot subscribe to the analysis of the factors determining the structure of arene complexes given by Hobza *et al.*[159] and by Hunter and Saunders,[157] *viz.* that the electrostatic interaction determines the structure and the dispersion the binding energy. This conclusion was based on a faulty analysis of the quadrupole–quadrupole interaction. The dispersion interaction constitutes the main contribution to the binding energy. To maximize this interaction the monomers will try to be as close to each other as possible. Acting against perpendicular arrangements are repulsive interactions due to the Pauli principle, much stronger than the electrostatic repulsion between quadrupoles in the parallel–displaced conformations. The precise minimum in the latter is, however, influenced by electrostatic interactions as a balance is struck between attraction and repulsion.

The MC minimum-energy search does not yield surprising low-energy structures. The difference with the manual-search structures are only slight tilts of the aromatic rings. The benzene dimer exhibits a more pronounced tilt (24° between the principal moments of inertia). The observed predominance of perpendicular orientations must be explained by the thermal population of such structures. In this respect, the 5 kJ/mol difference we find between parallel and perpendicular structures must be regarded as an upper bound. We have demonstrated that improvement of the out-of-plane component of the polarizability tensor stabilizes perpendicular arrangements more than parallel ones for the benzene dimer. It is to be expected that this will be the same for the other complexes studied here, although toluene and *o*-xylene will need less reparation of the polarizability than benzene because they have out-of-plane centres that carry polarizabilities.

Other Solvent Molecules Considered in this Thesis

To further investigate the generality of the proposed scheme to obtain force-field parameters, a comparison of calculated and experimental binding energies and equilibrium distances of acetonitrile (MeCN) and tetrachloromethane (CCl_4) dimers is reported in Table 5. Force-field parameters are given in Appendices 1 and 2.

Although the computed binding energy of the MeCN dimer is not as large as fits to experimental data give,[174] it does compare very well to Jorgensens liquid-phase interaction value of 16 kJ/mol.[173] Jorgensens model reproduced the heat of vaporization very well. The experimental uncertainty in the CCl_4-data is quite large, but the model interaction presented here compares well to those data. Note that CCl_4 was not part of the learning set from which atomic polarizabilities were fitted to molecular polarizabilities.[49] For the CCl_4 dimer a separate comparison was made for the repulsive part of the potential to test the CHARMM repulsion term (not shown).

Table 5: Calculated and experimental binding energies and equilibrium distances for MeCN and CCl_4 dimers.

Species	$-\Delta E_{binding}$ (kJ/mol)			R_{eq} (Bohr)	
	DRF[a]	Comp.[b]	exp.[c]	DRF[a]	exp.[c]
MeCN	15.5	16[173]	21.8[174]	6.64	6.52
CCl_4	3.1		3.8±1.1[175]	10.9	10.5±0.5

[a] Classical DRF force field. [b] *Ab initio* or other force field. [c] Experimental results.

The classical CHARMM repulsion was found to be a little too hard at the DRF equilibrium distance, compared to the orthogonalization energy in a DZP basis, so the present binding energy and equilibrium distance may be considered as upper limits.

Conclusion

The DRF force field is shown to provide a simple, general scheme to parameterize atom-based interaction functions that closely follow the theoretical intermolecular interaction components, electrostatic, induction, dispersion, and repulsion. The advantage of such a scheme is that the description can easily and systematically be improved according to the required accuracy as more detailed information on the molecules become available, either from experiment or from accurate quantum-chemical calculations. An important advantage of the DRF force field over other force fields such as CHARMM,[126] AMBER,[176, 177] and GROMOS[178, 179] is the clear separation of parameters, one set for each interaction component. In this way each component can be improved independently from the others. Especially the separation of electrostatic and induction interactions through explicit modelling of response properties avoids parameterization in which the immediate surrounding of an atom is incorporated in non-transparent ways. For example, there is no need to distinguish between alcoholic, aldehydic, and carboxylic oxygens for non-bonded interactions (except, of course, electrostatics) in the DRF force field.

Problems only arise at shorter distances where modelling of the consequences of the antisymmetry requirement on the total wave function becomes impossible. At intermediate distances the *ad hoc* repulsion potentials may be used to fine-tune the interaction potential depth and location of the minimum. There is a need for a more general repulsive potential in the spirit of the present approach.

Solvation 3.3

Theory

THE GIBBS ENERGY of solvation is the free energy associated with the process of bringing one molecule (the solute, A) from the gas phase into a liquid phase.[180] The liquid phase consists of a large number of molecules (the solvent, {S}):

$$A\ (g) + \{S\}\ (l) \longrightarrow \{A,\{S\}\}\ (l) \tag{8}$$

From both experimental and computational point of view, the interest in this process lies in the *interaction* between solute and solvent molecules and the changes it causes in both solute and solvent molecules. First, consider the computational route to the free energy. The Helmholtz free energy of a system is related to the partition function Z (section 1.2) by:

$$F = -\,kT \ln Z \tag{9}$$

It is impossible to calculate the partition function exactly, except for idealized situations.[5] At room temperature, these idealized situations are often good approximations to the actual ones—or at least serve as good points of departure. In order to make use of the simple equations for the partition function the total energy of the system should be expressible as a sum of *independent* components: electronic, vibrational, rotational, and translational energy for individual molecules, and interaction energy for collections of molecules. The partition function can then be expressed as a product of the independent component partition functions:

$$\begin{aligned} Z = \sum_i \exp\left(-E_i / kT\right) &\approx \sum_i \exp\left(-\left[\varepsilon_0 + E_i^{el} + E_i^{vib} + E_i^{rot} + E_i^{tr} + E_i^{int}\right] / kT\right) \\ &= \exp\left(-\varepsilon_0 / kT\right) \times z_{el} \times z_{vib} \times z_{rot} \times z_{tr} \times z_{int} \end{aligned} \tag{10}$$

in which ε_0 is the reference energy from which the contributions are counted. It can be shown that the translational motion can always be separated off exactly from the other types of motion, but the rotational and vibrational motions cannot.[16] For our purposes—simulating well-defined molecules at room temperature—the decoupling of rotational and vibrational motions is an accurate enough approximation. The vibrational motions shall be treated as harmonic oscillators and the rotational motions as those of a rigid rotor, which are further approximations to the exact partition functions.[181] Furthermore, z_{el} will be unity, since we deal with electronic ground-state molecules.

Now consider the partition functions before and after solvation. First of all, consider the solvent molecules already present in the liquid phase. The introduction of a new molecule is hardly expected to change the available phase space of their

degrees of freedom. The translational and rotational partition functions will not be affected by the solvation process. The vibrational contribution is absent if the molecules are assumed to be rigid. The same applies to the rotational and vibrational freedom of the solute. Relaxation of the rigid-molecule condition is expected to make little difference. The vibrations are usually low-amplitude motions and the surrounding solvent molecules are on average not close enough to significantly change the vibrational phase space. This is true for the overall rotational freedom as well, although the exploration may take more time, because the surrounding molecules hamper the rotation. This does not affect the partition function, though. For *internal* rotations the story may be different, but they are expected to play a minor role for the small molecules considered in this thesis.[182]

If we now start by keeping the solute fixed in space, the solvation free energy may be calculated as:

$$\Delta F_{solv} = - kT \ln\left(\sum_i \exp\left[- E_i^{int}(\mathbf{R}_0) / kT\right]\right) \tag{11}$$

in which i runs over all solvent-molecule configurations, and $\mathbf{R}_0$ signifies that the solute is kept fixed in space. $E_i^{int}(\mathbf{R}_0)$ is the interaction energy between solute and solvent molecules, i.e. the energy of the system additional to the same system without the solute molecule.

Experiment and computation may be connected by correcting the experimental values for the liberation free energy, i.e. the free energy the solute gains by removing the restraint that it be fixed in space. The liberation free energy is connected to the translational partition function:

$$z_{tr} = V\left(2\pi M kT / h^2\right)^{3/2} \tag{12}$$

in which V is the volume available to the system and M is its mass. The contribution of the liberation free energy may be estimated from the experimental liquid density ρ and the ideal-gas pressure p of the pure substance at temperature T:

$$\Delta G_{lib} = \Delta F_{lib} = - kT \ln\left(V_g / V_l\right) = kT \ln\left(pM / RT\rho\right) \tag{13}$$

Most authors tacitly include the liberation contributions in their tabulated values.[183] This makes it difficult to connect computed values to experimental data. We adopt the values given by Ben-Naim, as his view is conceptually simple and general. It can be shown that with this definition of the solvation process, the Gibbs and Helmholtz free energies are identical.[180]

Solvation Models and the Computation of the Solvation (Free) Energy

Dielectric continuum models

The simplest way to compute the solvation energy is to view the solvation process as immersing one solute molecule into a dielectric continuum, characterized by the dielectric constant ε_0 of the solvent. The solute is accommodated in a cavity in the dielectric. For small molecules, a spherical cavity might be a good model. In that case, the *electrostatic* component of the solvation energy is given by an analytic series in solute multipole moments:[103]

$$\Delta G_{solv}^{elst} = -\frac{1}{2}\sum_{l=0}^{\infty}\sum_{m=-l}^{l} a^{-(2l+1)}\frac{[(l+1)(\varepsilon_0-1)]}{[l+\varepsilon_0(l+1)]}\langle T_{lm}\rangle^2 \qquad (14)$$

in which a is the radius of the cavity and $\langle T_{lm}\rangle$ is the expectation value of the lm'th multipole moment expressed in spherical harmonics. The first two terms of this series, which give the energy of a charge and of a dipole in their own reaction fields, respectively, are called the Born and Onsager terms.[59, 60] The solvation energy is seen to be strongly dependent on the cavity radius. Several approaches to calculate the radius are in use, most of them based on the density of the pure liquid solute and solvent.[184, 185]

The spherical cavity approach is used profusely in solvent modelling, even for highly non-spherical solutes. An improvement to the spherical cavity is the general cavity, which follows the solute's shape. It may be constructed by defining spheres around the solute's nuclei, followed by tracing out the outer surface. The standard in this approach has been set by Connolly (see Figure 6).[61]

The radii of the nuclear spheres are subject to choice. Most models employ the van der Waals radii,[186] which may be scaled up slightly. This means the cavity surface is quite close to the solute. Analytic expressions for the energy of a charge

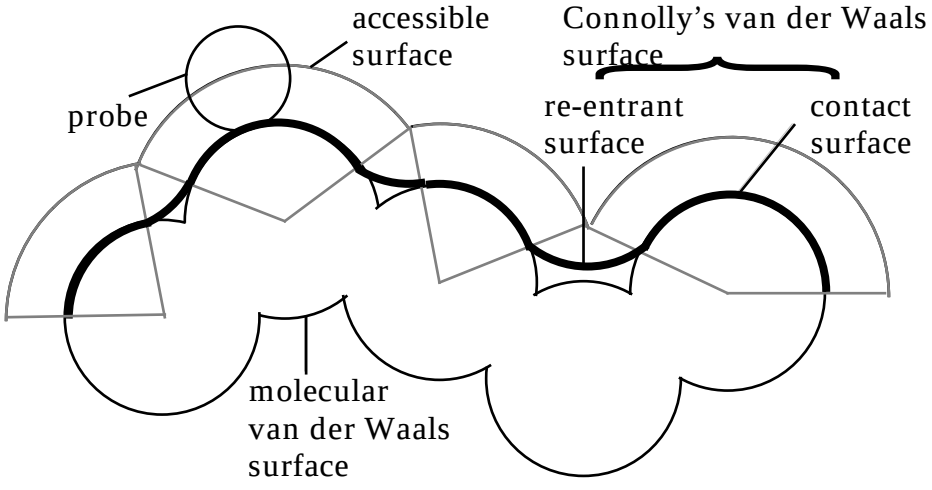

Figure 6. Definition of general shape cavity surfaces.

distribution in such a generally shaped cavity do not exist, but numerical procedures have been developed.[56-58] We employ the Melc suite of programs by Juffer *et al.*,[58] which is a boundary element method (BEM) to solve the Poisson equation for a charge distribution in a cavity, the surface of which is represented by a number of adjacent tiles. The program has several levels of accuracy regarding the representation of the reaction potential. The inhomogeneity of the induced surface dipole density on a tile may be accounted for by a Gaussian quadrature. If the inhomogeneity is not accounted for, one speaks of the constant element method, which we have employed throughout this work.

The continuum solvent model gives the *Gibbs free energy*, but of the electrostatic term only.[187] (In this context, the electrostatic term includes all orientation, vibration and electronic effects that go into the dielectric constant.) It is indeed a free energy because the dielectric constant is an average over all possible solvent configurations. Separate models for dispersion and repulsion are necessary because these terms are not included in Poisson's equation.[188, 189] Within the DRF approach, the dispersion term can easily be included for a quantum-mechanically described solute (sections 2.10 and 3.2, but note that the continuum should be represented by the *optic* dielectric constant for the computation of the dispersion component), but the repulsion term is still to be treated separately. Empirical formulas exist for the repulsion interaction between a solute molecule and the surrounding solvent molecules.[188] They are, however, highly parameterized, which means they are usually optimized in conjunction with other contributions. We shall not attempt this here, and will not consider this contribution.

A final contribution to the free energy that needs consideration in the continuum approach is the cost to create a cavity in the solvent to accommodate the solute. For the calculation of this cavitation free energy the semi-empirical method based on a hard sphere model due to Pierotti is used.[190]

$$\Delta G_{cav} = K_0 + K_1 \sigma_{12} + K_2 \sigma_{12}^2 + K_3 \sigma_{12}^3 ;$$

$$K_0 = kT \left\{ - \ln(1-y) + \frac{9}{2}\left(y/1-y\right)^2 \right\} - \frac{\pi p \sigma_1^3}{6} ; K_1 = - \frac{kT}{\sigma_1} \left\{ 6\left(y/1-y\right) + 18\left(y/1-y\right)^2 \right\} + \pi p \sigma_1^2 ; \quad (15)$$

$$K_2 = \frac{kT}{\sigma_1^2} \left\{ 12\left(y/1-y\right) + 18\left(y/1-y\right)^2 \right\} - 2\pi p \sigma_1 ; K_3 = \frac{4}{3}\pi p ; y = \frac{\pi \sigma_1^3 \rho}{6\,M} ; \sigma_{12} = \frac{1}{2}(\sigma_1 + \sigma_2)$$

in which σ_1 and σ_2 are the solvent and solute diameter, respectively. This expression is rooted in statistical mechanics and needs only solute and solvent diameter and solvent number density as parameters. The molecular radii may be calculated from the density, reducing the number of parameters by one, or fitted to experimentally determined cavitation free energies. This completes the theoretical view of solvation as a two-step process: first, a cavity is created in the solvent, after which the solute is 'grown' into it, gaining interaction free energy.

Explicit solvent models

Finally, the explicit solvent models include a number of solvent molecules, described either quantum chemically or classically, in the vicinity of the solute.[66, 67, 97, 99, 104, 134, 139, 191-193] The explicitly treated solvent shell(s) may be embedded in a dielectric continuum in the same way as the solute alone. The solvent molecules' coupling to the solute and their interaction functions have been discussed in Chapter 2 and discussed in section 3.2. The interaction term in eq. (11) may be split into electrostatic, induction, dispersion, and repulsion interactions. The explicit solvent model has the advantage that all interaction energy terms are included, but the disadvantage that it is very difficult to obtain a *free energy*, because that requires extensive sampling of the configuration space.[191] In this context, it is advantageous to look to the energy of solvation, given by:

$$\Delta U_{solv} = \Delta A_{solv} + T\Delta S_{solv} \tag{16}$$

in which ΔS_{solv} is the entropy of solvation. The energy of solvation may be calculated in the explicit solvent model by subtracting the average energy of the solvent molecules alone from the average energy of the solute plus solvent molecules:

$$\Delta U_{solv} = \langle U_{int} \rangle_s + \langle U_N \rangle_s - \langle U_N \rangle_0 \tag{17}$$

in which $\langle\,\rangle_s$ denotes an average over the configurations (obtained through appropriate thermodynamic sampling techniques) of the solvent molecules in the presence of the solute, and $\langle\,\rangle_0$ in the absence of the solute, but in the same volume. U_N is the total energy of the N explicitly treated solvent molecules, U_{int} the interaction energy between the solute and N solvent molecules.

The rest of this section will be devoted to the study of the numerical accuracy, validity and generality of the various solvent models applied to the process of solvation. To this end several solutes will be solvated in several solvents, using the various solvent models.

Solvation in Water

Z–E equilibrium of N-methylacetamide

The *Z–E* equilibrium of N-methylacetamide depicted in Figure 7 is unchanged when going from the gas phase to aqueous solution.[194, 195] Experimentally, both rotamers have a solvation free energy of about -42 kJ/mol. Of the computational approaches that have been applied to this equilibrium[196-198], only the explicit solvent model of Jorgensen,[196] with a Monte Carlo sampling of the solvent configuration space, has been able to reproduce experiment quite well: the solvation energy of the *E*-rotamer was found to be 0.4 kJ/mol larger than that of the *Z*-rotamer. The

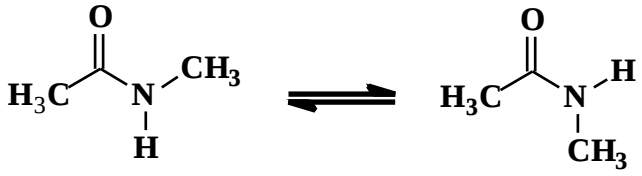

Figure 7. Z–E *rotamer equilibrium of N-methylacetamide.*

semi-empirical AM1–SM1 solvation model gave a solvation free energy difference of 5.6 kJ / mol in favour of the *E*-rotamer.[198]

Here, the rotamer equilibrium of N-methylacetamide is studied by the charge-distribution-in-a-cavity methods. The charge distribution was represented either classically, using the DPCs from a quantum-chemical vacuum calculation (parameters are given in Appendix 2), or left quantum mechanically. For the quantum-mechanically described charge distribution, the position of the boundary was varied, and the estimate of the dispersion interaction was added to the electrostatic interaction. The results are collected in Table 6.

If the standard, but physically incorrect van der Waals surface is used with either classical or quantum-mechanical charge representation (entries 2 and 3 in Table 6), the electrostatic component gives far too large a solvation energy. The explicit quantum-mechanical charge-representation can only be used in a perturbation approach, disallowing relaxation of the wave function in its own reaction field. Self-consistent coupling with the solvent reaction field is numerically unstable due to overlap effects resulting in the polarization catastrophe discussed in section 1.5.

Table 6. Electrostatic and dispersion contributions to solvation energies and solvation energy differences[a] of the *Z*- and *E*-rotamers of N-methylacetamide.

Solute / solvent model	ΔG_{solv} *Z*	ΔG_{solv} *E*	Δ_{solv} (*E* - *Z*)
Onsager approximation[b,c]	-18	-21	-3
DP charges, BEM, vdW[c,d,e]	-115	-72	+43
QM, BEM, vdW[e,f,g]	-116	-79	+37
QM, BEM, vdW+H_2O[e,h,i]	-8	-7	+1
QM, BEM, vdW+H_2O[h,i,j], disp[k]	-37	-38	-1
QM, BEM, vdW+H_2O[h,i], tot	-45	-45	0

[a] All energies in kJ / mol. Total vacuum energy in STO4-31G basis for *Z*-rotamer: -246.641773; for *E* -rotamer-246.636106 Hartree. [b] Sphere radius of 5.93 Bohr, from pure N-methylacetamide density. Computed vacuum dipole moments: *Z*: 4.38; *E*: 4.72 Debye (exp. 3.73 D). [c] ε_0 = 78.5. [d] DPCs and standard Thole polarizability representation (see Appendices 1 and 2). [e] Triangulated boundary surface (240 elements) from van der Waals surface. [f] STO4-31G basis set, vacuum density. [g] Connolly's van der Waals surface (ca. 500 elements) from van der Waals radii. [h] STO4-31G basis set, reaction field coupled self-consistently to the QM density. [i] Connolly's van der Waals surface (ca. 525 elements) from van der Waals + H_2O radii. [j] ε_∞ = 1.777. [k] Estimate of the dispersion energy [eqs. (2.A.32) and (2.A.33)], γ = 0.59 for both rotamers, from experimental ionization potentials.

Table 7. Experimental solvation free energies and computed cavitation, electrostatic, and dispersion component to solvation free energies[a] in the dielectric continuum model[b] of various solutes in water.

Solute[c]	ΔG_{exp}[d]	ΔG_{cav}[e]	ΔG_{int}[f]	μ[g]	Classical charge representation		Quantum mechanical charge representation			
					Onsager[h]	vdW[i]	vdW[j]	disp[k]	vdW+[l]	disp[k]
CH_3CN[m]	-16.3	+8.5	-24.8	4.23	-25	-37 (-54)	-44 (–)	-151	-6	-18
CH_3COCH_3[n]	-16.1	+7.3	-23.4	3.36	-11	-19 (-26)	-29 (–)	-195	-4	-30
H_2O[m]	-26.5	+13.8	-40.3	2.23	-21	-23 (-29)	-22 (-27)	-72	-3	-10
H_2O[n]	-26.5	+13.8	-40.3	2.60	-29	-32 (-39)	-30 (-35)	-70	-5	-10
CH_3OH[m]	-21.4	+9.6	-31.0	2.47	-7	-19 (-23)	-13 (-25)	-140	-2	-16
CH_3OH[n]	-21.4	+9.6	-31.0	2.32	-6	-29 (-34)	-16 (-21)	-137	-2	-16
$C_6H_5CH_3$[n]	-3.7	+6.3	-10.0	0.18	-0.1	-16 (-17)	-73 (–)	-386	-4	-53
C_6H_6[n]	-3.6	+6.7	-10.3	0.0	0	-8 (-8)	-45 (–)	-258	-8	-49
CCl_4[m]	+0.4	+6.5	-6.1	0.0	0	-0.1 (-0.2)	-1 (-1)	-225	0	-41

[a] All energies in kJ/mol, ε_0=78.5, ε_∞=1.777. [b] BEM implementation (see text). The number of boundary elements was approximately 300 for each surface considered. [c] Parameters are given in Appendix 2. [d] Experimental total solvation free energy. [e] Cavitation free energy from eq. (15). [f] $\Delta G_{int} = \Delta G_{exp} - \Delta G_{cav}$. [g] Computed vacuum dipole moment in Debye. [h] Onsager term with computed vacuum dipole moment, from eq. (14), solute cavity size from pure solute density. [i] Dipole Preserving charges (see section 1.4) in general shape cavity at standard scaled van der Waals distance (scaling factor is 1.2). The surface is the accessible surface as defined in Figure 6. Value in parenthesis reflects polarizable solute. [j] Same as i, but with quantum chemical charge representation. A (–) denotes failure of the wave function to converge.

[k] Dispersion interaction energy estimate, from eq. (6), γ from experimental ionization potentials (see Appendix 4). [l] Water-radius added to van der Waals radii to determine the boundary surface. [m] DZP basis set. [n] STO4-31G basis set.

With the safe solute-boundary distance, the electrostatic component is small, but adding the dispersion leads to quantitative agreement on both solvation energy and the difference between the rotamers (entries 4-6 in Table 6).

Various solutes

The *Z–E* rotamer equilibrium of N-methylacetamide provides an example of the possible usefulness of the dielectric-only solvation model if adjusted sensibly. The model is usually claimed to be successful with the close boundaries that, however, failed for this particular example. To investigate the scope of the dielectric-only solvent model a number of solutes were solvated using a variety of approaches. The calculated electrostatic and dispersion contributions to the solvation free energy of a number of solutes in water in the Onsager approximation, and in general shape dielectric-only solvent models are collected in Table 7. The charge distribution was described either classically or quantum mechanically, and the boundary surfaces were either close (scaled van der Waals radii) or distant (solvent accessible surface with van der Waals plus solvent radii). The experimental solvation energies and the model cavitation free energies are also shown in Table 7. In the dielectric-only model, the interaction free energy ΔG_{int} should be reproduced by the sum of electrostatic, dispersion, and repulsion interactions. The model does not allow for an estimate of the dispersion interaction for a classical charge representation, but an estimate can be given for a quantum-mechanically described solute. We have not attempted to calculate the repulsion interactions between solute and solvent.

It is clear from the results presented in Table 7 that there are grave problems with the dielectric-only models. None of the approaches can be applied consistently for all solutes. The Onsager model is too crude because it only considers the overall dipole. Other features of the charge distribution are ignored. The results for the electrostatic part of the interaction energy for the classical and quantum-mechanical representations of the solute are seen to agree reasonably for the smaller molecules, whether the polarizability of the solute is accounted for or not. This is a confirmation of the quality of the classical representation of the quantum-mechanical charge distribution, already pointed out in the previous section. Problems arise with the larger molecules like toluene and benzene. The standard van der Waals surface is too close to the solute and ‘charge leakage’ occurs, giving an artificially large interaction energy. This problem is seen more acutely when the solute is allowed to respond to its own reaction field. The charge density ‘creeps into’ the boundary, the total energy tending to minus infinity. This is the polarization catastrophe pointed out in section 1.5. It does occur for smaller molecules as well, depending on the details of the surface. The model we use has no mechanism to check this behaviour. Special measures have to be taken, e.g. compensating for the leaked charge, as is done by Miertuš *et al.*[62]

The sensitivity of the continuum model to the boundary-surface details is its major weakness. The dependence of the electrostatic and dispersion contributions to the free energy of solvation of water in water is shown in Figure 8. At the distance

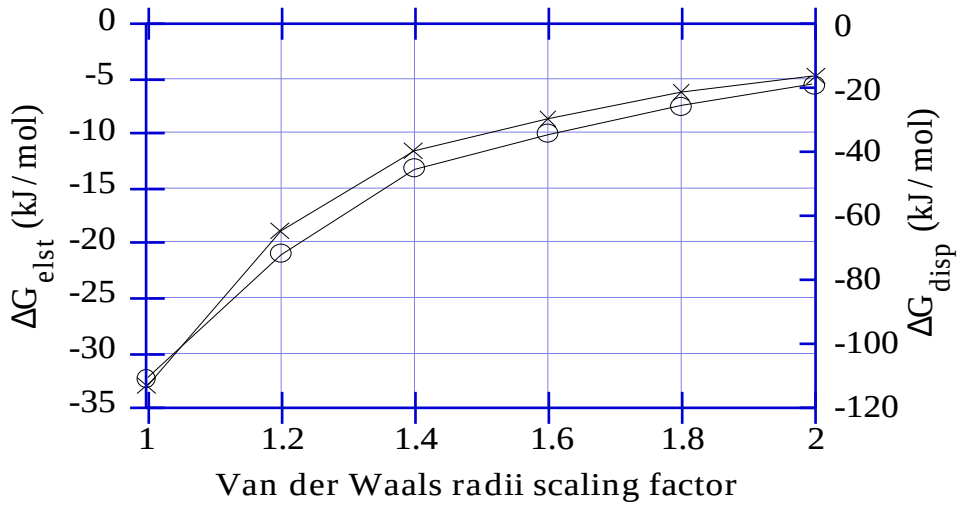

Figure 8. Continuum reaction-field stabilization energy of water in water as a function of the van der Waals radii scaling factor. ×: electrostatic component (left scale); ○: dispersion component (right scale). The boundary was Connolly's van der Waals surface with probe radius 3.64 Bohr (see Figure 6). The dielectric constant was 78.5, the optic dielectric constant 1.777.

we feel the requirements of non-overlapping systems and prevention of the polarization catastrophe are met (scaling factor of about 2, see the theoretical discussion in section 1.5), the electrostatic stabilization energy (≈5 kJ/mol) reasonably reflects the *bulk* contribution, but is far too small to be considered as *the* electrostatic part of the solvation energy. At smaller scaling factors the *electrostatic component alone* reproduces the free energy of solvation (26.5 kJ/mol, see Table 7). Several continuum models have been parameterized so the electrostatic component reproduces solvation free energies. This procedure has been validated by the observation that cavitation and dispersion–repulsion contributions tend to cancel.[188, 189]

If we consider the dispersion interaction as calculated in our approach, the failure of the dielectric-only model with the close boundary stands out. The dispersion energies are seen to be quite large, or even absurdly large. Realistic estimates may be made from explicit, polarizable solvent models, and we shall discuss the dispersion interaction in the next section, which deals with the explicit solvent models.

Explicit solvent models

Although computationally more costly than dielectric continuum models, explicit solvent models are worth studying in their own right since they provide so much more information on and insight into the factors that play a role in the solvation process. The main advantage is that explicit solvent models are expected to be more generally valid because their parameterization is at a deeper level than that of the dielectric models.

A number of the solutes studied in the previous section were immersed in a number (25 or 26) of our explicit, polarizable water molecules. A Monte Carlo sampling of the translational and orientational degrees of freedom was performed.

Table 8. Solvation energies[a] of various solutes in water, calculated by the explicit solvent model.[b]

Solute	ΔU_{elst}	ΔU_{disp}	ΔU_{rep}	ΔU_{int}	ΔU_{solv}	ΔU_{exp}
H_2O[c]	-66	-39	+40	-65 ± 8	-35	-41
CH_3COCH_3[c]	-52	-76	+53	-75 ± 12	-33	-40
CH_3CN[d]	-53	-56	+48	-61 ± 11	-32	-32
CH_3OH[d]	-40	-54	+40	-54 ± 8	-61	-44

[a] All energies in kJ/mol. [b] ΔU_{solv} is calculated by eq. (17). The solvent translational and rotational degrees of freedom are sampled in 50,000 Monte Carlo steps. [c] 26 surrounding water molecules. [d] 25 surrounding water molecules.

The energy of solvation was calculated by subtracting the average total energy of the solvent molecules alone from that of the solute plus solvent system [eq. (17)]. The interaction components have been analysed. The results are shown in Table 8.

The results of the explicit solvent model deserve some discussion. The solvation energies of water, acetone, and acetonitrile are seen to be in quite good agreement with experiment.[182] Only the solvation energy of methanol in water is some way off the experimental value. This may be due to insufficient sampling, in combination with equilibration of the system before collecting the data. In the runs we have performed the number of sampling steps is rather small (about 2,000 trial moves per solvent molecule). As far as the *interaction* energy between solute and solvent is concerned, proper equilibration was not very important. This was not so for the solvation energy, which is a difference between two total energies. The reliability of the results will improve if the sampling is extended—it is known that Monte Carlo sampling is thorough but slow. It would be well worthwhile to study the DRF force field with more sophisticated and direct thermodynamic ways to obtain the solvation energy. Nevertheless, the present results show the general validity of the explicit water model. Rullmann has applied this model to calculate protonation energies of amines in water,[99] obtaining excellent agreement with experiment, probably because his simulations were more extensive, both in number of MC steps and in number of solvent molecules considered.

The interaction energy of water in water was investigated in more detail. The aims of this study are the comparison of the quantum-chemical description of the solute to the classical one, and the investigation of the extent to which solvent molecules need to be described explicitly. First, the water pentamer was studied. The central water is surrounded by four water molecules. The surrounding molecules are placed at optimal distances and angles, taken from the water dimer. This configuration is studied both with and without a surrounding dielectric continuum to estimate the bulk contribution. Next, a Monte Carlo sampling of the orientational degrees of freedom is performed, keeping the centres of gravity at their original positions. Finally, translational freedom of the surrounding molecules is allowed as well. The results of these calculations are presented in Table 9.

Table 9. Total interaction energy of a water molecule with surrounding water and analysis of the interaction contributions.[a] Comparison of the description of the solute charge distribution.

Solute / Solvent Model[b]	ΔU_{int}	ΔU_{elst}	ΔU_{disp}	ΔU_{rep}
DZP / 4 classical[c]	-60±5 (-67)	-77 (-89)	-15 (-15)	+27 (+30)
DZP / 4 classical + diel.[d]	-66±5 (-81)	-79 (-89)	-18 (-18)	+26 (+30)
Clas. / 4 classical[c]	-58±5 (-76)	-74 (-81)	-26 (-27)	+28 (+30)
Clas. / 4 classical + diel.[d]	-70±5 (-86)	-72 (-82)	-25 (-27)	+28 (+30)
DZP / 26 classical + diel.[e]	-69±17 (-68)	-67 (-72)	-30 (-32)	+40 (+39)
Clas. / 26 classical + diel.[e]	-65±8 (-72)	-66 (-69)	-39 (-41)	+40 (+39)

[a] All energies in kJ/mol. The values in parentheses reflect the reference, or start, geometry. [b] DZP indicates the solute water being treated quantum mechanically in the DZP basis; Clas. indicates the solute water being treated classically, like the surrounding water molecules (parameters for the classical water [experimental molecular polarizability] may be found in Appendix 2); Diel. denotes the addition of a dielectric continuum term (the boundary is located at the solvent accessible surface, traced out from spheres located at the water centres of gravity). [c] 15,000 trial moves, rotation only. [d] 15,000 trial moves, rotation and translation. [e] 100,000 trial moves, rotation and translation.

The agreement between quantum-mechanical and classical descriptions has been pointed out before. There are some comments to be made on this, however. Although the agreement between mixed and fully classical descriptions is good for the total interaction energy between solute and solvent, this may not be so for the individual components. This is especially true for the dispersion interaction, which is invariably larger for the classical solute than it is for the quantum-mechanical one. This is explained by the fact that the classical solute model reproduces the experimental polarizability of water very well, whereas the DZP basis falls well short, which has been noted in section 3.2. On the other hand, the electrostatic interaction is seen to be larger in the quantum-mechanical solute case. This is due to the use of the basis set, which extends more into the solvent than the point charges do in the classical treatment.

The main solute–solvent interaction is seen to be captured by including only the first solvation shell. For water in water building the first solvation shell is easy, as the structure of the water pentamer is quite well known. For other solutes and solvents such a procedure would be more difficult. Including only the first solvation shell in the way it is done here can be deceptive, though. All solute–solvent interactions are optimal. This may be true at zero Kelvin and in the gas phase, but it is not a realistic picture of the condensed phase at room temperature. Allowing rotation of the four first-shell molecules already raises the energy, and allowing translation reenforces this trend. As more solvent molecules are added, saturation will occur. As far as the interaction between solute and solute is concerned we suggest that the 26 water molecules, which correspond to two to three solvent shells, are adequate. For accurate calculations on thermodynamic processes, such as solvation energy, boundary effects may necessitate more explicitly described solvent molecules before

Table 10. Solvation and transfer free energies[a] of benzene in various solvents in the dielectric-only solvent model.[b]

Solvent	$\Delta G_{solv,exp}$[c]	$\Delta G_{trans,exp}$[d]	ΔG_{cav}[e]	$\Delta G_{int,calc}$	$\Delta G_{trans,calc}$[d]
Benzene	-31.0	0	+25.8	-11	0
n-Hexane	-29.8	+1.2	+23.1	-11	-3
Methanol	-26.0	+5.0	+19.9	-25	-20
Water	-3.6	+27.4	+6.7	-57	-65

[a] All energies in kJ/mol. [b] The number of boundary elements was approximately 300. [c] Experimental solvation energy, ref. 200. [d] Free energy of transfer, respective to benzene. [e] Cavitation free energy, eq. (15), parameters are given in Appendix 4.

terminating in a continuum, as well as more extensive sampling or more advanced thermodynamic techniques.[191] Nevertheless, it is clear that addition of a discrete first solvent shell is an essential improvement on the dielectric-only model.

Transfer Free Energy of Benzene

The dielectric-only solvent model has been applied almost exclusively to aqueous solutions, and has been optimized for that purpose. In this section the generality of the dielectric-only and explicit solvent models is investigated by applying them to non-aqueous solvation. The transfer free energy is defined as the free energy of transferring a solute molecule from one solvent to another.[199] The solvation free energy of benzene in benzene, hexane, methanol, and water is calculated by the same procedure as used for the various solutes in water by the dielectric-only model. The boundary is placed at the 'van der Waals plus solvent' radii to comply with the no-overlap criterion advocated in section 1.5. (If the boundary surface is Connolly's van der Waals surface of benzene, the dispersion interaction [which is the dominant contribution] is calculated to be -340 kJ/mol.) The results are presented in Table 10.

It is all too clear from Table 10 that the dielectric-only model is not straightforwardly extended to accommodate solvents other than water. The lack of specific interactions in the dielectric continuum model must be repaired by choosing optimal solute–boundary distances for each solvent. The results for aqueous solvation discussed before do not give us confidence that such a reparameterization would lead to a solvent model that accommodates various solute classes, although such a parameterization was proposed recently for non-polar organic solvents.[88]

Conclusion

Dielectric-only solvent models encountered in the literature have been more or less parameterized to reproduce solvation energies for a number of solutes in water. The emphasis on aqueous solutions is understandable from its importance, especially in model studies of biological processes. In focusing on water, the specific interactions of water as a solvent must have entered the parameters other than the dielectric constant, limiting the generality of the dielectric continuum model. This necessitates reconsidering parameters that should be independent of solute and solvent, such as the boundary surface defining radii, if solvation in solvents other than water is of interest.

Modelling of the first solvation shell(s) by molecular electrostatic (and response) models does not suffer from the inconsistencies of the dielectric-only model. Such an approach is more costly, however, and there may be problems regarding the number of explicit molecules to be included before terminating the explicitly described region by a dielectric. Boundary effects should be minimized. The property of interest will decide to some extent the length to which one should go. If macroscopic thermodynamic properties are wanted, such as solvation energies one should not be easily satisfied. If, however, the potentials and fields at a microscopic region due to the surrounding medium are of interest explicit description of the first two shells will generally suffice.

Solvatochromism 3.4

Introduction

SOLVENT EFFECTS on electronic spectra have long been the subject of fundamental and applied studies.[201-204] The aim of that research has primarily been to provide both qualitative and quantitative characterization of the various solvents. Solvent polarity scales derived from electronic transitions serve in correlating structure and activity in many areas of chemistry.

The computation of solvent effects from molecular models has followed the qualitative theories in an attempt to quantify the parameters appearing in the theory.[103, 204] The standard models are based on a dielectric continuum description of the solvent surrounding the solute placed in a cavity. Variations on the generic Onsager 'dipole-in-a-sphere' model have evolved with computing resources and range from a description of the system as a simple dipole in a sphere to a semi-empirical or *ab initio* quantum mechanically described solute in an arbitrarily shaped cavity. Although useful, these methods fail to reproduce the red shift of electronic transitions in non-polar solvents, which has been attributed to the absence of dispersion interaction modelling. Recently, dispersion has been added to the model with good results,[185] but the dielectric-only models still fail to provide a detailed analysis of the interaction components and are not generally applicable to all solvents, so the need for explicit solvent models has been recognized and acted upon.

There are several methods that combine a quantum-mechanical description of the solute with a classical description of explicit solvent molecules for the calculation of solvent effects on electronic transition energies.[205-208] However, because of the lack of an explicit polarizability model of the solvent molecules, most of these models still fail to reproduce the red shift of electronic transitions in non-polar solvents. The Direct Reaction Field (DRF) approach does provide a way to estimate the dispersion interaction between solute and solvent through an explicit polarizability model for the classical mechanically described solvent molecules. This estimate is based on comparing the second order perturbation (SOP) expression in the Unsöld approximation to the two-electron reaction-field contributions to the total energy, as was demonstrated in section 3.2.

$\pi^* \leftarrow n$ Transition of Acetone

To elucidate the importance of the different interaction components contributing to the shift, and to investigate the usefulness of the different solvent models, the $\pi^* \leftarrow n$ transition of acetone was calculated in water, in acetonitrile (MeCN), and in tetrachloromethane (CCl_4).[209-211] The solvatochromic shift of this transition underlies one of the less successful solvent-polarity scales, Φ.[202] It was chosen because it

Table 11. Ionization energies and dispersion scaling parameters.

Molecule	IE (eV)[a]	γ in water[c]	γ in MeCN[c]	γ in CCl_4[c]
Acetone, S_0	9.69	0.565	0.557	0.543
Acetone, S_1	5.88[b]	0.682	0.675	0.662
Water	12.6			
MeCN	12.2			
CCl_4	11.5			

[a] Ionization energy, taken from the CRC Handbook of Chemistry and Physics. [b] The S_1 state was taken to be 3.81 eV above the S_0 state.(this is about halfway between the computed and experimental values). [c] $\gamma = U_S/(U_S+U_A)$, with U_S and U_A the IE of solvent and solute, respectively.

has been studied previously by other groups with both dielectric continuum[185, 212] and non-polarizable molecular solvent models,[205, 206, 208] and for reasons of computational feasibility.

Results

The solvent models employed in this study are the dielectric continuum model and an explicit solvent molecule model, in which 26 classically described, polarizable solvent molecules surround the solute, the solute and solvent molecules being surrounded by a dielectric. To comply with experimental conditions, a modest Monte Carlo (MC) sampling of the solvent molecules' translational and orientational degrees of freedom was performed. The solute is treated quantum mechanically, using the closed-shell RHF wave function for the ground (S_0) state and the open-shell ROHF wave function for the first singlet excited (S_1) state, as implemented in HONDO8.1. The scaling parameter γ for the dispersion interaction[29, 55] [eq. (6)] is different for the S_0 and S_1 states and for each solvent. The ionization energies and computed γ's are given in Table 11.

The computed transition energies, for the reference geometry as well as the Monte Carlo averages, are given in Table 12. The analysis of the different contributions for the explicit solvent model is presented in Table 13.

Discussion

The results presented in Table 12 show first of all that the standard dielectric-only model (Dielectric I) cannot be applied for all solvents in a consistent way. For water as a solvent, the standard model *without* dispersion reproduces the experimental blue shift very well, but adding dispersion destroys the agreement completely implying a reparameterization of the standard model for water if dispersion is to be included. A reparameterization will not be easy as the dispersion contribution to the shift is larger than the electrostatic contribution.

The standard model without dispersion (Dielectric I), that does so well for water, fails for MeCN. The reaction field from a dielectric continuum hardly differs between media with dielectric constants of 78.5 and 37.5. This can be seen from the

Table 12. Computed excitation energy shifts (in cm^{-1}) of acetone[a] in H_2O, MeCN, and CCl_4 for different solvent models.

Solvent model	Shift in H_2O[b]	Shift in MeCN[b]	Shift in CCl_4[b]
Dielectric I[c]	-1,803 (+1,624)	-1,848 (+1,579)	-4,203 (+675)
Dielectric II[d]	-171 (+293)	-44 (+166)	-33 (+411)
Explicit solvent, reference[e]	+1,639 (+2,788)	+620 (+1,597)	-216 (+57)
Explicit solvent, MC average[f]	+1,821 ± 330	+922 ± 310	-381 ± 75
Experimental[g]	+1,700 ± 200	+400 ± 200	-350 ± 200

[a] STO4-31G basis for acetone. Vacuum ground state energy: -191.6776986 Hartree; vacuum excitation energy: 26,962 cm^{-1} (exp.: 36,100±100 cm^{-1}, ref. 209). [b] A negative value indicates a red shift. The values in parentheses are the values obtained by removing the dispersion contribution. [c] Boundary at Connolly surface obtained with atomic radii equal 1.2 times the van der Waals radii (standard model). [d] Boundary at Connolly surface obtained with atomic radii equal the van der Waals plus solvent radii. [e] Lowest energy geometry in an all-classical MC sampling. [f] Average over 7,000 MC steps for water, 7,500 for MeCN, and 15,000 for CCl_4, treating the acetone molecule quantum mechanically. [g] From refs. 209-211.

generic Born and Onsager reaction-field stabilization energies, eq (14). As was the case for water, adding the dispersion contribution results in a red shift. When the solvent size is accounted for (Dielectric II) the model still fails, as it does for water. The shifts without dispersion are too small and adding dispersion only makes it worse. Reparameterization of the solute–solvent boundary distance, distinguishing between electrostatic and optical reaction-field components would be necessary to obtain a dielectric-only model with correlating power.

For CCl_4 the dispersion contribution in the standard dielectric-only model is far too large, as it is for water, but it is required to get a red shift in CCl_4 at all. Here, by moving the boundary to a larger distance agreement between model and experiment can be obtained, but this requires a new parameterization of the appropriate solvent and solute sizes. Moving the boundary by a full solvent radius is obviously too much to obtain quantitative agreement between experiment and dielectric model.

The discrete solvent model, apart from reproducing the experimental solvent shifts very well, provides valuable insight into the importance of different contributions to the shifts in such diverse solvents as water, MeCN, and CCl_4. It is seen in Table 13 that the dispersion plays an important role in both the blue shift in the polar solvent and the red shift in the non-polar solvent. Without accounting for the dispersion contribution, the shifts in water and MeCN are calculated too large by as much as 1,200 and 1,000 cm^{-1}, respectively, and the red shift in CCl_4 is not reproduced at all. For water, the electrostatic shift contribution is the dominant one, confirming the qualitative explanation of the blue shift as originating from preferential solvation of the ground state. In the non-polar CCl_4 the electrostatic contribution is negligible, as expected, and the shift is almost entirely due to the dispersion interaction.

Table 13. Analysis of the contributions to the excitation energy shifts (in cm^{-1}) of acetone in H_2O, MeCN, and CCl_4 for the explicit solvent model.

Energy component	H_2O		CH_3CN		CCl_4	
	ref[a]	MC[b]	ref[a]	MC[b]	ref[a]	MC[b]
Polarization	-608	-611	-518	-298	-48	-75
Induction	+888	+903	+974	+512	+96	+151
Electrostatic	+2,509	+2,726	+1,141	+1,673	+9	+18
Dispersion	-1,149	-1,197	-978	-965	-273	-475
Total	+1,639	+1,821	+620	+922	-216	-381
Experimental	+1,700 ± 200		+400 ± 200		-350 ± 200	

[a] Reference geometry, obtained after equilibrating solvent molecules to classically described acetone.
[b] Monte Carlo average. 7,000 steps for water, 7,500 for MeCN, and 15,000 for CCl_4.

The MC sampling of the solvent degrees of freedom does not modify the qualitative picture given above for water, but improves the quantitative agreement for CCl_4. The number of MC steps was limited to around 10,000 because of extremely high CPU demands (circa 90 CPU hours on a CRAY-YMP for 15,000 configurations). For water the number of MC steps is probably too small to give reliable statistics of the orientation polarization, and further sampling will be necessary on this system. This seems even more so for MeCN, for which the MC results deviate appreciably from the reference geometry result. Acetonitrile is a difficult solvent to model, because of the tendency to form dimers—in which the monomer dipole moments are anti-parallel—in the liquid phase. This is reflected in the fact that its dielectric constant is smaller than one expects from the acetonitrile dipole moment.[203] To overcome the computational demands, it may be worthwhile to generate an ensemble from an all-classical MC before applying the combined quantum-mechanical–classical mechanical calculations for ground and excited state.[205]

It is perhaps surprising that the dispersion contribution to the solvent shift is larger for water than it is for CCl_4, because the latter has the larger molecular polarizability. In fact, the dispersion *interaction* between acetone and water is larger than between acetone and CCl_4. This is due to the distance factor in the dispersion interaction. Recall the SOP expression for the dispersion [eq. (4)], in which the intermolecular distance enters to the inverse sixth power. The mean distances of the closest solvent molecules were calculated from the radial distribution functions of the Monte Carlo simulations and are shown in Table 14, together with the calculated dispersion interaction. The ratio between the dispersion interactions for water and CCl_4 is seen to compare very well between the London approximation for the closest six solvent molecules and the Monte Carlo results, confirming the quality of the approach adopted here. Although the molecular polarizability of CCl_4 is larger than that of water by a factor of 7 (see Appendix 4), the mean distance of the closest solvent molecules to the acetone molecule is smaller for water than for CCl_4 by a factor of 0.65, and so explains the larger interaction between acetone and water compared to CCl_4.

Table 14. Mean acetone–solvent distances for the six closest solvent molecules in Monte Carlo simulation for water and CCl_4, computed London prefactor, and computed total dispersion interaction between the solvent and acetone.[a]

Solvent	$\langle r_{Ap} \rangle$ (Bohr)[b]	Prefactor[c]	ΔE_{disp}^{London} [d]	ΔE_{disp}^{DRF} [e]	ratio[f]
H_2O	7.0	8.5	-17	-80	4.7
CCl_4	11.4	57.8	-6.5	-28	4.3

[a] All energies in kJ/mol. [b] Brackets denote average over ensemble as well as closest six molecules. [c] Prefactor for London formula, equal $3\alpha_2 U_2 / 2(U_1 + U_2)$, in which 1 denotes acetone and 2 the solvent. [d] London formula: $\Delta E_{disp}^{London} = -\{3\alpha_1\alpha_2 U_1 U_2 / 2(U_1 + U_2)\} \langle r_{Ap} \rangle^{-6} * 6$, with experimental polarizabilities and ionization energies (see Appendix 4). [e] Total dispersion interaction between acetone in ground state and surroundings in Monte Carlo simulation. [f] $\Delta E_{disp}^{DRF} / \Delta E_{disp}^{London}$.

Conclusion

Computation of the solvent effect on the electronic transition of acetone is possible with a general explicit solvent model for such diverse solvents as water, acetonitrile, and tetrachloromethane. Standard dielectric-only models fail in reproducing the solvent shifts. They could still be useful in an engineering sense if new parameterizations are found. The reparameterization should at least take the solvent size into account and should probably employ different cavity surfaces for electrostatic (ε_s) and optical (ε_∞) reaction-field components.

The computation of the dispersion interaction, as well as the induction and polarization components of the classical partition require an explicit polarizability representation of the classical partition, which is present in our force field. The only parameters required for the dispersion are the ionization energies (IEs) of solute and solvent, available from experiment or computation. The dispersion scaling factors [eq. (6)] are not very sensitive to errors in the IEs: a 10% error in the solute or solvent IE results in a 3-5% error in γ, corresponding to an error of 25–50 cm^{-1} in the calculated shift. The error made as a result of the Unsöld approximation itself is not included in this assessment. Thus the explicit solvent model with polarizability may be used to provide both qualitative insight in and quantitative information on electronic transition energy shifts in any solvent in a generally applicable formalism.

The Nature of Dielectric Behaviour 3.5

Introduction

IN THE PRECEDING APPLICATIONS of various solvent models it has become clear that the dielectric continuum-only model has severe limitations, although it may be very useful in obtaining quantitative solvation energies in an engineering context. The breakdown of this model is due to the violation of the assumptions under which the model has been derived, notably the non-linearity, or saturation, effects that dominate the behaviour of the first few solvent shells. This saturation expresses itself in the orientation component of the response in polar solvents: the dipolar interactions with the solute are strong enough to hamper rotation of the solvent molecules in the first solvent shells. Deviation from dielectric behaviour due to the electronic component is often assumed to be much smaller, or absent. Whereas for the orientation component the homogeneity and anisotropy of the first solvent shells is readily acknowledged, current practice for the electronic component assumes homogeneity and isotropy on a microscopic scale. This assumption shows up in the popular use of an 'internal dielectric constant' of 2 to 6 to screen charge–charge interactions in simulations of biomolecular systems. Another example of the use of dielectric constants appears in dielectric continuum reaction-field approaches for the computation of solvation energies and solvent effects. Here the interior of the cavity is given a low dielectric constant, effectively reducing the reaction field from the bulk. In this section the behaviour of charge–charge interactions moderated by explicit polarizabilities is examined to investigate the validity of the use of such 'local dielectric constants', and distance-dependent dielectric screening functions. The validity of using internal dielectric constants in continuum models is investigated by the calculation of the KCl dissociation curve in a dielectric.

The Dielectric Function

The dielectric constant (ε) of a material is derived for macroscopic systems as the response of a bulk-amount of material to an applied electric field (section 1.4).[52, 53] The electric field can be generated by charging two plates in a capacitor, for example. The effect of the material intervening between the plates is to reduce the interaction between the plates with respect to vacuum, so the repulsion or attraction (depending on whether the plates carry like or unlike charge) between the plates is less. This effect is called screening, as the presence of the charge on one plate is made less apparent to the charge on the other. The rearranged charge distribution in the intervening material generates a field that opposes that of the charged plate.

The dielectric constant is next encountered as a scaling parameter in Coulomb's law for the force between interacting charges q_i and q_j connected by a vector $\mathbf{r}_{ij}$:

$$\mathbf{F}_{ij} = \frac{q_i\, q_j\, \mathbf{r}_{ij}}{\varepsilon \left| \mathbf{r}_{ij} \right|^3} \tag{18}$$

with the same scaling holding for the potential energy. It is very important to keep in mind that eq. (18) is a 'macroscopic formula', i.e. it holds for macroscopic charges and distances, and moreover, only if the charges are *completely* immersed in the material for which 'ε' stands, which is supposed to be homogeneous and isotropic. One must realize that the linear response of (bulk) material is the result of averaging the microscopic responses over a volume which may be microscopic on an everyday scale, but must be macroscopic on the atomic scale. Jackson gives a volume of 10^6 cubic Å as an absolute lower limit to the macroscopic domain.[52] Hence, the charges in eq. (18) should be about 100 Å apart, and the boundaries of the bulk material in which they are immersed should also be that far away from them!

Computational chemists mainly deal with *microscopic* systems in which charge densities—and associated potentials, fields, and responses—vary wildly. However, all properties of such systems are also obtained as *averages*. For example, the induced polarization **P** in bulk material for a weak external electric field **E** is given by:

$$\mathbf{P} = \chi_e\, \mathbf{E} \tag{19}$$

in which χ_e is the electric susceptibility. **P** is the average dipole *density* of a macroscopic volume (ΔV) of that material, and gives rise to a dipole moment **M**:

$$\mathbf{M} = \left(\chi_e\, \Delta V\right) \mathbf{E} \tag{20}$$

reflecting the change in the average positions of (bound) charges due to the presence of the field. From eq. (20) we see that $\chi_e\, \Delta V$ may be interpreted as the macroscopic polarizability of ΔV.

If the description of the system is explicitly quantum mechanical, the average is taken over the charge density *via* the wave function, but, dropping mathematical rigor for the moment, it is effectively the average over a *volume* which is typical for the size of the system. For example, if the potential *inside* an atomic ion is calculated, the result will reflect the variations in the charge density. Restricting the integration over the charge-density to the volume inside a spherical surface, the result for a measurement-point just outside the volume of integration goes smoothly to that for a point charge located at the ion's nucleus in the limit of extending the integration beyond the last maximum in the charge density.

The microscopic analogue of eq. (20) is:

$$\mu_{ind} = \alpha\, \mathbf{E} \tag{21}$$

with α the system's polarizability, and again describes the changes in the average positions of the charges in the field. We note that eq. (21) is applicable only if **E** is *external*, i.e. sources are located outside the system's 'volume', and the averaging is

done over that complete volume as is implied in the expectation value of μ_{ind}. Here too, the details of the actual charge distribution are lost.

All this is well known of course and is the basis for systematically going from integral approximations in *ab initio* methods to semi-empirical approaches and, finally, to the development of classical 'force fields'. It is particularly in using screening parameters in force fields that many computational chemists tend to forget about the macroscopic nature of dielectrics and the dielectric constant. In microscopic force fields the screened Coulomb's law [eq. (18)] is applied between charges, the screening factor usually ranging from 2 to 6, based on measurements of the permittivity of proteins, while optimization of force fields even leads to distance-dependent 'dielectric constants'.

A number of popular force fields employ a distant-dependent effective dielectric function for the calculation of electrostatic interactions:

$$\Delta U_{elst} = \sum_{i<j} \frac{q_i\, q_j}{4\pi\, \varepsilon(r_{ij})\, r_{ij}} \tag{22}$$

accompanied by a reference to Warshel and Levitt. An effective $\varepsilon(r)$ was introduced by Warshel and Levitt[93] to calculate approximately self-consistent orientations of Langevin dipoles, modelling water surrounding lysozyme, in order to avoid the costly self-consistent calculations, such as described in Chapter 2. Their approach was an engineering one, first going through the self-consistent calculation and then finding a best fit of the $\varepsilon(r)$ to the effective field of source charges at the dipoles. They expressly mention that this effective, distance-dependent dielectric constant was *not* used in the calculation of the interaction between the source-charges within lysozyme. They did, however, use the same approach to calculate the induced dipoles at explicitly described polarizabilities within the lysozyme. For this, they found that the $\varepsilon(r)$ was hardly distance dependent, and used the average value of 1.36. Again, this effective ε was not applied to the direct charge–charge interactions. The effect of the polarizabilities on the total energy was obtained as the interaction between the induced dipoles and the charges:

$$U_{tot} = \frac{1}{2} \sum_{i,j} \frac{q_i\, q_j}{r_{ij}} + \frac{1}{2} \sum_{i,k,j} q_i \frac{\mathbf{r}_{ik}^{\dagger}\, \mathbb{\alpha}_k}{\varepsilon(r_{ik})\, r_{ik}^3} \frac{\mathbf{r}_{kj}}{r_{kj}^3}\, q_j \tag{23}$$

which can never be cast into the form of eq. (22), even with additional fitting, the main obstacle being the appearance of the scalar products of vectors in eq. (23). The same holds for the self-consistent solution of this problem which leads [cf. eq. (2.35)] to:

$$U_{tot} = \frac{1}{2} \sum_{i,j} \frac{q_i\, q_j}{r_{ij}} + \frac{1}{2} \sum_{i,k,l,j} q_i \frac{\mathbf{r}_{ik}^{\dagger}}{r_{ik}^3}\, \mathbb{R}_{kl}^{-1} \frac{\mathbf{r}_{lj}}{r_{lj}^3}\, q_j \tag{24}$$

Employing effective dielectric constants in microscopic calculations is a result of scaling the macroscopic concepts down to microscopic dimensions. Knowing the limitations set on a macroscopic dielectric—homogeneity, isotropy, and linearity—the validation of the use of local, microscopic, dielectric constants is all but clear. The case against the physical meaning of *any* linear response theory to the description of microscopic behaviour has even been made.[213] We therefore investigate how charge–charge interactions are influenced on a microscopic scale by polarizable material, and under what conditions macroscopic-like dielectric behaviour may be expected.

The microscopic model underlying a macroscopic dielectric consists of a filling of space with interacting polarizabilities of some magnitude. On the chemical scale, 'units' of polarizability are typically molecular polarizabilities. We therefore choose to fill the space with polarizable spheres of radius 3.64 Bohr and with a polarizability of 10 cubic Bohr. These values are obtained from liquid water properties at room temperature. We start with a one-dimensional system to get a grip on the basic rules governing the interactions between charges in a polarizable environment. We then generalize the insights gained from that exercise to three-dimensional systems. In the one-dimensional systems we use the term anisotropy to mean absence of left-right symmetry. This concurs with the three-dimensional notion of inequality of different directions.

The interaction between two test charges is calculated according to eq. (24), which in this specific case reads:

$$E(r_{12}) = E_{vac} + E_{scr}^{self} + E_{scr}^{int} = \frac{q_1\, q_2}{r_{12}} + \frac{1}{2}\sum_{k,l}\left\{ q_1 \frac{\mathbf{r}_{1k}^{\dagger}}{r_{1k}^3}\ \mathbb{R}_{kl}^{-1}\frac{\mathbf{r}_{l1}}{r_{l1}^3}\, q_1 + q_2 \frac{\mathbf{r}_{2k}^{\dagger}}{r_{2k}^3}\ \mathbb{R}_{kl}^{-1}\frac{\mathbf{r}_{l2}}{r_{l2}^3}\, q_2 \right\} + \frac{1}{2}\sum_{k,l}\left\{ q_1 \frac{\mathbf{r}_{1k}^{\dagger}}{r_{1k}^3}\ \mathbb{R}_{kl}^{-1}\frac{\mathbf{r}_{l2}}{r_{l2}^3}\, q_2 + q_2 \frac{\mathbf{r}_{2k}^{\dagger}}{r_{2k}^3}\ \mathbb{R}_{kl}^{-1}\frac{\mathbf{r}_{l1}}{r_{l1}^3}\, q_1 \right\} \tag{25}$$

in which k and l are the indices of the relay matrix $\mathbb{R}$ that formally couples all polarizabilities in the system [eq. (2.35)]. The interaction terms are the vacuum Coulomb interaction, the screening of the self interaction and the screening of the electrostatic interaction.

Basic Interaction Components

The first system studied is a one-dimensional array of polarizable spheres, shown in Figure 9. A linear array of polarizable spheres is touching each other exactly. Two spheres are given a unit charge at their centres, one positive, the other either positive or negative. The spheres carrying the charges are situated as indicated in Figure 9 with k left-neighbouring spheres, and m right-neighbouring spheres, and n spheres

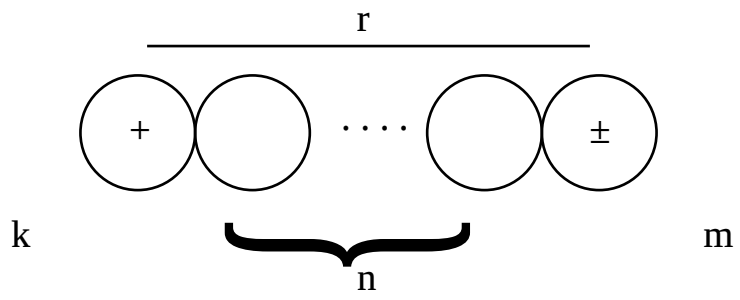

Figure 9. String of polarizabilities.

in between. The force between the charges is computed by finite difference from the interaction energy displacing the second charge by δ=0.01 Bohr in two directions:

$$\mathbf{F}_{\text{actual}}\ \mathrm{r} = -\frac{E\ \mathrm{r}+\delta - E\ \mathrm{r}-\delta}{2\delta} \tag{26}$$

and from this, the effective dielectric constant of that arrangement by:

$$\varepsilon(\mathrm{r}) = \frac{\mathrm{F}_{\text{vacuum}}(\mathrm{r})}{\mathrm{F}_{\text{actual}}(\mathrm{r})} \tag{27}$$

The first series of calculations are on a growing chain of polarizabilities with a fixed number (0, 1, or 4) of polarizable spheres just outside the charges. The computed effective ε as a function of interposed polarizabilities, ε(n), for both like and unlike charges for k=m=0 and k=m=1 are shown graphically in Figure 10.

It is immediately clear that the like and unlike charge combinations behave differently as concerns the effective screening on this microscopic scale. On closer examination, however, their behaviour operates on the same mechanism, *viz.* a tendency to be as close as possible to the *surplus* of polarizability. The unlike charges attract each other more than in vacuum, resulting in an ε<1, whereas the like charges start out behaving somewhat as if they were in a dielectric, but eventually start attracting each other, so that ε becomes negative. The cause of this effect is the anisotropy of the polarizable environment, combined with the increasing importance of the self-energy of the charges as the distance between them grows.

The contribution to the self-energy of a charge from a polarizable environment is the interaction between the charge and the dipoles it induces in the environment. The force from this contribution will be determined largely by the immediate surroundings, as the effective field at the surrounding polarizabilities falls off rather fast with the distance. As the direct charge–charge interaction becomes less, the behaviour of a charge will increasingly be determined by its immediate surroundings. The force resulting from the self-interaction of a charge in a polarizable environment as a function of anisotropy is shown in Figure 11, together with the magnitude of the self-interaction as the amount of polarizable material increases.

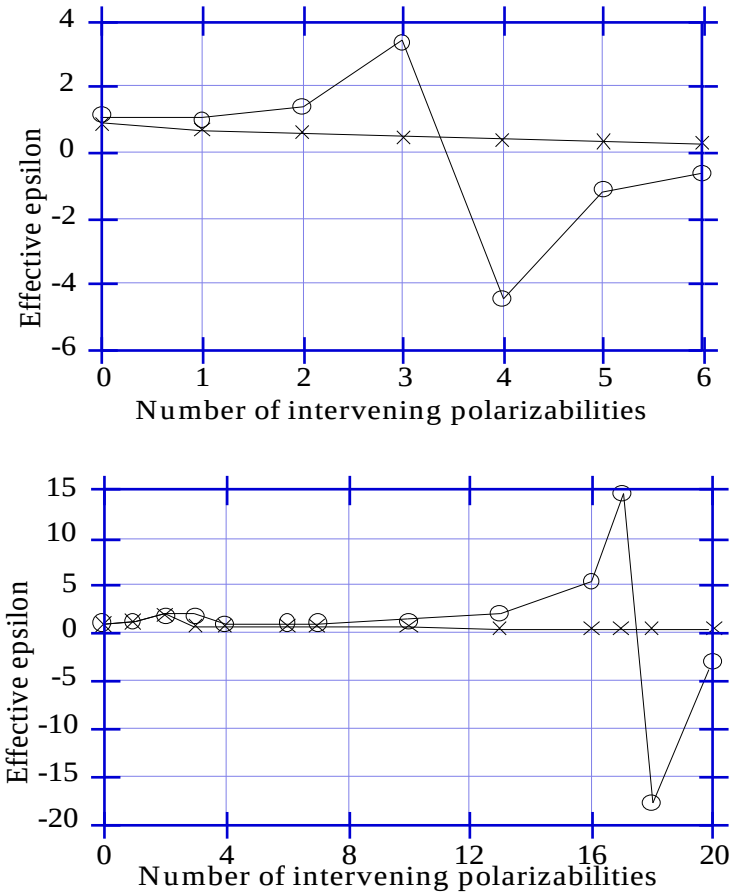

Figure 10. Effective ε for interacting charges in string of polarizabilities as a function of intervening polarizabilities.
○: + + charge combination; × : + - charge combination.
Top: figure 10a: k=m=0; bottom: figure 10b: k=m=1 (see Figure 9).

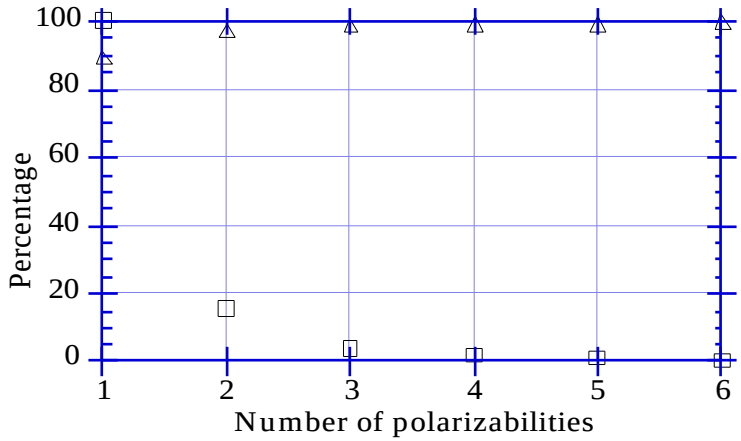

Figure 11. Study of self-interaction of a charge surrounded by polarizabilities. □: percentage of the force from the self-interaction on a single charge located at the ±-position in Figure 9, as a function of m, with k=29, relative to m=1; △: percentage of the self-interaction as a function of the number of neighbouring polarizabilities m, with k=m-1, relative to m=30 (see Figure 9).

The force from the anisotropy rapidly diminishes as more polarizable material is introduced on the right hand side of the charge, indicating that three to four polarizabilities should suffice to eliminate this component of the total force. Calculations with k=m=4 show that at distances of more than 200 Bohr (n>27), deviation from dielectric behaviour still occurs. Apparently the anisotropy, although energetically very small, eventually still dominates the charge–charge interaction.

Toward a Dielectric

Elimination of the anisotropy may be achieved by making sure the charges are surrounded by an infinite amount of polarizable material, which may be done in a computational sense by applying a dielectric continuum method. Therefore, the configuration of Figure 12 was examined. The dark spheres carrying the charges are embedded in a number of layers of polarizabilities, the whole being enveloped by a dielectric continuum, with ε=1.78. The result of the distance dependence of the effective screening between the charges for a box with fixed length of 31 polarizabilities is shown in Figure 13.

The most important conclusion to be drawn from the results presented in Figure 13 is that only in a situation in which the surroundings are as isotropic as possible, like and unlike charge combinations behave according to the same effective scaling law. Deviations seen from n=11 onwards indicate boundary effects, as the number of explicit polarizabilities between the charge and the dielectric becomes less than four.

The concept of a dielectric continuum, defined on a macroscopic scale, is not generally scaleable to microscopic dimensions. At microscopic dimensions, the requirement of anisotropy for dielectric behaviour will seldom be fulfilled, be it in the computational model or in the real system, as can be learned from looking at electronic density maps. It is the anisotropy of the immediate surroundings that cause deviation from dielectric behaviour, mainly because the self-energy of a charge

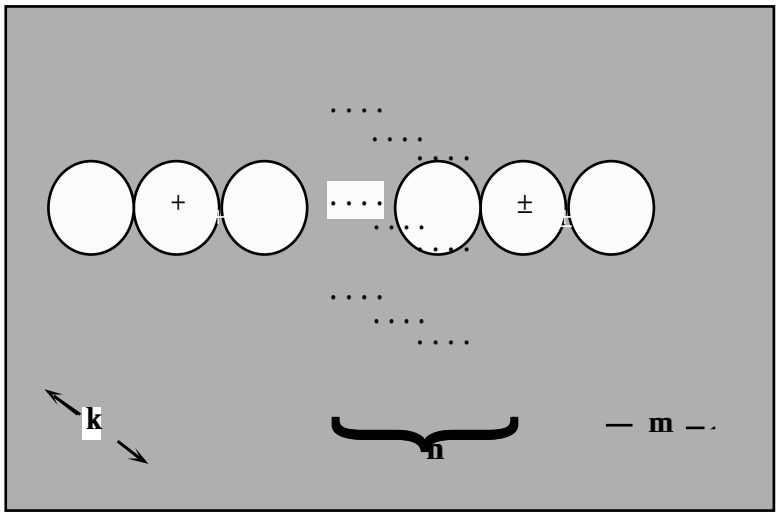

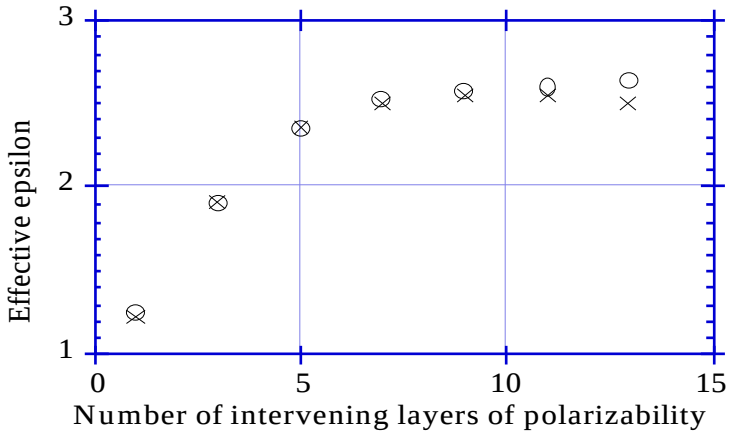

Figure 13. Effective ε for interacting charges in box filled with polarizabilities and surrounded by a dielectric continuum as a function of intervening layers (n) of polarizabilities (k=3, m=31, see Figure 12). ○: + + charge combination; × : + - charge combination.

is sensitive to the anisotropy. In a true dielectric, the self-energy of a charge is indifferent to the position of the charge in the dielectric, and hence does not contribute to the force.

On modelling 'low-dielectric' regions

In this section we investigate the effect of introducing a 'low-dielectric' region in the modelling of solvent effects as for example implemented in CHARMM[126] and DELPHI.[56] Solvation effects are often studied by solvating a vacuum Minimum Energy Reaction Path (MERP) in water by solving appropriate linearized Poisson-Boltzmann equations. To cite for instance Dejaegere *et al.*:[214]

> The solute molecules are treated as irregularly shaped objects whose interior has a uniform relative permittivity ε_i with point charges at positions corresponding to the atomic nuclei, as usual in a cavity in a dielectric continuum with ε=80. Any tendency for solvation to alter the charge distribution of the solutes (by electronic polarization effect, for example) is presumed to be included in ε_i; ε_i was set to 2.

Note that this is equivalent to setting ε_{out}=40, and leaving ε_i=1, since in the Poisson equation dielectric effects are only related to the *ratio* $\varepsilon_{out} / \varepsilon_i$.[58]

In the light of the preceding sections it is doubtful whether such a uniform screening is able to mimic the microscopic behaviour of the solutes. Therefore we treated a KCl molecule with our DRF approach. We first obtained part of the potential energy curve from RHF calculations, using a Wachters basis set for K[215] and Dunning's DZP basis for Cl.[148] Subsequently we solvated the system with the 'cavity-in-continuum-approach', first using the fully quantum-mechanical charge distribution and ε=80. This exercise was repeated, now using the DPCs[43] and ε=40, i.e. following the procedure suggested above. We also used a fully classical model

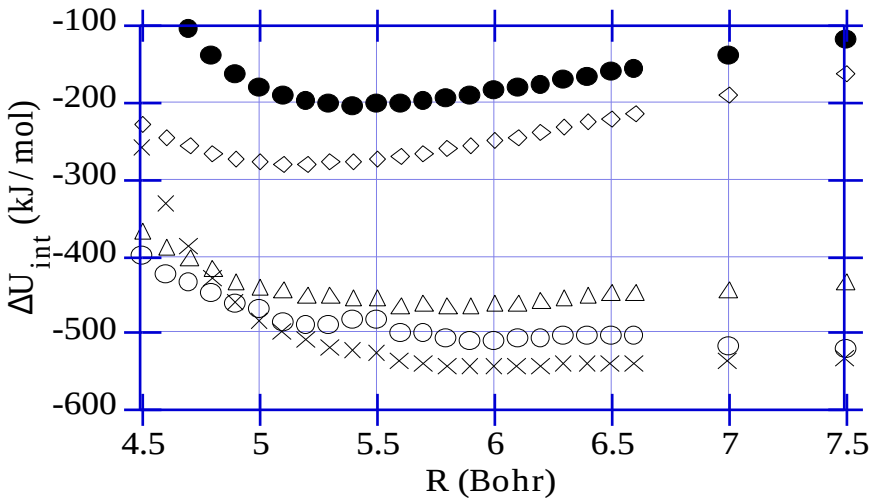

Figure 14. Solvation of KCl in various approximations. ◇: QM representation, vacuum; ●: Classical representation (charge-transfer correction), vacuum; ○: Solvated QM representation, ε=80; ×: Solvated classical representation, ε=80; △: Solvated point charges, ε=40.

with experimental atomic radii[216] and polarizabilities for K^+ and Cl^-.[123] In all reaction-field calculations we used a boundary defined by Connolly surfaces (see Figure 6), constructed anew for each interatomic distance, with the ionic radii multiplied by a factor of 1.3. This is slightly larger than the factor of 1.2 advocated by e.g. the Pisa group,[217] because for smaller distances no convergence was obtained in the SCF-DRF-RHF calculations, due to the relatively large basis set. Results are collected in Figure 14.

From Figure 14 we see that in vacuum the classical representation of KCl (●) does not do too badly in comparison with the RHF results (◇) although the DRF force field was not conceived for ionic cases. The agreement is obtained after correction with the experimental ionization energy and electron affinity. It leads to almost the same equilibrium distance and the curves have very similar shapes near this distance. The short-range repulsion is too hard, but only in the less important regime, as we have seen for the water dimer (section 3.2). Solvating the QM charge distribution in a dielectric with ε=80 (○) differs qualitatively from solvating only point charges in a dielectric with ε=40 (△), as expected. In the full treatment the molecule tends to dissociate, while in the point-charge-only treatment the atoms remain bound, albeit weakly. The difference between using a dielectric constant of 40 and 80 in either treatment is very small (maximal ≈2 kJ/mol, not shown). Accounting for the microscopic polarization of KCl is essential to get correct behaviour, which is demonstrated by the fully classical solvated case (×) which tends more to dissociation—like the fully quantum-mechanical case—than that of the solvated point charges.

Conclusion

The concept of a dielectric constant, defined on the macroscopic level, is not generally applicable at microscopic dimensions. Since the dielectric constant should be a real *constant* for homogeneous systems, or only a very slowly changing function of position, it is incompatible with a microscopic description of a system. The most important difference between 'dielectric' and 'microscopic' response behaviour is that the latter is dominated by local anisotropies which does not lead to general screening of Coulomb interactions. The actual difference between Coulomb interactions in vacuum and in the presence of some material with (linear) response on microscopic distances depends strongly on the geometry, the types and values of source charges, and on the response functions. Hence, in an arbitrary arrangement of charges of either type, with or without a dielectric around them, the 'response factor' can be anything. Failure of dielectric screening behaviour in proteins has been attributed to the nuclear response component.[218]

Fitting procedures are quite normal in the construction of force fields, but references to 'dielectric constants' in such procedures can be avoided—without any loss of validity within the fitting procedure—by using expressions like:

$$U = \sum_{i,j} \left[-\frac{A_{ij}}{r_{ij}^6} + \frac{B_{ij}}{r_{ij}^{12}} + \frac{C_{ij}\, q_i\, q_j}{r_{ij}} + \ldots \right] \tag{27}$$

for the 'non-bonded interactions', stressing that A, B, C, ..., and the q's are no more than (interdependent) fit-parameters which should not be interpreted as physically meaningful.

In contrast, the DRF parameters, in particular the charges and polarizabilities, are obtained as well-defined and independent properties of the subsystems and thus have to a large extent their usual physical contents. We conclude that the natural response functions for microscopic descriptions are local (dipole and higher) polarizabilities which are shown to behave to a large extent similarly to a full quantum-mechanical treatment of the system.

Conclusion 3.6

THE MODELLING of the condensed phase from first principles has been put to the test. The sensible models based on quantum-theoretical analysis of the interactions between molecules have proven feasible, useful, and necessary for the reliable calculation of solvent effects for a range of solutes and solvents. With the results of this work in hand we may step out confidently into application of this approach to many other areas of chemistry.

Future developments lie in improving the accuracy of the quantum-chemical and classical descriptions. This will be automatic as available computer power becomes available: the codes are there. The growing interest of computational chemists at the moment is in the dynamic properties of chemical systems. Chemists want to do chemistry! This is the edge of computational chemistry today. Codes are being written, refined, and generalized. The opportunity to step in with combined quantum-chemical–classical models must be taken.

A very important problem of the combined quantum-chemical–classical models is the transition between quantum-chemical and molecular mechanical regions, and between the discrete molecular and continuum regions. Especially the cutting of bonds, as it is encountered in cluster-calculations on solid-state and biological systems remains a most challenging problem. The models based on the separability into non-overlapping fragments fail. The development of a feasible approach to this problem in the spirit of the scheme presented in this thesis should be sought in the definition of small, transferable spectator groups which influence the electronic density through the (temporary) presence of occupied basis functions.

The practice of computational chemistry discussed in this chapter covers a wide range of specializations within the discipline. We have not been able to adhere to the standards of all disciplines. The wave functions could have been of higher quality, the thermodynamic averaging more extensive. The effort lies in the combination of specializations, mainly to demonstrate its possibility and added value. There remains a great need for sophistication and optimization of the techniques, to further enable the feasibility of sensible model calculations.

Appendix 3.7

1. General DRF force field parameters

Table A1. Atomic polarizabilities and radii for use in computation of induction, dispersion, and repulsion energies.

Damping[a]	Exponential	Linear	Repulsion	
Width-parameter[a]	2.089	1.662	I	II
Atom	polarizability[b]	polarizability[b]	radius[c]	radius[c]
H	2.881	3.469	2.516	2.267
C	8.672	9.482	3.518	3.213
N	6.526	7.457	3.247	2.929
O	5.304	5.871	2.989	2.872
F	3.200	3.577	–	2.778
Cl	17.61	17.61	4.324	3.307

[a] Thole's damping functions 1 and 4, respectively, see ref. 49. [b] In Bohr^3. [c] In Bohr.

The parameters given here are used throughout this thesis, unless noted otherwise. For the repulsion the radii of set I are used throughout, except for the benzene-derived dimers, for whom set II is used. Further deviation from the parameters given here is only for the polarizabilities of H and O in water when fitted to the DZP-polarizability (Table 1; Figure 2); and for H and C in the benzene SDPC, EDPC, SP and EP parameterizations, which are given in Appendix 3.

2. DRF Force-Field Parameters and Computed Molecular Properties for Molecules Used in this Thesis

Table A2. Atomic Cartesian co-ordinates, partial charges, computed overall dipole and quadrupole moments, and computed polarizability.

Molecule	X[a]	Y[a]	Z[a]	q[b]	μ, Θ[c]	α[d]
Water*					0.787	9.8
O	0.0	0.0	0.0	-0.796	-0.06	9.4
H (O1)	1.1031	1.4325	0.0	+0.398	1.26	12.3
H (O2)	1.1031	-1.4325	0.0	+0.398	-1.19	7.6

Table A2 (*continued*).

Molecule	X[a]	Y[a]	Z[a]	q[b]	μ, θ[c]	α[d]
Benzene†					0.0	61.5
C (1)	0.0	-2.63995	0.0	-0.1035	2.33	74.2
C (2)	-2.28626	-1.31997	0.0	-0.1035	2.33	74.2
C (3)	-2.28626	1.31997	0.0	-0.1035	-4.66	36.3
C (4)	0.0	2.63995	0.0	-0.1035		
C (5)	2.28626	1.31997	0.0	-0.1035		
C (6)	2.28626	-1.31997	0.0	-0.1035		
H (C1)	0.0	-4.68841	0.0	0.1035		
H (C2)	-4.06028	-2.34421	0.0	0.1035		
H (C3)	-4.06028	2.34421	0.0	0.1035		
H (C4)	0.0	4.68841	0.0	0.1035		
H (C5)	4.06028	2.34421	0.0	0.1035		
H (C6)	4.06028	-2.34421	0.0	0.1035		
Toluene†					0.11	74.4
C (1)	0.0	-2.63995	0.0	-0.1150	2.02	83.6
C (2)	-2.28626	-1.31997	0.0	-0.1097	2.00	92.0
C (3)	-2.28626	1.31997	0.0	-0.1533	-4.02	47.5
C (4)	0.0	2.63995	0.0	-0.1868		
C (5)	2.28626	1.31997	0.0	-0.1556		
C (6)	2.28626	-1.31997	0.0	-0.1043		
H (C1)	0.0	-4.68841	0.0	0.0991		
H (C2)	-4.06028	-2.34421	0.0	0.1016		
H (C3)	-4.06028	2.34421	0.0	0.1048		
C (7)	0.0	5.55013	0.0	0.3860		
H (C5)	4.06028	2.34421	0.0	0.1037		
H (C6)	4.06028	-2.34421	0.0	0.1015		
H (C71)	1.94202	6.23668	0.0	0.1028		
H (C72)	-0.97101	6.23668	1.68183	0.1118		
H (C73)	-0.97101	6.23668	-1.68183	0.1118		
o-Xylene†					0.20	86.8
C (1)	0.0	-2.63995	0.0	-0.1159	1.65	100
C (2)	-2.28626	-1.31997	0.0	-0.1205	1.73	103
C (3)	-2.28626	1.31997	0.0	-0.1563	-3.38	57.8
C (4)	0.0	2.63995	0.0	0.1331		
C (5)	2.28626	1.31997	0.0	0.1322		
C (6)	2.28626	-1.31997	0.0	-0.1566		
H (C1)	0.0	-4.68841	0.0	0.0973		
H (C2)	-4.06028	-2.34421	0.0	0.0973		
H (C3)	-4.06028	2.34421	0.0	0.1033		
C (7)	0.0	5.55013	0.0	-0.3815		
C (8)	4.80655	2.77507	0.0	-0.3849		
H (C6)	4.06028	-2.34421	0.0	0.1026		
H (C71)	1.94202	6.23668	0.0	0.1133		
H (C72)	-0.97101	6.23668	1.68183	0.1064		
H (C73)	-0.97101	6.23668	-1.68183	0.1064		
H (C81)	6.37213	1.43651	0.0	0.1036		
H (C82)	4.91511	3.96013	1.68183	0.1101		
H (C83)	4.91511	3.96013	-1.68183	0.1101		

Table A2 (*continued*).

Molecule	X[a]	Y[a]	Z[a]	q[b]	μ, θ[c]	α[d]
Fluorobenzene†					0.80	62.1
C (1)	0.0	-2.63995	0.0	-0.1243		74.6
C (2)	-2.28626	-1.31997	0.0	-0.1112		74.8
C (3)	-2.28626	1.31997	0.0	-0.2134		36.8
C (4)	0.0	2.63995	0.0	0.5658		
C (5)	2.28626	1.31997	0.0	-0.2134		
C (6)	2.28626	-1.31997	0.0	-0.1112		
H (C1)	0.0	-4.68841	0.0	0.1034		
H (C2)	-4.06028	-2.34421	0.0	0.1161		
H (C3)	-4.06028	2.34421	0.0	0.1213		
F (C4)	0.0	6.41657	0.0	-0.3705		
H (C5)	4.06028	2.34421	0.0	0.1213		
H (C6)	4.06028	-2.34421	0.0	0.1161		
Acetonitrile*					1.67	29.3
C (CN)	0.0	0.0	0.0	+0.5050	-1.52	38.3
N	-2.20	0.0	0.0	-0.5090	0.76	24.7
C (Me)	2.81	0.0	0.0	-0.8360	0.76	24.7
H (C21)	3.45	-1.81	0.0	+0.2800		
H (C22)	3.45	0.90	1.57038	+0.2800		
H (C23)	3.45	0.90	-1.57038	+0.2800		
Acetone[e]†					1.50	42.4
C (CO)	0.46479	0.95640	-0.00905	+0.61375	0.64	46.0
O	1.68667	2.89733	0.00450	-0.52335	-1.70	45.2
C (Me 1)	-2.37519	0.98510	-0.00004	-0.37730	1.06	36.0
H (C11)	-3.09296	0.00491	1.64946	+0.11070		
H (C12)	-3.10363	0.01723	-1.65125	+0.11070		
H (C13)	-3.05158	2.90761	0.01028	+0.11070		
C (Me 2)	1.71788	-1.59275	-0.02687	-0.37730		
H (C21)	1.20654	-2.64285	1.65643	+0.11070		
H (C22)	1.09693	-2.68784	-1.64194	+0.11070		
H (C23)	3.74285	-1.37428	-0.09414	+0.11070		
Methanol[f]*					0.76	22.5
C	-0.71167	-0.15571	0.27004	-0.0139	0.18	23.7
O	1.95454	-0.15571	0.27004	-0.6021	-0.63	21.3
H (OH)	2.49028	0.68843	-1.25289	0.4111	0.45	22.6
H (C21)	-1.46813	1.81716	0.27004	+0.0545		
H (C22)	-1.47096	-1.20376	-1.40218	+0.0545		
H (C23)	-1.26498	-1.14933	2.05319	+0.0959		
Tetrachloromethane*					0.0	73.5
C	-0.058959	0.0	0.043464	-0.1944	0.0	73.5
Cl (1)	3.266958	0.0	0.043464	0.0486	0.0	73.5
Cl (2)	-1.167662	-3.135811	0.043464	0.0486	0.0	73.5
Cl (3)	-1.167662	1.567906	2.759000	0.0486		
Cl (4)	-1.167662	1.567906	-2.672072	0.0486		

Table A2 (*continued*).

Molecule	X[a]	Y[a]	Z[a]	q[b]	μ, Θ[c]	α[d]
Z–N-methylacetamide[e*]					1.72	51.7
C (CO)	-3.73962	-0.09300	0.0	0.9995	4.67	64.7
O (CO)	-3.70680	-2.40791	0.0	-0.7774	-4.73	51.4
N	-5.92445	1.21486	0.0	-0.6092	0.06	39.0
H (N)	-5.89809	3.08396	0.0	0.3218		
C (Me C)	-1.33048	1.41587	0.0	-0.4922		
H (CC1)	-0.23408	0.90644	-1.64693	0.1504		
H (CC2)	-0.23408	0.90644	1.64693	0.1504		
H (CC3)	-1.63525	3.43365	0.0	0.0727		
C (Me N)	-8.34561	-0.07657	0.0	-0.0966		
H (CN1)	-8.53582	-1.25917	1.65374	0.1065		
H (CN2)	-8.53582	-1.25917	-1.65374	0.1065		
H (CN3)	-9.83478	1.31557	0.0	0.0676		
E–N-methylacetamide[e*]					1.86	51.3
C (CO)	-3.73974	-0.10386	0.0	0.9893	5.92	57.8
O (CO)	-3.81312	-2.41861	0.0	-0.7912	-6.97	57.3
N	-5.88881	1.27700	0.0	-0.6115	1.05	38.8
H (N)	-7.45965	0.24955	0.0	0.3479		
C (Me C)	-1.24366	1.25824	0.0	-0.4876		
H (CC1)	-0.18568	0.66825	-1.64539	0.1504		
H (CC2)	-0.18568	0.66825	1.64539	0.1504		
H (CC3)	-1.39505	3.28656	0.0	0.0932		
C (Me N)	-6.13996	4.00631	0.0	-0.1042		
H (CN1)	-5.30435	4.85414	-1.66201	0.0878		
H (CN2)	-5.30435	4.85414	1.66201	0.0878		
H (CN3)	-8.12783	4.45872	0.0	0.0877		

[a] Cartesian co-ordinate in Bohr. [b] Partial charge from HF wave-function DPC-analysis in atomic charge-units. * DZP basis; † STO4-31G basis set. [c] Overall dipole moment in a.u. (1 a.u.=2.54 D $=8.478\ 10^{-30}$ Cm), and xx, yy, and zz components of the Buckingham quadrupole-moment tensor in a.u. (1 a.u.=$4.487\ 10^{-40}$ Cm^2). [d] Isotropic polarizability, and xx, yy, and zz components of molecular polarizability tensor in $Bohr^3$. [e] STO4-31G-optimized geometry. [f] AM1-optimized geometry (CAChe-system).

3. Special Benzene Model Parameters

–A. Scaled models: SDPC and SP. The atomic charges and polarizabilities are scaled to yield the experimental quadrupole moment and isotropic molecular polarizability. The charges are -0.1626*e* and +0.1626*e*; the polarizabilites are 10.0 and 3.4 for C and H, respectively, with Thole's standard exponential damping model.

–B. Extra-centre models: EDPC and EP. Extra charge- and polarizability-points are added 1.8897 Bohr (1.0 Å) above and below the C-atoms in the z-direction. The extra points are given a charge of -0.07*e*, a polarizability of 1.3 $Bohr^3$, and a radius of 1.3 Bohr. Each C-charge is corrected to +0.0365*e* (from -0.1035*e*) to neutralize the charge-shift to the extra points. The H-charges are unaltered.

4. Selected Molecular and Bulk Properties

Table A3. Experimental molecular and bulk properties of various solvents.[a]

Species	M_W [b]	μ (D)[c]	α ($Bohr^3$)[d]	IE (eV)[e]	ρ (g/cm^3)[f]	ε_0 [g]	n_D^{20} [h]
H_2O	18.01	1.85	10	12.6	0.9971	78.5	1.333
CH_3CN	41.05	3.92		12.2	0.7856	37.5	1.344
CH_3OH	32.04	1.70	22	10.84	0.7914	32.6	1.329
$C_6H_5CH_3$	92.15	0.36		8.82	0.8669	2.38	1.494
n-C_6H_{14}	86.18			10.18	0.6603	1.89	1.372
C_6H_6	78.11	0	75	9.24	0.8787	2.30	1.501
CCl_4	153.8	0	71	11.5	1.5942	2.20	1.466
CH_3COCH_3	58.08	2.88		9.69	0.7899	20.7	1.359

[a] Sources: CRC Handbook of Chemistry and Physics, 64th edition and P.W. Atkins *Physical Chemistry*, 4th edition. [b] Molecular weight in atomic mass units. [c] Vacuum dipole moment in Debye. [d] Molecular isotropic polarizability. [e] Ionization energy in eV. [f] Liquid density at 298 K in g/cm^3. [g] Dielectric constant at 298 K. [h] Refractive index at 293 K.

References and Notes

1. *Guinness record boek 1992* (Uitgeverij Kosmos, Utrecht, 1992).
2. *General Chemistry: an Introduction to Descriptive Chemistry and Modern Chemical Theory*, L. Pauling (W.H. Freeman & Co., San Francisco, 1953).
3. *Taming the Atom—The Emergence of the Visible Microworld*, H.C. von Baeyer (Random House, 1992. Reprint, Penguin Books, London,1994).
4. Introduction to MOTECC-90, E. Clementi, In *MOTECC-90*, E. Clementi, Ed. (ESCOM, Leiden, 1990), p. 1-45.
5. *Thermodynamics, Kinetic Theory, and Statistical Thermodynamics*, F.W. Sears and G.L. Salinger (Addison-Wesley Publishing Co., Inc., Reading, 1975). 3rd Edition.
6. *Computer Simulation of Liquids*, M.P. Allen and D.J. Tildesley (Clarendon Press, Oxford, 1987).
7. Unified approach for molecular dynamics and density-functional theory, R. Car and M. Parrinello, *Phys. Rev. Lett.* **55**, 2471-2474 (1985).
8. Molecular dynamics without effective potentials via the Car–Parrinello approach, D.K. Remler and P.A. Madden, *Mol. Phys.* **70**, 921-966 (1990).
9. Selected topics in *ab initio* computational chemistry in both very small and very large chemical systems, E. Clementi, G. Corongiu, D. Bahattacharya, B. Feuston, D. Frye, A. Preiskorn, A. Rizzo and W. Xue, *Chem. Rev.* **91**, 679-699 (1991).
10. *The Character of Physical Law*, R.P. Feynman (British Broadcasting Company, London, 1965. Reprint, Penguin Books, London, 1992).
11. *Classical Mechanics*, H. Goldstone (Addison-Wesley Publishing Co., Inc., Reading, 1980). 2nd Edition.
12. *Quantum Mechanics*, A. Messiah (North Holland Publishing Co., Amsterdam, 1961).
13. *Quantum Mechanics*, A.S. Davydov (Gosudarstvennoye Izdatel'stvo Fiziko-matematicheskoi Literatury, Moscow, 1963. Reprint, translated from the Russian, with additions by D. ter Haar, Pergamon Press, Oxford, 1976). 2nd Edition.
14. *Advanced Quantum Theory—An Outline of Fundamental Ideas*, P. Roman (Addison-Wesley Publishing Co., Inc., Reading, 1965).
15. Atomic Units: Energy: 1 a.u.=1 Hartree=2625.5 kJ / mol; Electrostatics: charge: 1 a.u.= 1 e=1.60217733 10^{-19} C; vacuum permittivity $4\pi\varepsilon_0$=1=1.112665 10^{-10} C^2 / Jm; Length: 1 a.u.= 1 Bohr=52.917726 10^{-12} m.
16. The Born–Oppenheimer approximation, B.T. Sutcliffe, In *Methods in Computational Molecular Physics*, Vol. 293, S. Wilson and G.H.F. Diercksen, Eds. (Plenum Press, New York, 1992), p. 19-46.
17. *Vibronic Coupling: the Interaction between the Electronic and Nuclear Motions*, G. Fischer (Academic Press, London, 1984).
18. *Time-Dependent Quantum Molecular Dynamics*, J. Broeckhove and L. Lathouwers, Eds. (Plenum Press, New York, 1992).
19. *Modern Quantum Chemistry—Introduction to Advanced Electronic Structure Theory*, A. Szabo and N.S. Ostlund (Macmillan Publishing Co., 1982. Reprint, revised first edition, McGraw-Hill, Inc. New York, 1989.)

20. *Methods of Molecular Quantum Mechanics*, R. McWeeny (Academic Press, London, 1989). 2nd Edition.
21. *Quantum Electrodynamics—A Lecture Note and Reprint Volume*, R.P. Feynman (W.A. Benjamin, Inc., New York, 1962).
22. *Erewhon—or: over the Range*, S. Butler (1872. Reprint, Penguin Books, London, 1954).
23. Elaboration of approximate formulas for the interaction between large molecules: application in organic chemistry, P. Claverie, In *Intermolecular Interactions: From Diatomics to Biopolymers*, B. Pullman, Ed. (John Wiley & Sons, Chichester, 1978), p. 69-305.
24. Convergence properties of the intermolecular force series (1/R expansion), R. Ahlrichs, *Theor. Chim. Acta* **41**, 7-15 (1976).
25. On the convergence properties of the Raleigh–Schrödinger and the Hirschfelder–Silbey perturbation expansions for molecular interaction energies, G. Chalasinski, B. Jeziorski and K. Szalewicz, *Int. J. Quant. Chem.* **11**, 247-257 (1977).
26. Symmetry-adapted double-perturbation analysis of intramolecular correlation effects in weak intermolecular interactions. The He–He interaction, K. Szalewicz and B. Jeziorski, *Mol. Phys.* **38**, 191-208 (1979).
27. *Ab initio* studies of the interactions in van der Waals molecules, A. van der Avoird, P.E.S. Wormer, F. Mulder and R.M. Berns, In *Topics in Current Chemistry*, Vol. 93, F.L. Boschke, Ed. (Springer Verlag, Berlin, 1980), p. 1-51.
28. *Methods of Molecular Quantum Mechanics*, R. McWeeny (Academic Press, London, 1989). 2nd Edition, Chapter 14.
29. Quantum mechanical treatment of solvent effects, B.T. Thole and P.Th. van Duijnen, *Theor. Chim. Acta* **55**, 307-318 (1980).
30. On the theory of solvent-effect representations, O. Tapia, *J. Mol. Struct. (THEOCHEM)* **226**, 59-72 (1991).
31. Common theoretical framework for quantum chemical solvent effect theories, J.G. Ángyán, *J. Math. Phys.* **10**, 93-137 (1992).
32. Stationary perturbation theory, W. Kutzelnigg, *Theor. Chim. Acta* **83**, 263-312 (1992).
33. Theory and systematics of molecular forces, F. London, *Z. Phys.* **63**, 245-279 (1930).
34. Atomic multipole expansions of molecular charge densities. Electrostatic potentials, J. Bentley, In *Chemical Applications of Atomic and Molecular Electrostatic Potentials*, P. Pulitzer and D.G. Truhlar, Eds. (Academic Press, New York, 1981), p. 63-84.
35. Basic theory of intermolecular forces: applications to small molecules, A.D. Buckingham, In *Intermolecular Interactions: From Diatomics to Biopolymers*, B. Pullman, Ed. (John Wiley & Sons, Chichester, 1978), p. 1-67.
36. *Ab initio* determination of molecular electrical properties, C.E. Dykstra, S.-Y. Liu and D.J. Malik, In *Advances in Chemical Physics*, Vol. 75, I. Prigogine and S.A. Rice, Eds. (J. Wiley & Sons, Inc., New York, 1989), p. 37-111.
37. Representation of the molecular electrostatic potential by a net atomic charge model, S.R. Cox and D.E. Williams, *J. Comp. Chem.* **2**, 304-323 (1981).
38. An approach to computing electrostatic charges for molecules, U.C. Singh and P.A. Kollman, *J. Comp. Chem.* **5**, 129-145 (1984).
39. A comprehensive approach to molecular charge density models: from distributed multipoles to fitted atomic charges, J.G. Ángyán and C. Chipot, *Int. J. Quant. Chem.* **52**, 17-38 (1994).

40. Electronic population analysis on LCAO–MO molecular wave functions I., R.S. Mulliken, *J. Chem. Phys.* **23**, 1833-1840 (1955).
41. Distributed multipole analysis, or how to describe a molecular charge distribution, A.J. Stone, *Chem. Phys. Lett.* **83**, 233-239 (1981).
42. Distributed multipole analysis. Methods and applications, A.J. Stone and M. Alderton, *Mol. Phys.* **56**, 1047-1064 (1985).
43. A general population analysis preserving the dipole moment, B.T. Thole and P.Th. van Duijnen, *Theor. Chim. Acta* **63**, 209-221 (1983).
44. Potential energy models of biological macromolecules: a case for *ab initio* quantum chemistry, J.A.C. Rullmann and P.Th. van Duijnen, *CRC Reports in Molecular Theory* **1**, 1-21 (1990).
45. *Modeling Molecular Interactions in Proteins and Water; between Quantum Chemistry and Classical Electrostatics*, J.A.C. Rullmann, Ph.D. Thesis, University of Groningen, 1988. Chapter 2.
46. Atomic charge models for polypeptides derived from *ab initio* calculations, M.N. Bellido and J.A.C. Rullmann, *J. Comp. Chem.* **10**, 479-487 (1989).
47. Energy functions for peptides and proteins. I. Derivation of a consistent force field including the hydrogen bond from amide crystals, A.T. Hagler, E. Huler and S. Lifson, *J. Am. Chem. Soc.* **96**, 5319-5327 (1974).
48. The OPLS potential functions for proteins. Energy minimizations for crystals of cyclic dipeptides and Crambin, W.L. Jorgensen and J. Tirado-Rives, *J. Am. Chem. Soc.* **110**, 1657-1666 (1988).
49. Molecular polarisabilities calculated with a modified dipole interaction, B.T. Thole, *Chem. Phys.* **59**, 341-350 (1981).
50. Distributed polarisabilities, A.J. Stone, *Mol. Phys.* **56**, 1065-1082 (1985).
51. Local polarizabilities in molecules, based on *ab initio* Hartree-Fock calculations, G. Karlström, *Theor. Chim. Acta* **60**, 535-541 (1982).
52. *Classical Electrodynamics*, J.D. Jackson (John Wiley & Sons, New York, 1975).
53. *Theory of Electronic Polarisation*, C.J.F. Böttcher (Elsevier, Amsterdam, 1973). 2nd Edition.
54. The water–water MO-overlap was calculated with the program suites SYMOL (G.A. van der Velde, Ph.D. Thesis, University of Groningen, 1974) and GNOME (R. Broer, Ph.D. Thesis, University of Groningen, 1981), with optimized water-dimer orbitals in a DZP basis.
55. The direct reaction field hamiltonian: analysis of the dispersion term and application to the water dimer, B.T. Thole and P.Th. van Duijnen, *Chem. Phys.* **71**, 211-220 (1982).
56. Calculating the electrostatic potential of molecules in solution: method and error assessment, M.K. Gilson, K.A. Sharp and B.H. Honig, *J. Comp. Chem.* **9**, 327-335 (1987).
57. The rigorous computation of the molecular electric potential, R.J. Zauhar and R.S. Morgan, *J. Comp. Chem.* **9**, 171-187 (1988).
58. The electric potential of a macromolecule in a solvent: a fundamental approach, A.H. Juffer, E.F.F. Botta, B.A.M. van Keulen, A. van der Ploeg and H.J.C. Berendsen, *J. Comput. Phys.* **97**, 144-171 (1991).
59. Volumes and heats of hydration of ions, M. Born, *Z. Phys.* **1**, 45-48 (1920).
60. Electric moments of molecules in liquids, L. Onsager, *J. Am. Chem. Soc.* **58**, 1486-1493 (1936).
61. Solvent-accessible surface of proteins and nucleic acids, M.L. Connolly, *Science* **221**, 709-713 (1983).

62. Electrostatic interaction of a solute with a continuum. A direct utilization of *ab initio* molecular potentials for the prevision of solvent effects, S. Miertuš, E. Scrocco and J. Tomasi, *Chem. Phys.* **55**, 117-129 (1981).
63. Atom pair distribution functions of liquid water at 25°C from neutron diffraction, A.H. Narten, W.E. Thiessen and L. Blum, *Science* **217**, 1033-1034 (1982).
64. A combined *ab initio* quantum mechanical and molecular mechanical method for carrying out simulations on complex molecular systems: applications to the $CH_3Cl + Cl^-$ exchange reaction and gas phase protonation of polyethers, U.C. Singh and P.A. Kollman, *J. Comp. Chem.* **7**, 718-730 (1986).
65. A combined quantum mechanical and molecular mechanical potential for molecular dynamics simulations, M.J. Field, P.A. Bash and M. Karplus, *J. Comp. Chem.* **11**, 700-733 (1990).
66. A priori evaluation of aqueous polarization effects through Monte Carlo QM-MM simulations, J. Gao and X. Xia, *Science* **258**, 631-635 (1992).
67. A combined quantum chemical/molecular mechanical study of hydrogen-bonded systems, V.V. Vasilyev, A.A. Bliznyuk and A.A. Voityuk, *Int. J. Quant. Chem.* **44**, 897-930 (1992).
68. Microscopic models for quantum mechanical calculations of chemical processes in solutions: LD/AMPAC and SCAAS/AMPAC calculations of solvation energies, V. Luzhkov and A. Warshel, *J. Comp. Chem.* **13**, 199-213 (1992).
69. A hybrid approach for the solvent effect on the electronic structure of a solute based on the RISM and Hartree–Fock equations, S. Ten-no, F. Hirata and S. Kato, *Chem. Phys. Lett.* **214**, 391-396 (1993).
70. Influence of solvent on intramolecular proton transfer in hydrogen Malonate. Molecular dynamics simulation study of tunneling by density matrix evolution and nonequilibrium solvation, J. Mavri, H.J.C. Berendsen and W.F. van Gunsteren, *J. Phys. Chem.* **97**, 13469-13476 (1993).
71. Treatment of nonadiabatic transitions by density matrix evolution and molecular dynamics simulations, J. Mavri and H.J.C. Berendsen, *J. Mol. Struct.* **322**, 1-7 (1994).
72. The nature of K^+/crown ether interactions: a hybrid quantum mechanical–molecular mechanical study, M.A. Thompson, E.D. Glendening and D. Feller, *J. Phys. Chem.* **98**, 10465-10476 (1994).
73. An examination of a density functional/molecular mechanical coupled potential, R.V. Stanton, D.S. Hartsough and K.M. Mertz Jr., *J. Comp. Chem.* **16**, 113-128 (1995).
74. A multiconfiguration self-consistent reaction-field method, K.V. Mikkelsen, H. Ågren, H.J. Aa Jensen and T. Helgaker, *J. Chem. Phys.* **89**, 3086-3095 (1988).
75. Solvent effects. 1. The mediation of electrostatic effects by solvents, M.W. Wong, M.J. Frisch and K.B. Wiberg, *J. Am. Chem. Soc.* **113**, 4776-4782 (1991).
76. Reaction field factors for a multipole distribution in a cavity surrounded by a continuum, V. Dillet, D. Rinaldi and J.-L. Rivail, *Chem. Phys. Lett.* **202**, 18-22 (1993).
77. Liquid-state quantum chemistry: an improved cavity model, V. Dillet, D. Rinaldi and J.-L. Rivail, *J. Phys. Chem.* **98**, 5034-5039 (1994).
78. A multiconfiguration self-consistent reaction field response method, K.V. Mikkelsen, P. Jørgensen and H.J. Aa Jensen, *J. Chem. Phys.* **100**, 6597-6607 (1994).
79. A theoretical model of solvation in continuum anisotropic dielectrics, B. Mennucci, M. Cossi and J. Tomasi, *J. Chem. Phys.* **102**, 6837-6845 (1995).

80. Incorporation of reaction field effects into density functional calculations for molecules of arbitrary shape in solution, A.A. Rashin, M.A. Bukatin, J. Andzelm and A.T. Hagler, *Biophys. Chem.* **51**, 375-392 (1994).
81. Combined density functional, self-consistent reaction field model of solvation, R.J. Hall, M.M. Davidson, N.A. Burton and I.H. Hillier, *J. Phys. Chem.* **99**, 921-924 (1995).
82. The implementation of density functional theory with the polarizable continuum model for solvation, A. Fortunelli and J. Tomasi, *Chem. Phys. Lett.* **231**, 34-39 (1995).
83. Reaction field effects on the electronic structure of carbon radical and ionic centers, M.M. Karelson, T. Tamm, A.R. Katritzky, M. Szefran and M.C. Zerner, *Int. J. Quant. Chem.* **37**, 1-13 (1990).
84. General parameterized SCF model for free energies of solvation in aqueous solution, C.J. Cramer and D.G. Truhlar, *J. Am. Chem. Soc.* **113**, 8305-8311 (1991), and *ibid.*, p. 9901.
85. PM3–SM3: A general parameterization for including aqueous solvation effects in the PM3 molecular orbital model, C.J. Cramer and D.G. Truhlar, *J. Comp. Chem.* **13**, 1089-1097 (1992).
86. Multicavity reaction field method for the solvent effect description in flexible molecular systems, M. Karelson, T. Tamm and M.C. Zerner, *J. Phys. Chem.* **97**, 11901-11907 (1993).
87. A numerical self-consistent reaction field (SCRF) model for ground and excited states in NDDO-based methods, G. Rauhut, T. Clark and T. Steinke, *J. Am. Chem. Soc.* **115**, 9174-9181 (1993).
88. A semiempirical quantum mechanical solvation model for solvation free energies in all alkane solvents, D.J. Giesen, C.J. Cramer and D.G. Truhlar, *J. Phys. Chem.* **99**, 7137-7146 (1995).
89. Dielectric and thermodynamic response of a generalized reaction field model for liquid state simulations, H. Alper and R.M. Levy, *J. Chem. Phys.* **99**, 9847-9852 (1993).
90. A CFF91-based continuum solvation model: solvation free energies of small organic molecules and conformations of the alanine dipeptide in solution, F. Schmidt, *Mol. Simulation* **13**, 347-366 (1994).
91. Stabilization of helices in glycine and alanine dipeptides in a reaction field model of solvent, H.S. Shang and T. Head-Gordon, *J. Am. Chem. Soc.* **116**, 1528-1532 (1994).
92. A generalized reaction field method for molecular dynamics simulations, I.G. Tironi, R. Sperb, P.E. Smith and W.F. van Gunsteren, *J. Chem. Phys.* **102**, 5451-5459 (1995).
93. Theoretical studies of enzymatic reactions: dielectric, electrostatic, and steric stabilization of the carbenium ion in the reaction of Lysozyme, A. Warshel and M. Levitt, *J. Mol. Biol.* **103**, 227-249 (1976).
94. A new non-empirical force field for computer simulations, A. Wallqvist and G. Karlström, *Chemica Scripta* **29A**, 131-137 (1989).
95. A molecular dynamics study of polarizable water, P. Ahlström, A. Wallqvist, S. Engström and B. Jönsson, *Mol. Phys.* **68**, 563-581 (1989).
96. A local reaction field method for evaluation of long-range electrostatic interactions in molecular simulations, F.S. Lee and A. Warshel, *J. Chem. Phys.* **97**, 3100-3107 (1992).
97. Accurate solvation free energies of acetate and methylammonium ions calculated with a polarizable water model, E.C. Meng, P. Cieplak, J.W. Caldwell and P.A. Kollman, *J. Am. Chem. Soc.* **116**, 12061-12062 (1994).

98. Analysis of discrete and continuum dielectric models; application to the calculation of protonation energies in solution, J.A.C. Rullmann and P.Th. van Duijnen, *Mol. Phys.* **61**, 293-311 (1988).
99. A polarizable water model for calculation of hydration energies, J.A.C. Rullmann and P.Th. van Duijnen, *Mol. Phys.* **63**, 451-475 (1988), and *ibid.*, p. 557.
100. Quantum chemistry in the condensed phase: an extended direct reaction field approach, P.Th. van Duijnen, A.H. Juffer and J.P. Dijkman, *J. Mol. Struct. (THEOCHEM)* **260**, 195-205 (1992).
101. HONDO: a general atomic and molecular electronic structure system, M. Dupuis, A. Farazdel, S.P. Karma and S.A. Maluendes, In *MOTECC-90*, E. Clementi, Ed. (ESCOM, Leiden, 1990), p. 277-342.
102. Are direct reaction field methods appropriate for describing dispersion interactions?, J.G. Ángyán and G. Jansen, *Chem. Phys. Lett.* **175**, 313-318 (1990).
103. Theory of solvent effects on electronic spectra, H. Ågren and K.V. Mikkelsen, *J. Mol. Struct. (THEOCHEM)* **234**, 425-467 (1991).
104. Theoretical treatment of solvent effects on electronic spectroscopy, M.M. Karelson and M.C. Zerner, *J. Phys. Chem.* **96**, 6949-6957 (1992).
105. Equilibrium and nonequilibrium solvation and solute electronic structure III. Quantum theory, H.J. Kim and J.T. Hynes, *J. Chem. Phys.* **96**, 5088-5110 (1992).
106. Taming cut-off induced artifacts in molecular dynamics studies of solvated polypeptides. The reaction field method, H. Schreiber and O. Steinhauser, *J. Mol. Biol.* **228**, 909-923 (1992).
107. On the implementation of Friedman boundary conditions in liquid water simulations, A. Wallqvist, *Mol. Simulation* **10**, 13-17 (1993).
108. *On the Modelling of Solvent Mean Force Potentials—From Liquid Argon to Solvated Macromolecules*, A.H. Juffer, Ph.D. Thesis, University of Groningen, 1993.
109. Dynamic surface boundary conditions. A simple boundary model for molecular simulations, A.H. Juffer and H.J.C. Berendsen, *Mol. Phys.* **79**, 623-644 (1993).
110. Success and pitfalls of the dielectric continuum model in quantum chemical calculations, A.H. de Vries, P.Th. van Duijnen and A.H. Juffer, *Int. J. Quant. Chem., Quant. Chem. Symp.* **27**, 451-466 (1993).
111. The effective fragment potential method. An approximate *ab initio* MO method for large molecules, K. Ohta, Y. Yoshioka, K. Morokuma and K. Kitaura, *Chem. Phys. Lett.* **101**, 12-17 (1983).
112. Simulation of ionic transition-metal crystals: the cluster model and the cluster–lattice interaction in the light of the theory of electronic seperability, V. Luaña and L. Pueyo, *Phys. Rev. B* **39**, 11093-11112 (1989).
113. Molecular models in *ab initio* studies of solids and surfaces: from ionic crystals and semiconductors to catalysts, J. Sauer, *Chem. Rev.* **89**, 199-255 (1989).
114. A representation of the exchange operator useful for large molecules, R. Colle and O. Salvetti, *Theor. Chim. Acta* **80**, 63-70 (1991).
115. *Ab initio* model potential study of local distortions around Cr^{+} and Cr^{3+} defects in fluorite, L. Seijo and Z. Barandarian, *J. Chem. Phys.* **94**, 8158-8164 (1991).
116. Effective potentials for spectator groups in molecular systems I. Potential curves and binding energies, M. von Arnim and S.D. Peyerimhoff, *Theor. Chim. Acta* **87**, 41-57 (1993).

117. Reaction field effects on proton transfer in the active site of Actinidin, B.T. Thole and P.Th. van Duijnen, *Biophys. Chem.* **18**, 53-59 (1983).
118. *Interstitial Transition Metals in Silicon; Ab Initio Electronic Structure Calculations on Cluster Models*, G. Aissing, Ph.D. Thesis, University of Groningen, 1988.
119. The active site of Papain. All-atom study of interactions with protein matrix and solvent, J.A.C. Rullmann, M.N. Bellido and P.Th. van Duijnen, *J. Mol. Biol.* **206**, 101-118 (1989).
120. Papain in aqueous solution and the role of Asp-158 in the mechanism: an *ab initio* SCF+DRF+BEM study, J.P. Dijkman and P.Th. van Duijnen, *Int. J. Quant. Chem., Quant. Biol. Symp.* **18**, 49-59 (1991).
121. On the quantum mechanical treatment of solvent effects. II: Comparison of exact and expanded field operators, P.Th. van Duijnen, M. Dupuis and B.T. Thole, IBM DSD report KGN-38, May 18, 1986.
122. Extended Mulliken electron population analysis, S. Huzinaga, Y. Sakai, E. Miyoshi and S. Narita, *J. Chem. Phys.* **93**, 3319-3325 (1990).
123. *Handbook of Atomic Data*, S. Fraga, K.M.S. Saxena and J. Karwowski (Elsevier, Amsterdam, 1976).
124. Medium effects on the molecular electronic structure. I. The formulation of a theory for the estimation of a molecular electronic structure surrounded by an anisotropic medium, H. Hoshi, M. Sakurai, Y. Inoue and R. Chûjô, *J. Chem. Phys.* **87**, 1107-1115 (1987).
125. *Numerical Recipes, The Art of Scientific Computing*, W.H. Press, B.P. Flannery, S.A. Teukolsky and W.T. Vetterling (Cambridge University Press, Cambridge, 1986). The routines LUDATF and LUELMF were taken from the IMSL library.
126. CHARMM: a program for macromolecular energy, minimization and dynamical calculations, B.R. Brooks, R.E. Bruccoleri, B.D. Olafson, D.J. States, S.J. Swaminathan and M. Karplus, *J. Comp. Chem.* **4**, 187-217 (1983).
127. The van der Waals forces in gases, J.C. Slater and J.G. Kirkwood, *Phys. Rev.* **37**, 682-697 (1931).
128. Accurate non-local electron–Argon pseudopotential for condensed phase simulation, D.A. Estrin, C. Tsoo and S.J. Singer, *Chem. Phys. Lett.* **184**, 571-578 (1984).
129. Origins of structure and energetics of van der Waals clusters from *ab initio* calculations, G. Chalasinski and M.M. Szszesniak, *Chem. Rev.* **94**, 1723-1765 (1994).
130. The calculation of small molecular interactions by the differences of separate total energies. Some procedures with reduced errors, S.F. Boys and F. Bernardi, *Mol. Phys.* **19**, 553-566 (1970).
131. State of the art in counterpoise theory, F.B. van Duijneveldt, J.G.C.M. van Duijneveldt-van de Rijdt and J.H. van Lenthe, *Chem. Rev.* **94**, 1873-1885 (1994).
132. SCF, MP2, and CEPA-1 calculations on the OH··O hydrogen bonded complexes $(H_2O)_2$ and $(H_2O–H_2CO)$, R.J. Vos, R. Hendriks and F.B. van Duijneveldt, *J. Comp. Chem.* **11**, 1-18 (1990).
133. A new two-body water–water potential, E. Clementi and P. Habitz, *J. Phys. Chem.* **87**, 2815-2820 (1983).
134. A new intermolecular energy calculation scheme: applications to potential energy surface and liquid properties of water, A. Wallqvist, P. Ahlström and G. Karlström, *J. Phys. Chem.* **94**, 1649-1656 (1990).

135. Towards an accurate intermolecular potential for water, C. Millot and A.J. Stone, *Mol. Phys.* **77**, 439-462 (1992).
136. Intermolecular potential functions and the properties of water, J.R. Reimers, J.O. Watts and M.L. Klein, *Chem. Phys.* **64**, 95-114 (1982).
137. Isothermal–isobaric molecular dynamics simulation of liquid water, I. Ruff and D.J. Diestler, *J. Chem. Phys.* **93**, 2032-2042 (1990).
138. Interaction models for water in relation to protein hydration, H.J.C. Berendsen, J.P.M. Postma, W.F. van Gunsteren and J. Hermans, In *Intermolecular Forces; Proceedings of the 14th Jerusalem Symposium on Quantum Chemistry and Biochemistry*, B. Pullman, Ed. (Reidel, Dordrecht, 1981), p. 331-342.
139. Comparison of simple potential functions for simulating liquid water, W.L. Jorgensen, J. Chandraskhar, J.D. Madura, R.W. Impey and M.L. Klein, *J. Chem. Phys.* **79**, 926-935 (1983).
140. The missing term in effective pair potentials, H.J.C. Berendsen, J.R. Grigera and T.P. Straatsma, *J. Phys. Chem.* **91**, 6269-6271 (1987).
141. A polarizable model for water using distributed charge sites, M. Sprik and M.L. Klein, *J. Chem. Phys.* **89**, 7556-7560 (1988).
142. A new water potential including polarization: application to gas-phase, liquid, and crystal properties of water, P. Cieplak, P. Kollman and T. Lybrand, *J. Chem. Phys.* **92**, 6755-6760 (1990).
143. Molecular dynamics simulation for liquid water using a polarizable and flexible potential, G. Corongiu, *Int. J. Quant. Chem.* **42**, 1209-1235 (1992).
144. Variation–perturbation treatment of the hydrogen bond between water molecules, B. Jeziorski and M. van Hemert, *Mol. Phys.* **31**, 713-729 (1976).
145. A theoretical study of the water dimer interaction, K. Szalewicz, S.J. Cole, W. Kolos and R.J. Bartlett, *J. Phys. Chem.* **89**, 3662-3673 (1988).
146. Convergence to the basis-set limit in *ab initio* calculations at the correlated level on the water dimer, J.G.C.M. van Duijneveldt-van de Rijdt and F.B. van Duijneveldt, *J. Chem. Phys.* **97**, 5019-5030 (1992).
147. *Ab initio* studies of hydrogen bonds: the water dimer paradigm, S. Scheiner, *Ann. Rev. Phys. Chem.* **45**, 23-56 (1994).
148. Gaussian basis sets for molecular calculations, T.H. Dunning Jr. and P.J. Hay, In *Methods of Electronic Structure Theory*, H.F. Schaefer III, Ed. (1977), p. 1-27.
149. Thermodynamic properties of gas-phase hydrogen-bonded complexes, L.A. Curtiss and M. Blander, *Chem. Rev.* **88**, 827-841 (1988).
150. *Ab initio* calculation of Raman intensities; analysis of the bond polarizability approach and the atom dipole interaction model, M.C. van Hemert and C.E. Blom, *Mol. Phys.* **43**, 229-250 (1981).
151. Electric dipole moments of low J-states of H_2O and D_2O, T.R. Dyke and J.S. Muenter, *J. Chem. Phys.* **59**, 3125-3126 (1973).
152. Magnetic properties and molecular quadrupole tensor of the water molecule by beam-maser Zeeman spectroscopy, J. Verhoeven and A. Dymanus, *J. Chem. Phys.* **52**, 3222-3233 (1970).
153. Perturbation theory of the electron correlation effects for atomic and molecular properties. Second- and third-order correlation corrections to molecular dipole moments and polarizabilities, G.H.F. Diercksen and A.J. Sadlej, *J. Chem. Phys.* **75**, 1253-1266 (1981).

154. Molecular electric properties in excited states: multipole moments and polarizabilities of H_2O in the lowest $^1B_1$ and $^3B_1$ excited states, M. Urban and A.J. Sadlej, *Theor. Chim. Acta* **78**, 189-201 (1990), and references cited therein.
155. Dipole moments and polarizabilities of molecules in excited electronic states, W. Liptay, In *Excited States*, Vol. I, E.C. Lim, Ed. (Academic Press, New York, 1974), p. 129-229.
156. From intermolecular potentials to the spectra of van der Waals molecules, and *vice versa*, A. van der Avoird, P.E.S. Wormer and R. Moszynski, *Chem. Rev.* **94**, 1931-1974 (1994).
157. The nature of π–π interactions, C.A. Hunter and J.K.M. Saunders, *J. Am. Chem. Soc.* **112**, 5525-5534 (1990).
158. π–π interactions: the geometry and energetics of phenylalanine–phenylalanine interactions in proteins, C.A. Hunter, J. Singh and J.M. Thornton, *J. Mol. Biol.* **218**, 837-846 (1991).
159. Potential energy surface of the benzene dimer: *ab initio* theoretical study, P. Hobza, H.L. Selzle and E.W. Schlag, *J. Am. Chem. Soc.* **116**, 3500-3506 (1994).
160. Formation of mixed binary clusters in a supersonic molecular beam: a nice case of RRK kinetics, B.R. Veenstra, H.T. Jonkman and J. Kommandeur, *J. Phys. Chem.* **98**, 3538-3543 (1994).
161. Multiphoton ionization and dissociation of mixed van der Waals clusters in a linear reflectron time-of-flight mass spectrometer, B. Ernstberger, H. Krause, A. Kiermeier and H.J. Neusser, *J. Chem. Phys.* **92**, 5285-5296 (1990).
162. Binding energies of small benzene clusters, H. Krause, B. Ernstberger and H.J. Neusser, *Chem. Phys. Lett.* **184**, 411-417 (1991).
163. Binding energy and structure of van der Waals complexes of benzene, H.J. Neusser and H. Krause, *Chem. Rev.* **94**, 1829-1843 (1994).
164. Structure and properties of benzene-containing molecular clusters: nonempirical *ab initio* calculations and experiments, P. Hobza, H.L. Selzle and E.W. Schlag, *Chem. Rev.* **94**, 1767-1785 (1994).
165. Intermolecular potentials for the H_2O–C_6H_6 and the C_6H_6–C_6H_6 sytems calculated in an *ab initio* SCF CI approximation, G. Karlström, P. Linse, A. Wallqvist and B. Jönsson, *J. Am. Chem. Soc.* **105**, 3777-3782 (1983).
166. Computed structure of small benzene clusters, B.W. van de Waal, *Chem. Phys. Lett.* **123**, 69-72 (1986).
167. Benzene, aromatic rings, van der Waals molecules, and crystals of aromatic molecules in Molecular Mechanics (MM3), N.L. Allinger and J.-H. Lii, *J. Comp. Chem.* **8**, 1146-1153 (1987).
168. Aromatic–aromatic interactions: free energy profiles for the benzene dimer in water, chloroform, and liquid benzene, W.L. Jorgensen and D.L. Severance, *J. Am. Chem. Soc.* **112**, 4768-4774 (1990).
169. The rotational spectrum, structure and dynamics of a benzene dimer, E. Arunan and H.S. Gutowsky, *J. Chem. Phys.* **98**, 4294-4296 (1993).
170. Intermolecular Raman bands in the ground state of benzene dimer, V.A. Venturo and P.M. Felker, *J. Chem. Phys.* **99**, 748-751 (1993).
171. The electric quadrupole moments of benzene and hexafluorobenzene, M.R. Battaglia, A.D. Buckingham and J.H. Williams, *Chem. Phys. Lett.* **78**, 421-423 (1981).
172. *CRC Handbook of Chemistry and Physics*, (CRC Press, Inc., Boca Raton, Florida, 1983-1984).
173. Monte Carlo simulation of liquid acetonitrile, W.L. Jorgensen and J.M. Briggs, *Mol. Phys.* **63**, 547-558 (1988).

174. An effective pair potential for liquid acetonitrile, H.J. Böhm, I.R. McDonald and P.A. Madden, *Mol. Phys.* **49**, 347-360 (1983).
175. Cluster-collision frequency: the long-range interaction potential, A.S. Amadon and W.H. Marlow, *Phys. Rev. A* **43**, 5483-5492 (1991).
176. A new force field for molecular mechanical simulation of nucleic acid acids and proteins, S.J. Weiner, P.A. Kollman, D.A. Case, U.C. Singh, C. Ghio, G. Alagona, S. Profeta and P. Weiner, *J. Am. Chem. Soc.* **106**, 765-784 (1984).
177. An all atom force field for simulations of proteins and nucleic acids, S.J. Weiner, P.A. Kollman, D.T. Nguyen and D.A. Case, *J. Comp. Chem.* **7**, 230-252 (1986).
178. A consistent empirical potential for water–protein interactions, J. Hermans, H.J.C. Berendsen, W.F. van Gunsteren and J.P.M. Postma, *Biopolymers* **23**, 1513-1518 (1984).
179. A molecular dynamics study of the C-terminal fragment of the L7/L12 ribosomal protein. Secondary structure motion in a 150 picosecond trajectory, J. Åqvist, W.F. van Gunsteren, M. Leijonmarck and O. Tapia, *J. Mol. Biol.* **183**, 461-477 (1985).
180. *Solvation Thermodynamics*, A. Ben-Naim (Plenum Press, New York, 1987).
181. *Quantum Chemistry*, H. Eyring, J. Walter and G.E. Kimball (Wiley, Inc., New York, 1944).
182. Solvation thermodynamics of nonionic solutes, A. Ben-Naim and Y. Marcus, *J. Chem. Phys.* **81**, 2016-2027 (1984).
183. Group contributions to the thermodynamic properties of non-ionic organic solutes in dilute aqueous solution, S. Cabani, P. Gianni, V. Mollica and L. Lepori, *J. Solution Chem.* **10**, 563-595 (1981).
184. The size of molecules, A.Y. Meyer, *Chem. Soc. Rev.* **15**, 449-474 (1985).
185. Calculation of dispersion energy shifts in molecular electronic spectra, N. Rösch and M.C. Zerner, *J. Phys. Chem.* **98**, 5817-5823 (1994).
186. Van der Waals volumes and radii, A. Bondi, *J. Phys. Chem.* **68**, 441-451 (1964).
187. Free energy of a charge distribution in concentric dielectric continua, D.L. Beveridge and G.W. Schnuelle, *J. Phys. Chem.* **79**, 2562-2566 (1975).
188. The extended polarizable continuum model for calculation of solvent effects, S. Miertuš, V. Frecer and M. Májeková, *J. Mol. Struct. (THEOCHEM)* **179**, 353-366 (1988).
189. Evaluation of the dispersion contribution to the solvation energy. A simple computational model in the continuum approach, F. Floris and J. Tomasi, *J. Comp. Chem.* **10**, 616-627 (1989).
190. A scaled particle theory of aqueous and nonaqueous solutions, R.A. Pierotti, *Chem. Rev.* **76**, 717-726 (1976).
191. Excess free energy of different water models computed by Monte Carlo methods, M. Mezei, *Mol. Phys.* **47**, 1307-1315 (1982).
192. Self-consistent reaction field calculations of photoelectron binding energies for solvated molecules, C. Medina-Llanos, H. Ågren, K.V. Mikkelsen and H.J.Aa Jensen, *J. Chem. Phys.* **90**, 6422-6435 (1989).
193. Proton solvation in liquid water, an *ab initio* study using the continuum model, I. Tuñón, E. Silla and J. Bertran, *J. Phys. Chem.* **97**, 5547-5552 (1993).

194. Infrared studies of the less stable *cis* form of N–methylformamide and N–methylacetamide in low-temperature nitrogen matrices and vibrational analysis of the *trans* and *cis* forms of these molecules, S. Ataka, H. Takeuchi and M. Tasumi, *J. Mol. Struct.* **113**, 147-160 (1984).
195. Influence of solvent water on protein folding: free energies of solvation of cis and trans peptides are nearly identical, A. Radzicka, L. Pedersen and R. Wolfenden, *Biochemistry* **27**, 4538-4541 (1988).
196. Cis–trans energy difference for the peptide bond in the gas phase and in aqueous solution, W.L. Jorgensen and J. Gao, *J. Am. Chem. Soc.* **110**, 4212-4216 (1988).
197. Aqueous solvation of N–methylacetamide conformers: comparison of simulations and integrals equation theories, H.-A. Yu, B.M. Petitt and M. Karplus, *J. Am. Chem. Soc.* **113**, 2425-2434 (1991).
198. Molecular orbital theory calculations of aqueous solvation effects on chemical equilibria, C.J. Cramer and D.G. Truhlar, *J. Am. Chem. Soc.* **113**, 8552-8554 (1991), and *ibid.*, p. 9901.
199. Standard thermodynamics of transfer. Uses and misuses, A. Ben-Naim, *J. Phys. Chem.* **82**, 792-803 (1978).
200. *Chemical Kinetics, the Study of Reaction Rates in Solution*, K.A. Connors (VCH, New York, 1990), p. 421.
201. Solvent-shift effects on electronic spectra and excited-state dipole moments and polarizabilities, A.T. Amos and B.L. Burrows, In *Advances in Quantum Chemistry*, Vol. 7, P.-O. Löwdin, Ed. (Academic Press, New York, 1973), p. 289-313.
202. Empirische Parameter der Lösungsmittelpolarität als linear Frei Enthalpie Beziehungen, C. Reichardt, *Angew. Chem.* **91**, 119-131 (1979).
203. *Solvent Effects in Organic Chemistry*, C. Reichardt (Verlag Chemie, Weinheim, 1979).
204. Solvatochromic shifts: the influence of the medium on the energy of electronic states, P. Suppan, *J. Photochem. Photobiol.* **A50**, 293-330 (1990).
205. Solvent effects on optical absorption spectra. The $^1A_1 \rightarrow {}^1A_2$ transition of formaldehyde in water, J.T. Blair, K. Krogh-Jespersen and R.M. Levy, *J. Am. Chem. Soc.* **111**, 6948-6956 (1989).
206. A theoretical examination of solvatochromism and solute-solvent structuring in simple alkyl carbonyl compounds. Simulations using statistical mechanical free energy perturbation methods, S.E. DeBolt and P.A. Kollman, *J. Am. Chem. Soc.* **112**, 7515-7524 (1990).
207. Microscopic calculations of solvent effects on absorption spectra of conjugated molecules, V. Luzhkov and A. Warshel, *J. Am. Chem. Soc.* **113**, 4491-4499 (1991).
208. Monte Carlo QM-CI/MM simulation of solvent effects on the $n \rightarrow \pi^*$ blue shift of acetone, J. Gao, *J. Am. Chem. Soc.* **116**, 9324-9328 (1994).
209. *Photochemistry*, J. G. Calvert and J. N. Pitts (Wiley, New York, 1966). p. 377.
210. Solvent effects on the intensities and weak ultraviolet spectra of ketones and nitroparaffins - I, N.S. Bayliss and G. Wills-Johnson, *Spectrochim. Acta* **24A**, 551-661 (1968).
211. Solvent and substituent effects on the $n \rightarrow \pi^*$ absorption bands of some ketones, W.P. Hayes and C.J. Timmons, *Spectrochim. Acta* **21**, 529-541 (1965).
212. On the n-π^* blue shift accompanying solvation, M. Karelson and M.C. Zerner, *J. Am. Chem. Soc.* **112**, 9405-9406 (1990).
213. The case against linear response theory, N.G. van Kampen, *Physica Norvegica* **5**, 279-284 (1971).

214. Phosphate ester hydrolysis: calculation of gas-phase reaction paths and solvation effects, A. Dejaegere, X. Liang and M. Karplus, *J. Chem. Soc., Faraday Trans.* **90**, 1763-1770 (1994).
215. Gaussian basis sets for molecular wavefunctions containing third-row atoms, A.J.H. Wachters, *J. Chem. Phys.* **52**, 1033-1036 (1970).
216. *Physical Chemistry,* P.W. Atkins (Oxford University Press, Oxford, 1994). 5th Edition, p. C24.
217. Molecular interactions in solution: an overview of methods based on continuous distributions of the solvent, J. Tomasi and M. Persico, *Chem. Rev.* **94**, 2027-2094 (1994).
218. Intramolecular dielectric screening in proteins, T. Simonson, D. Perahia and G. Bricogne, *J. Mol. Biol.* **218**, 859-886 (1991).

Summary

THE TREATMENT of solvent effects is attracting ever growing interest in computational chemistry because it marks the meeting of two mainstream developments in approaching chemistry by computation rather than by experiment: *quantum chemistry*, which attempts to calculate molecular properties and reaction profiles from first principles, i.e. by solving the Schrödinger equation for nuclei and electrons, the building blocks of matter as far as the chemist is concerned; and *molecular mechanics*, which attempts at calculating macroscopic properties from microscopic representations of matter by statistical thermodynamics, operating at a higher level of aggregation than does quantum chemistry, *viz.* that of atomic or molecular building blocks. Interest from experimental chemistry is also bountiful, because direct observation of microscopic key-events in condensed-phase experiments is very difficult.

The computational approaches suffer from technological limitations in their application. The first-principle methods are very detailed descriptions, rendering these techniques very CPU and memory intensive, barring statistical thermodynamic calculation of large samples; by stepping up a level of aggregation to molecular mechanics such calculations become feasible, be it at the expense of much detail. The loss of detail may seriously undermine the physical meaning and interpretability of the results. The problems with the physical meaning and interpretability of statistical thermodynamic calculations lie especially in the description of the atomic building blocks. Although the descriptors are cast in forms that are based on sound theoretical analysis of intermolecular interactions, the numerical values, the parameters, are usually fit to macroscopic properties, and thus the ‘atoms’ are not the same as they would be in isolation, but effective macroscopic atoms. The fitting procedure causes a mixing of physical effects to enter parameters that stand for clearly defined interaction components, and thus obfuscates the analysis.

The approach followed in this thesis chooses the first-principle methods as the starting point for building a molecular mechanics description of molecular aggregates. In this way, a hierarchical description of the condensed phase is built up from depth, retaining the physical meaning of the interaction energy components of the molecules. An especially important feature of this approach is that it allows *mixing* of the first-principles and molecular descriptions in a transparent and consistent way. The mixing is necessary if one wants to describe processes that cannot be dealt with without the quantum mechanics of the electrons and/or nuclei of at least part of the system, such as the spectrum, electron-transfer processes, and reactions.

Starting with a clear-cut analysis of interaction at the level of nuclei and electrons, criteria for both application and the building of molecular representations that preserve the physical meaning of the parameters—distributed charges and polarizabilities, completed by *ad hoc* repulsion parameters—are derived. The criterion for application of the molecular representation is spatial separation of the

molecules, i.e. they should be recognizable as such. The properties of interest for building the molecular model are the electrostatic and electric response properties of the molecules that can be obtained from the molecules in isolation, i.e. without having to resort to the macroscopic.

The application of the molecular model to condensed-phase systems constitutes a border-line case. The molecules are close, yet they are recognizable. Some special measures have to be taken to prevent accidents due to the spatial extent of the molecules. These may again be rooted in sound theoretical analysis at the deepest level, or rather *ad hoc*. Whatever choices are made, checking is necessary.

The outline of this thesis is the following. In Chapter 1 the analysis of intermolecular interactions from quantum theory is elaborated in the mathematical language, emphasizing the assumptions underlying the transition from quantum-chemical to classical representation of the molecules. The classical molecular description in terms of the properties of isolated molecules is derived from the quantum-theoretical formulas. The molecular electrostatic and response models are introduced and put under some scrutiny as concerns the internal consistency and limits of applicability. Chapter 2 provides the computational chemist with the tools to put his ideas into action, as the implementation of the molecular model in combination with standard quantum-chemical is detailed on. Finally testing and application of the molecular model to various chemically interesting systems is carried out in Chapter 3. These include the water dimer and van der Waals complexes, solvation, both aqueous and non-aqueous, and solvatochromism of acetone. It is shown that the approach advocated by us provides a general and straightforward scheme to attack very different systems. The treatment of the various systems is not always entirely satisfactory, but at least the approach leaves little doubt about the improvements necessary to obtain better agreement with highly accurate *ab initio* calculations and experiment. The chapter closes with an analysis of the nature of dielectric behaviour, demonstrating that although the macroscopic is a result of the goings-on of the microscopic, the microscopic may not be represented as a scaled-down macroscopic. Finally, a section for the interested readers commanding the Dutch language is included presenting a broader introduction to quantum chemistry and molecular models in the light of computational science as a means to study nature. The ideas behind the approach chosen in this work are introduced by appealing to everyday analogues.

The aim of the work presented in this thesis is to work toward a consistent, sensible, and applicable model for condensed-phase phenomena, preserving physical meaning handed down by quantum theory. This approach is believed to be more fruitful than approaches based on fitting to macroscopic properties because it is more general and not hampered by mixing of separable effects in the molecular descriptions.

Quantumchemie en moleculemodellen

Laten we er vooral allemaal anders over denken.

C. BUDDINGH'

Sommige mensen... Aforismen verzameld door Gerd de Ley (1971)

Inleiding A.1

SINDS MENSENHEUGENIS houdt onze soort zich bezig met de dingen der natuur en de natuur der dingen. Kennis van de dingen der natuur is noodzakelijk om ons te handhaven; kennis van de natuur der dingen moet ons helpen de natuur te beheersen en, nog verdergaand, naar onze hand te zetten. Het begin van deze kennis ligt in directe zintuiglijke waarneming van natuurverschijnselen. Daarna ook in indirecte waarnemingen gedaan met behulp van vervaardigde instrumenten. Tenslotte door waarnemingen in door ons geforceerde situaties, ofwel experimenten.

De sleutel tot het handhaven in, en het beheersen en manipuleren van de natuur ligt in het *ordenen* van de waarnemingen. Een zinvolle ordening doet regelmatigheden naar voren komen die helpen situaties te herkennen en te voorspellen, waardoor het mogelijk is op tijd passende maatregelen te treffen. Regelmatigheden leiden tot formulering van 'natuurwetten': vaste verbanden tussen verschijnselen. Deze helpen bij het beheersen van de natuur, en bij het manipuleren ervan. Experimenteren langs de gevonden regels van oorzaak en gevolg is de basis voor technologie: het vervaardigen van voorwerpen om een bepaalde taak uit te voeren.[1] Hierbij is vooral belangrijk dat het voorwerp doet wat ervan verwacht wordt en is de vraag naar diepere achtergronden minder interessant.

Van oudsher is de mens echter ook op zoek naar inzichten die de veelheid aan natuurverschijnselen onder één noemer brengen. Het bestaan van één algemeen principe dat àl het waarneembare verklaart vervult blijkbaar een diepe behoefte in ons bewustzijn. In tegenstelling tot technologie gaat het hierbij vooral om de algemeenheid, de schoonheid, de eenvoud en de consistentie van de aangedragen verklaring. De moderne natuurwetenschap verschilt van andere wegen tot het vinden van algemene waarheden doordat zij natuurwetten formuleert die niet vertrouwen op alledaagse, aan de natuurlijke waarnemingen zèlf ontleende concepten, maar veeleer uitgaan van ideale, bedachte toestanden.[2] Niettemin heeft zij als enig toegestane toetssteen de meetbare werkelijkheid. Neem als voorbeeld de beweging van voorwerpen. In de alledaagse beleving moet voortdurend moeite gedaan worden een voorwerp in beweging te houden. Men moet een kracht op het voorwerp uitoefenen. Aristoteles verwoordde deze 'natuurwet' die twee millennia stand hield. Toen bleek een radicaal ander concept, namelijk dat een voorwerp haar baan onveranderd van snelheid en richting voortzet als daar *geen* kracht op wordt uitgeoefend, te leiden tot een dieper inzicht, en konden uiteindelijk de bewegingen van de

1 *The Evolution of Technology*, G. Basalla (Cambridge University Press, Cambridge, 1987. In vertaling verschenen onder de titel: *Geschiedenis van de technologie*, Uitgeverij Het Spectrum B.V., Utrecht, 1993.)
2 *The Unnatural Nature of Science*, L. Wolpert (Faber and Faber Ltd., London, 1993); *The Character of Physical Law*, R.P. Feynman (British Broadcasting Company, London, 1965. Ook bij Penguin Books, London, 1992); *Physics and Philosophy*, W. Heisenberg (Harper & Row, New York, 1962. Ook bij Penguin Books, London, 1990).

hemellichamen, vallende appels en veren, en van gas in een buis in één en de-zelfde theorie (de klassieke mechanica) worden ondergebracht.

Het inzicht dat leidde tot de algemeen geldige beschrijving van bewegende objecten kwam tot stand met behulp van een gedachtenexperiment. Galileo stelde zich een situatie voor waarin een voorwerp met niets in aanraking zou komen. Een luchtledige dus, iets dat in de natuur niet voorkomt, getuige de klassieke spreuk 'Natura abhorret vacuum', 'De natuur verafschuwt het ledige'. Nadat de afkeer van het idee van een luchtledige was overwonnen en men op zoek ging naar bewijs voor het bestaan ervan, bleek het succes van de nieuwe zienswijze. Niet alleen werden de bewegingswetten getoetst en correct bevonden (in het luchtledige valt een appel even snel als een veer), maar er opende zich ook een geheel nieuwe tak van technologie en wetenschap rond het vacuüm, uitmondend in de eerste stoommachine.

Toch komt ook in de wetenschap een einde aan het begrijpen. De mechanica werd geformuleerd in termen van 'krachten' die op objecten werken. Hoe die 'krachten' tot stand kwamen wist men niet, en weet men voor een deel nog steeds niet. Het concept is echter zó krachtig dat men er zich in eerste instantie niet om bekommert wat de fysische betekenis ervan is. Zo worden in de wetenschap *modellen* opgesteld die de werkelijkheid beschrijven, en wel in *kwantitatieve* zin. De nadruk op kwantitatief juiste theorieën kenmerkt de moderne wetenschap meer dan iets anders. Waar het in de klassieke wetenschap vooral belangrijk was of een inzicht esthetisch was, moet een theorie tegenwoordig waarnemingen getalsmatig beves-tigen en de uitkomst van metingen voorspellen. Daarbij blijft natuurlijk het streven naar eenvoud bestaan, maar een esthetisch aansprekende theorie die geen kwanti-tatieve voorspellingen doet is waardeloos. Als gezegd is de enig toegestane toets-steen de meetbare werkelijkheid, het experiment.

Door het getalsmatige van de huidige wetenschap is zij bijzonder wiskundig van aard.[3] Er wordt voortdurend gerekend. Omdat de kennis van de natuur beperkt is, zijn de opgestelde modellen dat ook. Maar er is ook een beperking aan de hoeveelheid detail die in een model gestopt kan worden om het nog mogelijk te maken berekeningen uit te voeren. In dit verband heeft de enorme vooruitgang in computerkracht de mogelijkheden van de natuurwetenschapper net zo spectaculair vergroot als die van de videospelletjesfanaat. Zo is het nu mogelijk de bewegingen van een redelijk groot aantal wisselwerkende deeltjes (of dat nu revolverhelden in cyberspace of elementaire deeltjes in versnellers zijn) 'levensecht' te beschrijven. Om de levensechtheid van computerspelletjes te waarborgen worden minder belangrijke objecten ruwer weergegeven. Het weglaten van die decorstukken zou echter een hinderlijk gat achterlaten. Iets dergelijks geldt in de scheikunde als we eigenschappen van moleculen in oplossing willen berekenen, hetgeen in dit proefschrift centraal staat.

---

3 *Mathematics in Western Culture*, M. Kline (Oxford University Press, Oxford, 1953. Ook bij Penguin Books, London, 1982).

Een zeer algemeen model voor het beschrijven van de natuur is het opgebouwd denken van materie uit elektrisch geladen deeltjes, genaamd protonen en elektronen, die met elkaar een wisselwerking aangaan. De wetten waaraan die deeltjes moeten voldoen zijn uitermate eenvoudig en het model is toepasbaar op letterlijk alle verschijnselen, van atoomspectra tot de onderlinge bewegingen van sterrenstelsels. De rekeninspanning die vereist is om de bewegingen van de deeltjes te beschrijven is echter bijzonder groot, en er zijn onnoemelijk veel deeltjes betrokken bij de verschijnselen van alledag, zodat de vragen die beantwoord kunnen worden met deze zeer gedetailleerde beschrijving beperkt zijn tot die waarin een klein aantal protonen en elektronen een cruciale rol spelen. Het nut is echter uit te breiden door uit de beschrijving in termen van protonen en elektronen *collectieve* eigenschappen af te leiden die kunnen dienen voor grofstoffelijker beschrijvingen. Vergelijk de situatie met het weergeven van een muur in een videospel. De afzonderlijke stenen hoeven niet getoond te worden als het erom gaat aan te geven dat de bewegingsmogelijkheden van de held beperkt zijn. Een ondoordringbaar vlak, het collectieve effect van zoveel stenen, brengt de boodschap over. Detail kan echter noodzakelijk zijn, als er bijvoorbeeld een losse steen gezocht moet worden waarmee een verborgen deur geopend kan worden. In de buurt van de held moet de muur zijn weergegeven als losse stenen, maar verderop volstaat een vlak. Zo hangt de benodigde hoeveelheid detail af van de situatie waarin we geïnteresseerd zijn.

Hetzelfde geldt in de scheikunde bij de beschrijving van eigenschappen van stoffen. Het detail van protonen en elektronen is niet altijd nodig. Of het is slechts plaatselijk van belang. Er is dan behoefte aan een gecombineerd model. Gedetailleerd waar het moet, globaal waar het kan. In dit proefschrift wordt beschreven hoe men kan komen van een beschrijving van materie op het niveau van protonen en elektronen tot een beschrijving op het niveau van moleculen en van op het niveau van moleculen tot op het niveau van vloeistoffen. Deze procedure heeft tot doel de niveaus te kunnen combineren op een manier die consistent is met het diepste niveau, zodat de toepasbaarheid maximaal blijft, en tegelijkertijd de toepassingsmogelijkheden vergroot worden door vermindering van de benodigde rekeninspanning. Het gaat in dit proefschrift om de praktische uitwerking van de vereenvoudigde modellen. Het onderzoek beoogt criteria aan te geven waaraan de molecule- en vloeistofmodellen moeten voldoen om te mogen worden gebruikt en om te worden gecombineerd met de gedetailleerde beschrijving.

Grondslagen van de quantumchemie A.2

QUANTUMCHEMIE is de toepassing van quantumtheorie op vraagstukken die spelen bij scheikundig onderzoek. De quantumtheorie is in het eerste deel van deze eeuw ontwikkeld naar aanleiding van een groot aantal experimenten op het raakvlak van natuur- en scheikunde waarvan men de resultaten niet kon rijmen met de theorieën die destijds golden met betrekking tot het gedrag van de bouwstenen van materie. In de loop der tijden is de mens erin geslaagd materie steeds gedetailleerder te bekijken. Met de eerste microscopen werd het bestaan van cellen aangetoond, later volgden bacteriën, nog later grote moleculen zoals DNA, en pas sinds een aantal jaren kleinere moleculen en atomen.

Hoewel we pas nu atomen 'direct' kunnen zien door een microscoop is er al veel langer indirect bewijs voor het bestaan van deze bouwstenen van het heelal.[4] De atomen zelf bestaan uit nog weer kleinere bouwstenen. Men denkt atomen als zijnde opgebouwd uit een relatief immobiele 'harde pit', de kern, met daaromheen een ijle wolk snelle deeltjes, de elektronen. In de kern is een hoeveelheid protonen verzameld die samen het atoom zijn 'karakter' geven: bij één proton hoort waterstof, bij twee helium, bij zes koolstof, bij zeven stikstof en bij tweeënnegentig hoort uranium, om vijf van de ruim honderd bekende atoomsoorten te noemen.

Elk proton draagt één positieve elektrische lading, dus in de kern van een atoom bevindt zich een opeenhoping van positieve lading. Gelijke ladingen stoten elkaar af. Dat de protonen toch bij elkaar in de kern blijven is te danken aan de aanwezig-heid van nog weer andere deeltjes in de kern, neutronen genaamd, die door hun wisselwerking met de protonen onder andere als 'kleefstof' dienst doen. Ook de kern zelf bestaat dus uit nog weer kleinere deeltjes. Het lijkt wel of in ieder brokje materie weer nieuwe, kleinere brokjes materie te vinden zijn. Men is er nog niet uit of dat een keer ophoudt. In ieder geval bestaan protonen en neutronen uit drie zogenaamde quarks, waarvan er zes typen moeten zijn. Voor scheikundigen is het eigenlijk niet zo belangrijk wat zich allemaal in die kern afspeelt omdat de verschijnselen die zij bestuderen de kern ongemoeid laten. Wie meer wil weten over de bouw van kernen moet zich wenden tot de subatomaire natuurkunde.[5]

Voor de scheikunde zijn de snelle deeltjes rond de kern, de elektronen, belangrijk, en dan vooral de manier waarop de elektronen zich rond de kern kunnen verdelen. Elk elektron draagt één negatieve elektrische lading. Ongelijke ladingen trekken elkaar aan volgens dezelfde wetmatigheid als waarmee gelijke elektrische ladingen elkaar afstoten. De kern trekt de elektronen aan en de elektronen stoten elkaar af. De grote vraag aan het begin van deze eeuw was waarom de elektronen zich niet op de

4 *Taming the Atom—The Emergence of the Visible Microworld*, H.C. von Baeyer (Random House, 1992. Ook bij Penguin Books, London,1994).
5 *De bouwstenen van de schepping—Een zoektocht naar het allerkleinste*, G. 't Hooft (Ooievaar Pockethouse, Amsterdam, 1992).

kern storten, net als een steen op de aarde valt door de zwaartekracht. Men stelde zich voor dat de elektronen in banen om de kern cirkelen, net als de planeten om de zon. Zo'n baan wordt gekarakteriseerd door een grootheid genaamd energie (dat geldt ook voor planeten om de zon). De energie bestaat uit twee componenten, potentiële energie en bewegingsenergie. Voor een stabiele, ofwel stationaire, baan moet er een vaste verhouding zijn tussen de twee, dat is het zogenaamde viriaaltheorema. Verlies van bewegingsenergie betekent verlies van potentiële energie en een cirkelbaan dichter bij de kern. Van elektronen was bekend dat zij energie verliezen als zij bewegen. Dat gebeurt in de vorm van straling. (Dat straling ook een vorm van energie is merkt men tijdens het doorbrengen van een dag in de zon.) Door de beweging bij het cirkelen rond de kern zou een elektron steeds een beetje energie *moeten* afgeven en daardoor dichter bij de kern komen totdat het erin zou vallen. Zou dit het geval zijn, dan nam alle materie ongeveer honderdduizend keer zo weinig ruimte in beslag als nu het geval is.

De oplossing voor dit probleem werd voorgesteld door de natuurkundige Niels Bohr.[6] Hij bekeek het waterstofatoom, dat bestaat uit één proton en één elektron. Hij veronderstelde nu een aantal dingen. Ten eerste verbood hij het elektron zomaar een willekeurige hoeveelheid energie uit te stralen. Dat verbod was niet zo uit de lucht gegrepen als het lijkt, want al eerder had een andere natuurkundige, Max Planck, ontdekt dat er met straling iets bijzonders aan de hand is. Om zijn experimenten te verklaren moest Planck ervan uitgaan dat stralingsenergie slechts met bepaalde hoeveelheden tegelijk wordt afgegeven of opgenomen. Hij noemde die hoeveelheden quanten. Ten tweede postuleerde Bohr dat het elektron alleen zeer goed bepaalde hoeveelheden energie kan hebben. Het elektron kan nu van de ene baan naar de andere 'springen' door opname of afgifte van stralingsquanten. Nu zou het nog mogelijk kunnen zijn dat het elektron kan springen naar een baan waarbij het zich permanent in de kern bevindt. Vergelijking van de maximale energie-sprong van het waterstofatoom met de mogelijke energie van de diepstliggende baan leidt echter tot de conclusie dat het elektron zich niet permanent op de kern kan bevinden, waarmee de stabiliteit van atomen is verklaard.

Hoewel aanvankelijk als 'lapmiddel' geformuleerd, bleek de theorie van Bohr wel degelijk betekenis te hebben. Verder onderzoek leidde tot de theorie van de quanten, de quantumtheorie, en leerde dat er in het kleine 'universum van het atoom' andere wetten heersen dan in de wereld die we van het leven van alledag kennen. De kleinschaligheid die bereikt is in de beschrijving van materie leidt soms tot vreemde denkbeelden die we ontwikkelen om ons een voorstelling te maken. Zo hebben we nu protonen en elektronen steeds 'deeltjes' genoemd, daarbij het beeld oproepend van kluitjes materiaal. Dat beeld is maar ten dele correct, want protonen en elektronen gedragen zich in sommige opzichten alsof het 'golven' zijn. Een deeltje kan maar op één plaats zijn, een golf is overal, denk aan een golf gemaakt door het gooien van een steen in een vijver. Wil men dus realiteitswaarde aan de kleine bouwstenen van materie toekennen, dan zijn ze *zowel* 'deeltjes' als 'golven'. Het

6 *A History of Mechanics*, R. Dugas (Édition du Griffon, Neuchâtel, 1955. In Engelse vertaling verschenen bij Dover Publications, New York, 1988).

gebrek aan passende beeldspraak maakt het voor veel mensen moeilijk de quantumtheorie te begrijpen.[7] Zij zijn in goed gezelschap. Niels Bohr zelf zei dat iemand die de quantumtheorie niet moeilijk vindt haar niet begrepen heeft.

De quantumtheorie is dus de verzameling van wetten die gelden op atomaire schaal. Uit die wetten volgt de quantummechanica, dat is de wiskundige formulering van de *bewegingsvergelijkingen* voor de deeltjes – in ons geval kernen en elektronen – waarmee hun onderlinge bewegingen kunnen worden uitgerekend. Zo kunnen berekeningen worden gedaan aan atomen, bestaande uit één kern en een aantal elektronen, maar ook aan moleculen, die bestaan uit meerdere kernen met daaromheen elektronen. De onderlinge bewegingen van de kernen en elektronen kunnen niet zoals de baan van een kanonskogel met de klassieke mechanica heel precies van tijdstip naar tijdstip worden berekend, maar als een *waarschijnlijkheid* dat een deeltje zich op een bepaalde tijd op een bepaalde plaats in de ruimte bevindt. De waarschijnlijkheidsverdeling van de kernen en elektronen over de ruimte definieert een *toestand*. Er bestaan allerlei mogelijke toestanden die meer of minder gunstig zijn. De mate van gunstig zijn wordt uitgedrukt in de *energie* van de toestand. Elke toestand die stabiel is, dat wil zeggen dat de bijbehorende waarschijnlijkheidsverdeling een tijdje kan standhouden, heeft een bepáálde energie. Het vóórkomen van bepaalde toestanden is afhankelijk van de beschikbare energie.

Quantumchemie houdt zich bezig met het oplossen van de bewegingsvergelijkingen van de kernen en elektronen met als doel het begrijpen en voorspellen van molecule- en stofeigenschappen. Dat is belangrijk omdat de quantummechanische natuur der dingen doorwerkt in het alledaagse. Neem bijvoorbeeld kleur. Kleur ontstaat doordat materiaal waarop wit licht valt een deel van dat licht opneemt, absorbeert. (Wit licht bestaat uit een mengsel van alle kleuren licht, iets dat men kan zien aan de regenboog die ontstaat als het licht van de zon gebroken wordt door water in de atmosfeer.) Het materiaal kan alleen dat deel van het licht gebruiken dat overeenkomt met de energie die nodig is om van de ene naar de andere toestand te komen. De energie van de rest van het licht ‘past’ niet bij een overgang tussen twee toestanden en wordt teruggekaatst. Wat wij zien is wit licht verminderd met het geabsorbeerde deel. Welke kleur het materiaal krijgt wordt bepaald door de samenstelling van het materiaal in termen van de onderlinge verdeling van kernen en elektronen en de mogelijke toestanden.

Zo kan men eigenlijk alle stofeigenschappen uiteindelijk verklaren met behulp van de quantumtheorie, en kwantitatieve voorspellingen doen met behulp van de quantummechanica. Alle wetenschap houdt zich bezig met het leggen van relaties tussen structuur en gedrag. Steeds meer disciplines bereiken daarbij het niveau van moleculen, het terrein van de scheikunde. Zo krijgt de scheikunde een steeds belangrijkere rol in wetenschap en technologie, van elektrische schakelingen in ‘chips’ tot ontwikkeling van geneesmiddelen, van eigenschappen van nieuwe materialen tot de

---

[7] *Alice in Quantumland*, R. Gilmore (Sigma Science, Wilmslow, 1994); *Mr. Tomkins Explores the Atom*, G. Gamov (Cambridge Unversity Press, Cambridge, 1945. Opnieuw verschenen als *Mr. Tomkins in Paperback*, Canto edition, 1994)

samenstelling van interstellaire gassen. Quantumchemie heeft een plaats waar scheikunde een plaats heeft, als complementair gereedschap bij experimentele technieken. Zowel als hulp bij de verklaring en interpretatie van experimentele gegevens, maar ook als techniek op zichzelf, voor het uitvoeren van ‘numerieke experimenten’, om inzichten te verwerven waarvoor geen experimentele techniek beschikbaar is.

Moleculemodellen en quantumchemie A.3

HET EENVOUDIGSTE EN MEEST ALGEMENE MOLECULEMODEL is de beschrijving van ‘moleculen’ als een verzameling bij elkaar horende kernen en elektronen, deeltjes die zich gedragen volgens de quantummechanica, zoals beschreven in de vorige paragraaf. Met dit model kunnen in principe alle eigenschappen van individuele moleculen, alsmede interacties tussen en reacties van moleculen, worden voorspeld door het uitvoeren van berekeningen. De beperking van de beschikbare rekenkracht verhindert echter een zo grootschalige aanpak van chemische probleemstellingen. Het is echter ook lang niet altijd nodig zo diep terug te grijpen in de theorie. Bepaalde materiaaleigenschappen kunnen ook op een minder hoog niveau worden begrepen.

Neem bijvoorbeeld de verdamping van vloeistoffen. Methaan (aardgas) is bij kamertemperatuur geen vloeistof maar een gas. Het is een vloeistof bij temperaturen ver onder nul graden Celcius. Water daarentegen is bij kamertemperatuur een vloeistof en kookt pas bij honderd graden Celcius. De verklaring hiervoor is dat stoffen bestaan uit een grote hoeveelheid moleculen. Water bestaat uit watermoleculen, methaan uit methaanmoleculen. Omdat methaanmoleculen veel minder aan elkaar ‘kleven’ dan watermoleculen kunnen ze makkelijker de vloeistof verlaten en zal de vloeistof makkelijker verdampen. De minder sterke interactie tussen de methaanmoleculen kan verklaard worden door te kijken naar een aantal eigenschappen van de moleculen. Methaanmoleculen hebben een andere verdeling van de lading dan watermoleculen. In methaanmoleculen is de positieve en negatieve lading evenwichtiger verdeeld over het molecule: de moleculen zijn minder polair. Minder polaire moleculen hebben minder sterke wisselwerking met elkaar dan polaire moleculen. De molecule-eigenschap ‘polariteit’, iets dat te meten is, bepaalt dus (mede) de verdampingssnelheid van een vloeistof.

Het verschil in polariteit tussen methaan- en watermoleculen vindt haar oorsprong in de verdeling van de kernen en elektronen waaruit de moleculen zijn opgebouwd. Een methaanmolecule bestaat uit één koolstof- en vier waterstofkernen en tien elektronen; een watermolecule uit één zuurstof- en twee waterstofkernen en eveneens tien elektronen. Gezien vanuit de koolstofkern wijzen de vier waterstofkernen in methaan allemaal een andere kant op; de twee waterstofkernen in water liggen aan één kant van het molecule ten opzichte van de zuurstofkern. In het methaanmolecule zijn de positieve ladingen veel evenwichtiger verdeeld dan in water, zodat ook de elektronen evenwichtiger verdeeld zijn. De stofeigenschap hangt uiteindelijk wel af van de dieper liggende quantummechanica van de kernen en elektronen, maar wij kunnen haar ook duiden in termen van *collectieve* eigenschappen van een aantal kernen en de daarbij behorende elektronen. We hebben dan een stap gemaakt van de beschouwing van materie op het kern-en-elektronniveau naar een moleculair beeld: materie bestaat uit een verzameling moleculen, die door hun onderlinge interacties de eigenschappen van de stof bepalen. Op het molecu-

laire niveau doen de gedragingen van de individuele kernen en elektronen er niet meer toe.

Het collectief optreden van groepen kernen en elektronen is te vergelijken met het voeren van cao-onderhandelingen door vertegenwoordigers van werkgevers en werknemers. De individuele werkgevers en werknemers zullen elkaar vaak nauwelijks kennen, zeker niet als ze in verschillende bedrijven werken, maar gezamenlijk oefenen ze wel degelijk invloed op elkaar uit. De onderhandelaars verwoorden de collectieve belangen van hun achterban. Komt er een akkoord, dan kan het voorkomen dat individuen het daarmee niet eens zijn, maar het collectief zal zich tevreden tonen. Zouden individuele werkgevers en werknemers met elkaar hebben onderhandeld, dan zouden (in een redelijke maatschappij) sommigen het heel slecht, sommigen het heel goed en de meesten het naar tevredenheid treffen, maar gemiddeld zou het resultaat niet veel verschillen van de centraal gemaakte afspraken. Voor het begrijpen van het resultaat is dus geen kennis vereist van de verlangens van alle betrokken individuen, maar volstaat kennis van het gezamenlijk en gemiddeld belang.

Het voordeel van het gebruik van moleculemodellen boven het kern-en-elektronmodel is, naast het vereenvoudigde inzicht, de enorme besparing op de benodigde rekeninspanning, net als centraal overleg onnoemelijk veel tijd bespaart. Het kern-en-elektronmodel heeft belangrijke rekentechnische nadelen. Ten eerste het werken met waarschijnlijkheden. Van deeltjes die zich volgens de klassieke mechanica gedragen, zoals de kanonskogel uit paragraaf 2, hoeft per deeltje maar één plaatscoördinaat, dat zijn drie getallen, op elk tijdstip te worden bijgehouden; voor quantumdeeltjes een waarschijnlijkheid in èlk stukje van de ruimte, dat zijn in principe oneindig veel getallen. Het probleem kan toch hanteerbaar gemaakt worden door gebruik te maken van eenvoudige recepten, *functies,* die bij een plaats in de ruimte een waarschijnlijkheid geven volgens een vaste formule. Zo hoeft niet op elke plaats in de ruimte een waarschijnlijkheid bewaard te worden, maar kan deze worden uitgerekend met behulp van het recept. Vanwege het ‘golfkarakter’ van de deeltjesbeschrijving noemt men de functie die de waarschijnlijkheidsverdeling oplevert de golffunctie. De makkelijkste manier om de golffunctie van àlle deeltjes hanteerbaar te maken is haar uit te schrijven als produkt van golffuncties van de losse deeltjes. Er is echter een addertje onder het gras dat een groot struikelblok voor de quantumchemie oplevert.

Elektronen zijn ononderscheidbaar: het is onmogelijk een ‘mentaal naamplaatje’, zoals een nummer, aan individuele elektronen te hangen. Eigenlijk is de term ‘individueel elektron’ al fout. De golffunctie die ontstaat door het produkt te nemen van alle losse-deeltjesfuncties is niet correct omdat daarin de elektronen tòch genummerd zijn. Deze fout kan goedgemaakt worden door alle elektronen in de genummerde golffunctie op alle mogelijke manieren met elkaar te verwisselen. Als er N elektronen zijn dan bestaat de echte golffunctie uit N! (dat is N×(N-1)×(N-2)×...×2×1) van dezelfde, maar verschillend genummerde golffuncties. Het vervelende is dat al deze golffuncties op een bepaalde manier moeten worden opgeteld, en wel zó dat de golffuncties die ontstaan door een oneven aantal verwisselingen van elektronen met een minteken tellen, en de golffuncties die door een even aantal

verwisselingen ontstaan met een plusteken. Deze antisymmetrie-eis voor elektronen is een voorbeeld van het zogenaamde Pauli-principe voor fermionen die de toepassing van de quantummechanica grote beperkingen oplegt door de overweldigende rekeninspanning die zij vereist. Door over te schakelen op het moleculemodel wordt al deze ellende omzeild – er is immers geen sprake meer van elektronen – en blijft alleen het klassieke technische rekenprobleem over, dat voor het berekenen van de bewegingen van N deeltjes N×(N-1) interacties nodig zijn, hetgeen overigens ook nog beperkingen oplegt aan het aantal te beschouwen moleculen.

Hoewel het moleculemodel dus enorme besparing levert op de rekeninspanning en zo berekeningen mogelijk maakt, blijft de fundamentelere beschrijving noodzakelijk. Voor het uitrekenen van het elektronische deel van een *moleculespectrum*, dat zijn de energieën die een molecule kan opnemen of afstaan door van de ene naar de andere elektronische toestand te gaan, is een quantummechanische beschrijving vereist. De energieën van de verschillende toestanden worden bepaald door elektronenbanen die zich over het hele molecule kunnen uitspreiden. Ook de directe omgeving van het molecule is voor de elektronenbanen belangrijk. Het spectrum van een geisoleerd molecule verschilt in het algemeen van dat van het molecule in een vloeistof of oplossing, en soms maakt het soort oplosmiddel dramatisch verschil voor het spectrum. Een praktische toepassing van deze eigenschap is te vinden bij allerlei indicatoren, waarvan de kleur informatie geeft over de polariteit van de omgeving. In zo'n geval moet het molecule quantumchemisch worden beschreven en kan de invloed van de omgeving niet weggelaten worden. Hier biedt het moleculemodel uitkomst als het *gecombineerd* kan worden met het kern-en-elektronmodel.

De belangrijkste eis die in dit verband aan het moleculemodel gesteld moet worden is dat de verschijnselen die beschreven worden *plaatselijk* (men zegt ook wel lokaal) van aard zijn. Dat wil zeggen dat de belangrijke elektronentoestanden zich over een klein deel van de ruimte uitstrekken. Goed beschouwd is dat eigenlijk nooit het geval, en wel vanwege het Pauli-principe. Bij benadering mag echter 'gezondigd' worden tegen dit principe, door de elektronen tòch te nummeren en toe te wijzen aan moleculen. Voor de moleculen in de nabijheid van het bestudeerde worden de elektronen samen met de kernen als collectief beschreven; de elektronen die zijn toegewezen aan het bestudeerde molecule houden hun oorspronkelijke, uitgebreide beschrijving. De verwisselingen van de elektronen in het quantumchemisch beschreven stuk met die in het moleculair beschreven stuk worden weggelaten. De kwintessens van de getrapte beschrijving is echter dat men terug kan grijpen op het kern-en-elektronmodel zodra het moleculemodel faalt, en zo altijd controle heeft op de terechtheid van de gemaakte vereenvoudigingen.

Het is mogelijk nòg verder te gaan in de reductie van benodigde rekenkracht dan het geval is door toepassing van het moleculemodel. Dan beschrijft men het collectief gedrag van vele duizenden moleculen en komt tot stofmodellen. Het stofmodel relevant voor combinatie met het moleculemodel en het kern-en-elektronmodel is die van de stof als diëlektrisch continuüm, waarmee de elektrische eigenschappen van een stof worden beschreven. Het gaat dan om het collectieve gedrag van enkele tienduizenden moleculen. Het is duidelijk dat er in zo'n model veel detail verloren

gaat, meer nog dan in het moleculemodel. Het is dan ook de vraag in hoeverre het nog geoorloofd is voor de beschrijving van verschijnselen die zo sterk afhangen van het gedrag van de elektronen het diëlektrisch model te combineren met het kern-en-elektronmodel. Ook hiervoor zijn vanuit de quantumtheorie, net als bij de opstelling van het moleculemodel, grenzen aan te geven. Zij zijn eigenlijk precies dezelfde, daarmee de kracht, consistentie en algemeenheid aangevend van de quantum-mechanische beschrijving van de natuur.

Tenslotte nog iets meer over de aard van de collectieve eigenschappen die door het moleculemodel moeten worden weergegeven. De kernen en elektronen hebben wisselwerking met elkaar door hun elektrische lading. De molecule-eigenschappen die van belang zijn, zijn dus elektrische. Vanuit het oogpunt van consistentie is de beste aanpak de collectieve elektrische eigenschappen van moleculen te onderscheiden in twee soorten, vacuüm en respons. De vacuümeigenschappen worden bepaald door het molecule in isolatie, wanneer het geen enkele invloed van andere moleculen voelt (weer een geïdealiseerde toestand die alleen op papier – en in de computer! – te verwezenlijken is). Deze geven aan hoe het molecule de eerste confrontatie aangaat.

De responseigenschappen geven aan hoe de verdeling van kernen en elektronen zal reageren op de aanwezigheid van andere kernen en elektronen. Als twee groepen kernen en elektronen met elkaar wisselwerking aangaan is het een kwestie van geven en nemen, op zoek naar een nieuw evenwicht, net als in cao-onderhandelingen beide partijen wat zullen moeten inschikken, hoe fraai hun uitgangspunten ook waren. Een verschil tussen onderhandelaars en moleculen is dat de responseigenschappen van moleculen makkelijk te berekenen zijn. De ‘inschikkelijkheid’ – in vakjargon spreekt men van polariseerbaarheid – van een molecule is een intrinsieke eigenschap van het molecule. De polariseerbaarheid kan alleen op het kern-en-elektronniveau worden berekend, hetgeen tot problemen kan leiden in verband met de benodigde rekenkracht. Niettemin is deze aanpak vruchtbaar aangezien de analyse van allerlei invloeden direct gerelateerd kan worden aan fysische processen.

Bijna alle bestaande moleculemodellen brengen de scheiding tussen vacuüm- en responseigenschappen niet aan, maar gebruiken ‘effectieve’ elektrische eigenschappen, waarin de responseigenschappen zijn opgenomen gebaseerd op experimentele gegevens van een aantal voorbeeldsystemen. De hoop is dan dat deze effectieve eigenschappen ook bruikbaar zullen zijn voor andersoortige systemen. Vaak blijkt echter dat dan toch flinke aanpassingen nodig zijn. Om weer de metafoor van de cao-onderhandelingen aan te halen: het is alsof de uitkomst van de onderhandelingen in de metaalsector voorspeld worden in termen van de uiteindelijke resultaten van die in de bouw, de detailhandel en het bankwezen, zonder dat is gekeken hoe daar het proces van geven en nemen in z’n werk is gegaan. Kennis van die zaken had wellicht kunnen voorzien wat nu als verrassing komt. De aanpak die hier wordt voorgesteld vereist aanvankelijk meer werk en is rekenintensiever, maar de verwachting is dat het uiteindelijk zal leiden tot breder toepasbare en inzichtelijker modellen, die ons het minder interessante werk zullen besparen.

Samenvatting en conclusie A.4

IN DIT PROEFSCHRIFT wordt beschreven hoe men vanuit de gedetailleerde quantumchemische beschrijving van materie op het kern-en-elektronniveau kan komen tot moleculemodellen, die het *collectieve* gedrag van een aantal kernen en elektronen vereenvoudigd weergeven. Een niveau hoger wordt het collectieve gedrag van enkele tienduizenden moleculen beschreven door een diëlektrisch continuüm. De beschrijving van collectief gedrag vereist aanzienlijk minder inspanning, waardoor het mogelijk wordt realistischer voorstellingen van gecompliceerde systemen te maken en door te rekenen. De voor de scheikunde interessante processen vereisen vaak slechts een gedetailleerde beschrijving van een deel van het macroscopische systeem. Door de molecule- en continuümmodellen af te leiden uit de quantummechanica van de kernen en elektronen kunnen zij gebruikt worden *in combinatie* met het kern-en-elektronmodel. Het te bestuderen macroscopische systeem wordt in stukken verdeeld die in verschillend detail worden behandeld, al naar gelang het verwachte belang van verschillende onderdelen. Dit wordt geïllustreerd in de onderstaande figuur.

Het interessante gedeelte (het quantumsysteem) wordt zeer gedetailleerd beschreven m.b.v. quantumchemie. Hier beschrijven we de bewegingen van kernen en elektronen. De invloed van directe buurmoleculen (expliciet klassiek systeem) wordt beschreven door gebruik te maken van vereenvoudigde moleculemodellen, die nog wel enig detail vertonen, maar waarin afzonderlijke kernen en elektronen niet meer zichtbaar zijn. Tenslotte kan de rest van het macroscopisch systeem worden weergegeven als een diëlektrisch continuüm, waarin ook individuele moleculen niet meer zichtbaar zijn, maar hun collectieve gedrag wordt weergegeven door betrekkelijk eenvoudige, algemene vergelijkingen met één of twee molecule-specifieke parameters.

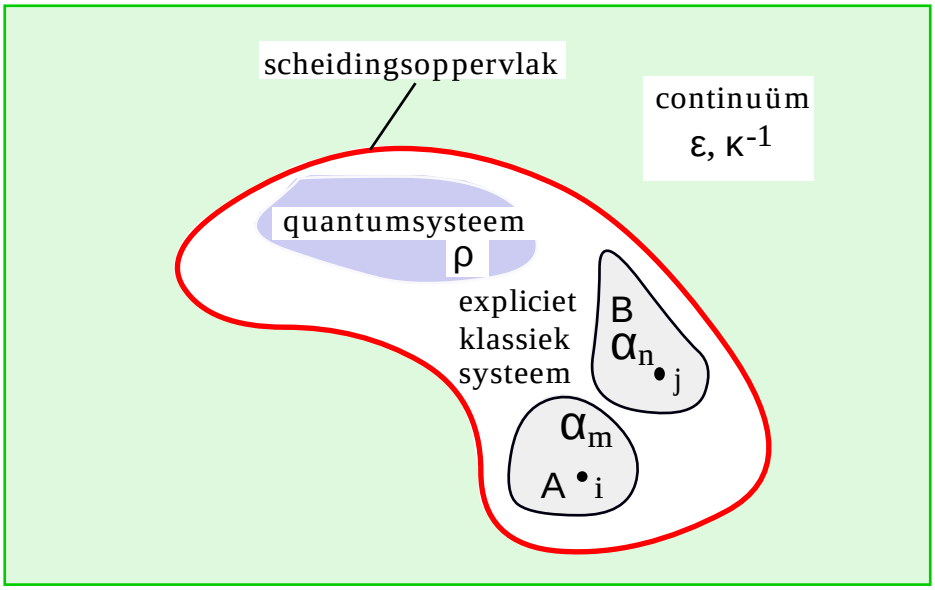

Het proefschrift doorloopt de fasen van de beschreven modelvorming. Hoofdstuk 1 behandelt de wiskunde van de voorgestelde modelvorming, met de nadruk op de beperkingen die het model opgelegd krijgt door de benodigde benaderingen. Getoond wordt dat het de elektronische eigenschappen van de moleculen zijn die de spil vormen van het moleculemodel. Deze zijn zowel toegankelijk via experiment als door berekening, waarmee theorie en experiment worden verbonden. In hoofdstuk 2 wordt het instrumentarium voor het doen van berekeningen met de gecombineerde modellen uitgestald. Het gaat om praktische vergelijkingen en formules die men in een computerprogramma moet verwezenlijken om de voorgestelde methode te gebruiken.

Het derde hoofdstuk bevat de toepassingen van de gecombineerde aanpak. Eerst wordt aan de hand van de interacties tussen twee moleculen – in zogeheten dimeercomplexen – bekeken in hoeverre het moleculemodel beantwoordt aan de verwachtingen. De totaal verschillende dimeren van water enerzijds en benzeenderivaten anderzijds blijken met hetzelfde recept heel behoorlijk te beschrijven. Nu durven we ook de stap te zetten naar grotere verzamelingen van moleculen en gaan dan proberen de oploswarmte van moleculen uit te rekenen. Dit blijkt veel moeilijker, maar dat ligt niet aan een slechte beschrijving van de interacties tussen de moleculen. Veeleer is het aantal moleculen om het centrale molecule die worden beschreven te klein en worden niet alle mogelijke manieren waarop deze zich om het centrale molecule kunnen bevinden effectief en afdoende afgezocht, hetgeen wel erg belangrijk is voor het berekenen van de oploswarmte. De verschuiving van het *spectrum* van een molecule ten gevolge van naburige moleculen blijkt wèl goed te berekenen met een beperkt aantal nabuurmoleculen, ook al worden niet alle mogelijke posities van de nabuurmoleculen afgezocht. Het moleculemodel beschreven in dit proefschrift leverde de eerste succesvolle beschrijving van zowel blauw- als roodverschuiving op van de zogenaamde $\pi^* \leftarrow n$ overgang van aceton in zeer uiteenlopende oplosmiddelen (water, acetonitril en tetrachloorkoolstof).

Door het proefschrift heen blijkt steeds weer dat de combinatie van kern-en-elektronmodel met het diëlektrisch continuümmodel zonder tussenliggende expliciet beschreven moleculen leidt tot inconsistenties. De scheiding tussen de verschillende onderdelen, quantum, klassiek en continuüm, moet duidelijk aan te brengen zijn. De continuümbeschrijving is te grof om binnen de theoretische grenzen van toepasbaarheid met het quantumsysteem te combineren. Hoewel het expliciet beschrijven van moleculen veel duurder is dan het gebruik van het continuümmodel, moet het toch gedaan worden om een realistisch beeld van de microscopische werkelijkheid te scheppen.

Hoofdstuk 3 sluit af met een gedeelte dat laat zien dat het naar beneden schalen van macroscopische eigenschappen, zoals het diëlektrisch continuüm dat beschrijft, naar microscopische dimensies onjuist is en leidt tot foutieve inzichten. Aangetoond wordt dat de directe omgeving van de microscopisch interessante delen van macroscopische systemen het gedrag stuurt, en dat het essentieel is deze directe omgeving in enig detail te beschrijven.

Het succes van de scheikundige manier van kijken naar stoffen is gelegen in het uitleggen van alledaagse, *macroscopische* stofeigenschappen in termen van eigenschappen van en interacties tussen *microscopische* bouwstenen, atomen en moleculen. Het achterhalen van molecule-eigenschappen en intermoleculaire interacties door middel van experimenten is echter allerminst eenvoudig en vaak zelfs onmogelijk door de complexiteit van het macroscopische systeem.

Verrassenderwijs brengt een nòg gedetailleerder zienswijze van materie hier uitkomst: de quantumchemie. In de quantumchemie wordt materie beschreven op het niveau van kernen en elektronen, de bouwstenen van moleculen. De onderlinge bewegingen van de kernen en elektronen bepalen de molecule-eigenschappen en uiteindelijk alle stofeigenschappen. Quantumchemie verschaft het theoretisch en praktisch instrumentarium om de molecule-eigenschappen niet alleen globaal te begrijpen, maar ook *uit te rekenen* door het oplossen van de bewegingsvergelijkingen waaraan de kernen en elektronen moeten voldoen. Op deze manier zijn de eigenschappen van een individueel, niet al te groot molecule goed toegankelijk. In het macroscopische systeem is het molecule echter niet meer alleen, maar wordt omgeven door zeer veel andere moleculen. Door interactie met de omgeving veranderen de eigenschappen van het molecule in het macroscopisch systeem. De omgeving bevat zoveel kernen en elektronen dat het niet mogelijk is deze op het gedetailleerde, quantumchemische niveau te beschrijven. Gelukkig is dat ook niet altijd nodig. In plaats daarvan doet men een beroep op vereenvoudigde omgevingsmodellen.

In het onderzoek beschreven in dit proefschrift, dat zich richt op het berekenen van eigenschappen van moleculen in oplossing, zoals bijvoorbeeld de optische eigenschappen van aceton in verschillende oplosmiddelen (water, tetra en acetonitril), vormen de omgevingsmodellen zèlf het belangrijkste aandachtsgebied. Er zijn twee niveaus waarop de omgeving vereenvoudigd kan worden weergegeven: het moleculaire en het diëlektrische. Op het moleculaire niveau wordt het *collectieve* gedrag van maximaal enkele honderden kernen en elektronen beschreven; op het diëlektrisch niveau worden enkele tienduizenden moleculen ‘samengepakt’. Met iedere vereenvoudiging gaat een zekere hoeveelheid detail verloren. Onderzocht wordt in hoeverre het verlies aan detail fouten veroorzaakt in de berekende eigenschappen van het molecule in oplossing. Vaak wordt aangenomen dat het moleculaire niveau kan worden overgeslagen. Het detail dat door het moleculaire niveau wordt verschaft blijkt echter essentieel voor een consistent en betrouwbaar rekenmodel, hetgeen zowel in theorie als in praktijk wordt aangetoond. De algemeenheid van dit omgevingsmodel wordt geïllustreerd door het toe te passen op zeer uiteenlopende systemen.

Bibliography

The texts in this thesis are based on a number of papers that have found their way into the scientific literature, or are close to doing so. A number of applications of the method have not been treated in this thesis, but are (being) published.

Theoretical calculation of tautomer equilibria of 4-substituted imidazoles in the gas phase and in solution, A.H. de Vries and P.Th. van Duijnen, *Biophysical Chemistry*, **43** (1992) 139-147.

Succes and pitfalls of the dielectric continuum solvent model in quantum chemical calculations, A.H. de Vries, P.Th. van Duijnen, and A.H. Juffer, *International Journal of Quantum Chemistry, Quantum Chemistry Symposium*, **27** (1993) 451-466.

Implementation of reaction field methods in quantum chemistry computer codes, A.H. de Vries, P.Th. van Duijnen, A.H. Juffer, J.A.C. Rullmann, J.P. Dijkman, H. Merenga, and B.T. Thole, *Journal of Computational Chemistry*, **16** (1995) 37-52.

Solvatochromism of the $\pi^* \leftarrow n$ transition of acetone by combined quantum mechanical–classical mechanical calculations, A.H. de Vries and P.Th. van Duijnen, *International Journal of Quantum Chemistry* (1995), in press.

Utopia dielectrica, P.Th. van Duijnen and A.H. de Vries, *International Journal of Quantum Chemistry, Quantum Chemistry Symposium*, **29** (1995), in press.

The Direct Reaction Field force field: A consistent way to connect and combine quantum-chemical and classical descriptions of molecules, P.Th. van Duijnen and A.H. de Vries, *International Journal of Quantum Chemistry* (1995), accepted for publication.

Polarization of the excited states of twisted ethylene in a non-symmetrical environment, R.W.J. Zijlstra, P.Th. van Duijnen, and A.H. de Vries, *Chemical Physics* (1995), submitted for publication.

The subject of this thesis is the theory, implementation, and practice of combined quantum-mechanical and classical descriptions of liquid-phase chemistry.

It is shown that a diversity of solvents may be treated consistently only if a few solvent layers around the solute are included at the molecular level, modelling electrostatic and electric response properties of solvent molecules.

In dit proefschrift wordt beschreven hoe fysisch-chemische eigenschappen van moleculen in oplossing kunnen worden uitgerekend.

Voor een realistisch, zinvol en praktisch hanteerbaar model dienen verschillende niveaus van detail met elkaar te worden gecombineerd.

Het voorgestelde model kent drie lagen van details die het elektrisch gedrag van respectievelijk:
- kernen en elektronen;
- moleculen en
- vloeistoffen

beschrijven.